CCFE-R(15)28
June 2015

Michael Fleming
Jean-Christophe Sublet

Validation of FISPACT-II Decay Heat and Inventory Predictions for Fission Events

www.ccfe.ac.uk

Validation of FISPACT-II Decay Heat and Inventory Predictions for Fission Events

Michael Fleming
Jean-Christophe Sublet

June 2015

UK Atomic Energy Authority
Culham Science Centre
Abingdon
Oxfordshire
OX14 3DB

Contacts Dr Michael Fleming
Dr Jean-Christophe Sublet

UK Atomic Energy Authority
Culham Science Centre
Abingdon
Oxfordshire
OX14 3DB
United Kingdom

Telephone: +44 (0)1235-466884
email: michael.fleming@ccfe.ac.uk

Telephone: +44 (0)1235-466400
email: jean-christophe.sublet@ccfe.ac.uk

Facsimile: +44 (0)1235-463435

Disclaimer

Neither the authors nor the United Kingdom Atomic Energy Authority accept responsibility for consequences arising from any errors either in the present documentation or the FISPACT-II code, or for reliance upon the information contained in the data or its completeness or accuracy.

Acknowledgement

The authors would like to gratefully acknowledge the invaluable assistance of W. Schier, P.-I. Johansson and T. Yoshida, who provided original data and translations without which this report could not be written. We are also indebted to the UKAEA librarian, H. Bloxham, for her tireless scouring of international libraries for original documents. Additional thanks are due to K.-H. Schmidt and B. Jurado (CENBG) for the most recent GEF libraries, as well as the advice of I. Gauld.

We also acknowledge the work of J.W. Eastwood and J.G. Morgan from Culham Electromagnetics Ltd in the development of FISPACT-II.

CCFE is the fusion research arm of the United Kingdom Atomic Energy Authority.

CCFE is certified to ISO 9001 and ISO 14001.

Executive Summary

Decay heat and inventory calculations for irradiated fission fuels comprise two of the fundamental tasks for time-dependent Bateman solvers in the nuclear industry. Detailed and accurate knowledge of these time-dependent characteristics, as well as trustworthy uncertainty values, are of primary importance for reactor safety cases and the handling of irradiated fuel – issues which cover a great many activities representing billions of euros in current and future effort.

Development of the FISPACT-II code has resulted in new and unique simulation methods for a variety of nuclear observables, including fission decay heat and inventory calculations. To perform these simulations, massive libraries which contain the complete probability distributions for fission product formation, as well as the complete decay data for all of these products (reaching from the long-lived to those with sub-second half-lives), must be maintained and validated with sophisticated and sturdy simulation software. All of the physics of nuclear interactions, fissions and decays is contained within the nuclear data files, which hide one half of the simulation within the evaluation method behind those files. The fundamental point is that simulations cannot be performed by codes or data libraries, but the union of these into a code/data suite.

While most time-dependent inventory and observables codes rely upon *one* bespoke nuclear data library, the ability to harness any dataset affords a unique opportunity to cross-check data and provide feedback which ultimately improves the code/data system. By performing a verification and validation on FISPACT-II with all of the major international nuclear data libraries, this exercise goes beyond demonstrating the capabilities of the code/data system in simulating decay heat and inventories, giving precise information on which nuclides should have their fission yield or decay data re-evaluated and in which library.

To ensure that this validation is as robust as possible, a thorough effort has been made to revisit as many high-quality decay heat experiments with complementary neutron spectra, irradiation schedules, measurement techniques and nations of origin. Simulations from theoretical fission bursts to full-day irradiations have been performed, using a variety of nuclear data combinations, and compared with the available experiments. Good agreement between calculation and experiment (C/E) is found for total heat from the major fresh fuel components in actual LWRs, however spectroscopic partial heat and decay heat in thorium fuel cycle nuclides remains discrepant – both in C/E and C/C. For minor actinides where no experimental data was available, C/C comparisons also show substantial differences between data libraries.

Detailed (spectroscopic and total) decay heat break-down by nuclide is also performed for select cooling times and fissiles, using different decay or fission yield libraries to demonstrate the precise cause of the C/C discrepancies. These are found to primarily be due to incomplete adoption of TAGS results for Pandemonium nuclides, but many other decay data and fission yield differences have been identified. Given the tendency for relative agreement on total values, it is clear that many compensating effects are still present.

Contents

1 Introduction

The thermal fission of ^{235}U results in the release of some 200 MeV which is carried by the numerous outgoing particles. In a typical fission, more than 80% of this 200 MeV manifests as kinetic energy of the two main fission fragments, while approximately 10 MeV is carried by neutrinos and some 4-8 MeV are taken by each of the following: prompt neutrons, prompt gammas, fission product betas and fission product gammas. The β- and γ-decays of the fission products are commonly referred to as the **decay heat** due to the the fission. These are of tremendous importance to the nuclear power industry as they are generated over time-scales relevant to reactor operation and the wider fuel cycle. The events at the Fukushima Daiichi power plant underline this point; even though decay heat represents a small fraction of total reactor power, the integrated energy output after shutdown is more than enough to break safety limits in a reactor or storage pool.

In order to safely develop fission plants it was necessary to determine the heat output of fission events through careful experiments. All potential fuels, as well as the fissionable products of neutron absorption of those fuels, were irradiated in experiments with various neutron energies and pulse durations. These experiments are generally separated by their measurement approach, which include some combination of radiation-specific or calorimetric instruments. Each is burdened with its own drawbacks; difficulty measuring short ($<$ 10 s) cooling times, inability to contain noble gases, challenges in quantifying the fission rate, *etc.*

Simulations of decay heat rely upon tremendously complex fission yield and decay data, as well as code systems which can accurately use this information to track inventories which include most of the periodic table with many unstable nuclei and numerous decay chains. The distribution of fission products is additionally non-constant as a function of incident neutron energy and can be evaluated for a variety of energies. Moreover, a multi-group energy structure complemented with an equal number of fission yields (more than 1-3) could be used for robust, spectrum-dependent fission yield calculations[1].

Validation of decay heat calculations necessarily involves analysis over time-scale orders of magnitude and meaningful conclusions cannot be drawn from comparisons with dozens of experiments, each including many measurements. Selection of individual experiments in this report has been guided by availability and the international recognition of quality experiments[2], but extended to include as many reliable sources as possible. They are all described in the following section.

Although there is broad agreement between calculation-derived (C) and experimental (E) decay heat values, a well-known misallocation of β/γ decay paths remains for many data libraries. This was demonstrated in a paper by Hardy *et al* [6] using a fictional

[1] This is a novel capability of GEF fission yield files [1, 2] which is **not** a feature of legacy libraries. The ability to utilise this more complete data remains, to our knowledge, a unique feature of EASY-II. While the operation of LWRs may not require more n-incident data-points for fission yields, many other applications demand it.

[2] Largely following the work of Tobias [3]. See also the validation reports for ORIGEN-S and SCALE [4, 5]

nuclide, Pandemonium[3], whose β and γ levels and feeding parameters were artificially generated[4]. It was demonstrated that with typical efficiency functions for HPGe γ detectors, which are commonly used for these measurements, many high-energy γ decays would not be detected. The so-called 'Pandemonium effect' occurs when poor detector efficiency prohibits the detection of high-energy γ-rays. When β-decay occurs in the same pathway, the absence of high-energy γ measurements results in the incorrect attribution of energy to the β-decay which was emitted in the hidden γ-ray(s), as shown schematically in Figure 1.

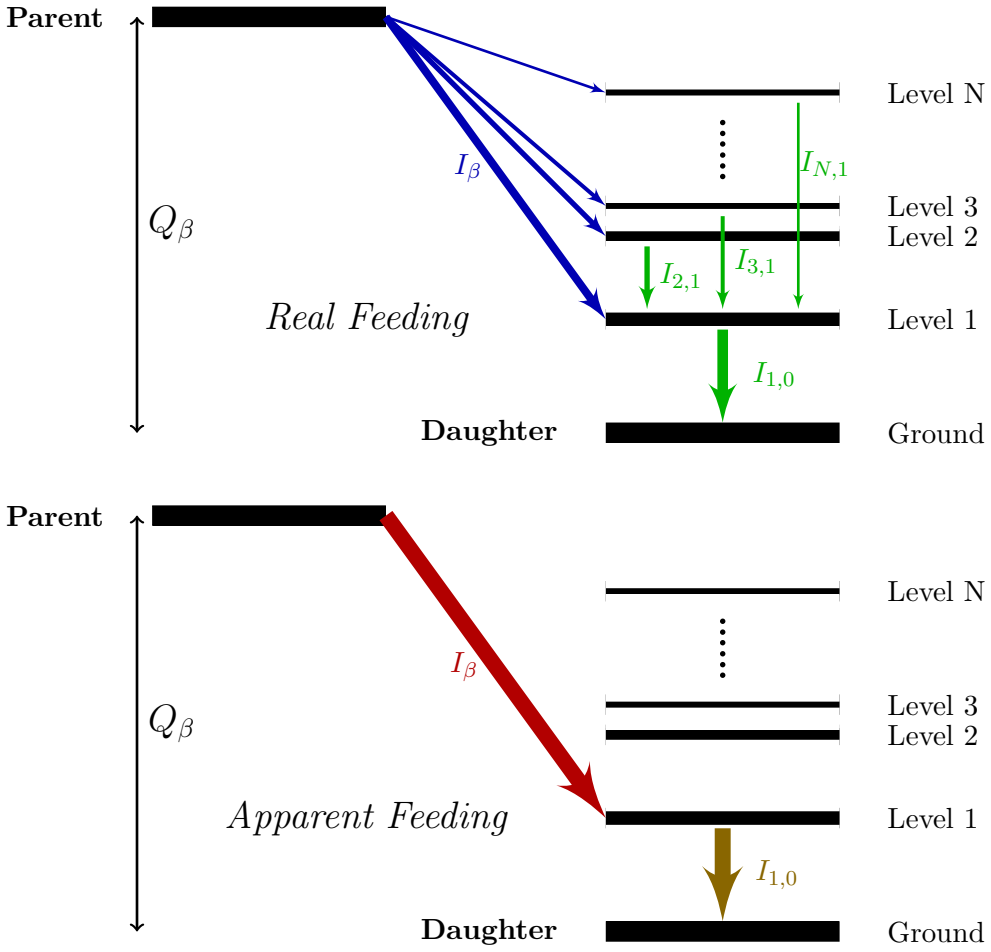

Figure 1: Difference between real (top) and apparent (bottom) β-decay feeding of daughter excited states, yielding an overestimated β-energy contribution.

The highest energy beta decays could be inferred from the lowest level gamma decays as

$$I_\beta = I_{1,0} \text{ assuming } I_{i\neq 1,0} = 0. \quad (1)$$

[3] "Of Sovran power, with awful Ceremony
And Trumpets sound throughout the Host proclaim
A solemn Councel forthwith to be held
At Pandæmonium, the high Capital
Of Satan and his Peers"
Milton *Paradise Lost* I-753

[4] Although fictional, it was taken as spin $\frac{1}{2}^+$ with A=145 N=64 to draw comparisons with the data for the real nuclide ^{145}Gd.

With the inclusion of higher-energy gamma transitions which were not resolved in previous experiments, $\sum_{i=2}^{N} I_{i,0} \neq 0$ and a variety of lower-energy beta decay feeds must be added, ultimately subtracting from the beta feed to the first level and decreasing the % beta heat per decay of the parent nuclide.

The search for decay data which incorrectly attributed β and γ feeding led to a set of total absorption gamma spectroscopy (TAGS) measurements performed by Greenwood *et al* [7]. Some 69 nuclides were considered and data was made available for the improvement of decay data which would lead to more accurate fission decay heat simulations. This was followed by a new list, from WPEC subgroup 25, of high-priority nuclides for TAGS measurements[5] [8]. Data from several of these nuclides have been slowly assembled and used to re-evaluate the decay data which ultimately improves the agreement between simulation experimental results from decay heat experiments.

To illustrate the challenges faced by evaluators who must produce fission yield and decay libraries, Figure 2 shows the decay heat from a thermal fission pulse of ^{235}U using ENDF/B-VII.1 data. Each radionuclide is placed at (x,y) coordinates which are the half-life and end of irradiation (EOI) heat production, respectively. The tremendous number of nuclides – which cannot be distinguished by eye – should impress upon the reader the convoluted nature of fission decay heat. The ability to simulate such a system with reasonable accuracy is testament to the quality of the code system, fission yields and decay data files used.

Considering the same decay process, Figure 3 shows only those nuclides which have been the subject of previous and ongoing TAGS measurement campaigns. These nuclides represent a substantial proportion of the decay heat during several time-periods following a fission pulse and revision of the decay files has a profound effect on spectroscopic decay heat simulations. The identification of these nuclides is due to a combination of theoretical considerations with a focus on nuclides which are essential for reactor responses. This report provides another perspective: detailed analysis of fuel decay heat responses which can probe the discrepancies between nuclear data files and fix potential errors.

[5]Which include re-measurements of a few 'Greenwood' nuclides.

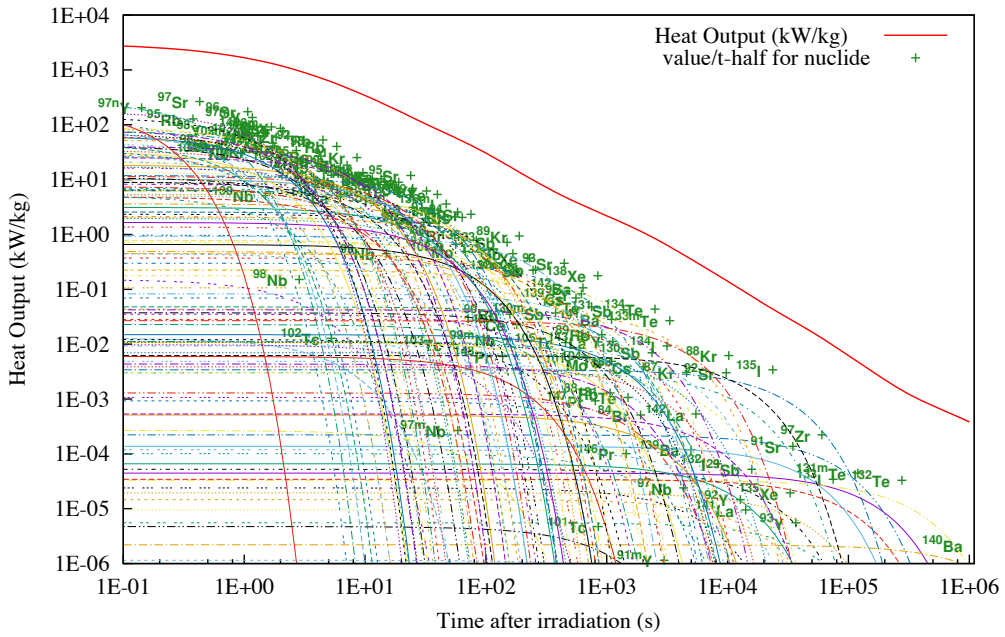

Figure 2: Total decay heat from $^{235}U_{th}$ pulse with radionuclide labels at = ($t_{1/2}$, heat(EOI)).

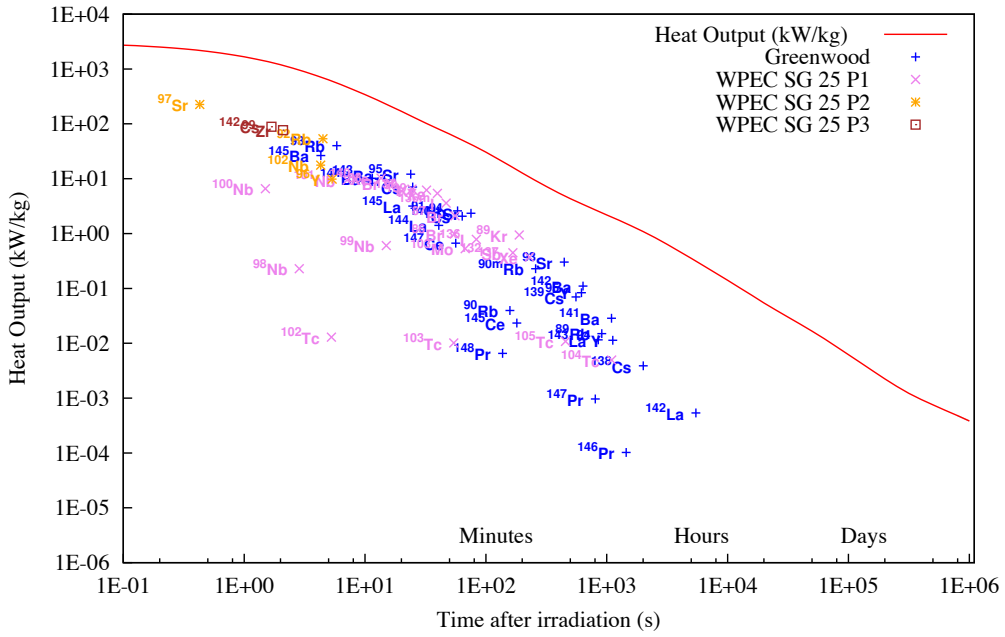

Figure 3: Total decay heat from $^{235}U_{th}$ pulse with TAGS radionuclide labels at (x,y) = ($t_{1/2}$, heat(EOI)). WPEC subgroup 25 nuclides are labelled as PX = priority X.

2 Codes and libraries

The European Activation System, EASY-II [9], has been used to perform this validation exercise. The FISPACT-II code [10] allows the use of a variety of decay data (DD) and neutron-induced fission yield (nFY) libraries, of which the following are used:

- **JEFF-3.1.1** [11] European library containing nFY and decay files
- **ENDF/B-VII.1** [12] American library containing nFY and decay files
- **JENDL-4.0** [13] Japanese library containing nFY and decay files
- **GEF-4.2** [1, 2] Centre d'études nucléaires de Bordeaux Gradignan GEF-based fission-fragment yield library
- **UKDD-12** UKAEA decay data file built from EAF-2007 decay data [14] with inclusion of some updates and increased set of short-lived nuclides to cover further TENDL daughter nuclides

The various libraries contain not only different data for the same nuclides, but also cover different sets of nuclides. This is summarised in Table 1, where the columns show the number of nuclides with neutron-incident, decay, neutron-induced fission and spontaneous fission yield (sFY) files, respectively. The methodologies behind TENDL and GEF allow for more robust files, notably containing any target nuclides and a large range of incident neutron energies.

Table 1: Overview of the number of nuclides which have files within each nuclear data library.

Library	n-incident	DD	nFY	sFY
TENDL-14	2632	—	—	—
GEF-4.2	—	—	119	109
UKDD-12	—	3875	—	—
ENDF/B-VII.1	423	3818	31	9
JENDL-4.0u	406	1380	31	9
JEFF-3.2/3.1.1	472	3854	19	3

Comparisons are initially made between paired neutron-induced fission yield and decay data from the same continent, but in section 6, the JEFF-3.1.1 nFY file is used for all calculations, while different decay libraries are used for comparison. Fission yields are generally stored for three separate incident neutron energies: a thermal value of 0.025 eV, a 'fast' value of 400 keV and a 'high-energy' value of 14 MeV. The experiments that are considered in this report use either thermal or fast neutron irradiations and are simulated within the FISPACT-II code as irradiations of a mono-energetic neutron flux. Pulses are performed using a 1 μs irradiation of 1E19 $\mathrm{n \cdot cm^{-2} s^{-1}}$ neutron flux, while a variety of specific experiments are simulated using the precise flux/duration reported. The decay heat is measured in MeV/fission in order to probe the fission and decay heat

data exclusively[6].

3 Fission Decay Heat Experiments

Fission yields are generally a function of energy and several experiments have been performed with various nuclides and neutron energies to determine heat output as a function of time. In this report the data are drawn from the sources listed in Table 2. Neutron spectra are separated into either thermal (th) or fast (f), denoted with a subscript on the fissile nuclide.

Table 2: Decay heat data sources with a primary author, experimental information and indicative year.

Author, Institute	Nuclide(s)	Method	Irrad. (s)	Year
Fisher, LANL	$^{232}Th_f$, $^{233}U_f$, $^{235}U_f$, $^{238}U_f$, $^{239}Pu_f$	γ	< 1	1964
McNair, UKAWRE	$^{235}U_{th}$, $^{239}Pu_{th}$	β	10-1E5	1969
MacMahon, SRRC	$^{235}U_{th}$	β	10-1E4	1970
Scobie, SRRC	$^{235}U_{th}$	β	1E4-1E5	1971
Lott, CEA	$^{235}U_{th}$	Total	1E2-5E3	1973
Yarnell, LANL	$^{233}U_{th}$, $^{235}U_{th}$, $^{239}Pu_{th}$	Total	2E4	1978
Jurney, LANL	$^{233}U_{th}$, $^{235}U_{th}$, $^{239}Pu_{th}$	γ	2E4	1979
Murphy, UKAEA	$^{235}U_f$, $^{239}Pu_f$	β	1E5	1979
Dickens, ORNL	$^{235}U_{th}$, $^{239}Pu_{th}$, $^{241}Pu_{th}$	γ & β	1-100	1980
Baumung, Karlsruhe	$^{235}U_{th}$	Total	200	1981
Akiyama, JAEA	$^{233}U_f$, $^{235}U_f$, $^{238}U_f$, $^{239}Pu_f$	γ & β	10-300	1982
Akiyama, JAEA	$^{232}Th_f$, $^{nat}U_f$	γ	10-300	1983
Johansson, Uppsala	$^{235}U_{th}$	γ & β	4-120	1987
Tobias Berkeley NL	$^{235}U_{th}$, $^{239}Pu_{th}$	Stat.	-	1989
Schier, UM Lowell	$^{235}U_{th}$, $^{238}Pu_f$, $^{239}Pu_{th}$	γ & β	<1	1997
Ohkawachi, JAEA	$^{235}U_f$, $^{237}Np_f$	γ & β	10-300	2002

The ORNL [15, 16], JAEA [17, 18], Uppsala [19] and UML [20] data all include separate β and γ decay heat measurements for fission pulses. All except the work by Johansson [19] are compared as pulse data, while for that work finite-irradiation-to-pulse correction were not applied and the full treatment is presented. Separate γ-only measurements

[6]More precisely, power per fission multiplied by cooling time, MeV/s/fission × t. In some few cases the data is shown without this time factor and this is referenced in the text.

of ^{232}Th and ^{nat}U, also taken at the JAEA YAYOI fast reactor, were obtained from the doctoral thesis of M. Akiyama [21]. A more recent set of experiments carried out with the YAYOI reactor considered ^{237}Np [22]. A few calorimetric measurements were considered, including the Karlsruhe data [23] from a 200s irradiation, LANL data from a longer 20000s irradiation [24, 25] and three irradiation sets performed by the CEA [26]. A companion campaign at LANL also measured gamma heat using the same reactor and irradiation conditions [27]. A range of irradiations between 10s and 10^5s were performed at the Scottish Research Reactor Centre [28, 29], the UK Atomic Weapons Research Establishment [30, 31] and the UKAEA [32], which probed spectroscopic heat at longer irradiations. Several decay heat experiments performed using Godiva-II are also presented for short cooling validation of a variety of fissile nuclides [33].

To provide the reader with some context of the experimental conditions used for each set of measurements, the following sections are provided with brief summaries for each experimental dataset.

3.1 Oak Ridge National Laboratory data

Measurements using the Oak Ridge Research Reactor by Dickens *et al* [15] were made on the thermal fission of ^{235}U, ^{239}Pu and ^{241}Pu. Samples of approximately 1-10 μg of 93.5% enriched $^{235}U_3O_8$ were dissolved in nitric acid and precipitated. Irradiations of plutonium were carried out with 1 and 5 μg samples of 99% enriched ^{239}Pu and ^{241}Pu oxides, respectively. In all cases, blank sample holders were used for calibration and Au/Mn foils for flux characterisation, to estimate 'epithermal' fissions fraction. A neutron flux of approximately 4E13 n/cm^2/s was available at the target location. The rabbit transfer limited the cooling time to a minimum of 2 seconds and irradiations were run for a range of 1-100 seconds, with varying irradiation sets for the different nuclides.

3.2 Japanese Atomic Energy Agency data

A large set of irradiations were performed by Akiyama *et al* [17, 18, 21] using the YAYOI fast reactor. Samples of 99.44% ^{233}U, 97.652% ^{235}U and 99.107% enriched ^{239}Pu around 1.6 mg were electrodeposited onto 18 mm diameter titanium foils. These were encased within mylar film with PVC rings and calibrated against 'dummy' samples without the fissile material. 99.95% ^{238}U and 99.96% ^{232}Th samples were machined into metallic foils of diameter 12.7 mm, thickness 0.025 mm and 0.10 mm, respectively.

Gamma-ray dection was performed with a NaI(Tl) scintillator calibrated with a response function between 0.06 and 5.0 MeV. A well-type plastic scintillator connected to a transmission type counter using an argon/methane gas was used for beta-ray detection. The responses were calculated using monoenergetic electron beams with energies between 0.3 and 2.7 MeV.

The same experimental set-up was used by Ohkawachi *et al* [22] to remeasure the ^{235}U decay heat and perform measurements using a 0.5 mg sample of ^{237}Np deposited onto a titanium foil. Some efforts were made to correct for the natural and capture decay heat, but no experimental uncertainty or detailed methodology for these corrections, or for the finite-irradiation-to-pulse correction, were available to the authors of this report.

Various irradiation durations of 10, 60, 100 and 300 s were performed and used to generate 'corrected' values for comparison with instantaneous pulse calculations.

3.3 Kernforschungszentrum Karlsruhe data

A 'reduced tandem calorimeter' with thermal constant of a few seconds was used by Baumung [23] to measure total decay heat from ^{235}U from 15 to 4000s following a 200s irradiation. The fraction of escaping gamma-heat was measured using a Moxon-Rae type energy-flux detector. Several pellets of UO_2 and uranium metal with length 15mm and diameter 8-15mm were used for the experiments.

The total gamma heat at certain cooling times rises to approximately 50% of the decay heat, of which the KfK experimentalists estimate 30-60% escaped the calorimeter and were corrected for using their gamma detector. It is noted in the discussion that discrepancies with the then ANS decay heat standard support an over-estimation of the gamma heat escaping the calorimeter.

3.4 University of Uppsala data

A 6 MeV Van de Graff accelerator was used by Johansson *et al* [19] to generate neutrons using the ^{9}Be(p,n)^{9}B reaction followed by thermalisation within a paraffin cube. A flux of approximately 1E8 $ns^{-1}cm^{-2}$ was produced with a fast to thermal neutron ratio estimated at 0.002 using stochastic calculations. Both ^{235}U and ^{239}Pu samples were electrodeposited onto a titanium foil and covered with another titanium foil to prevent escape of fission products. Both were enriched to 99.3% although for γ measurements of ^{239}Pu a larger sample enriched to 93.3% was used.

Gamma detection was performed with a NaI(Tl) crystal shielded with 10 cm Cu/Cd-coated lead and 10 cm of paraffin. 35 different mono-energetic gamma sources over 59.5 to 4071.9 keV were used to calibrate the response function. Beta measurements were made with a Si(Li) detector calibrated using ^{207}Bi conversion electrons.

Samples were placed in various permutations of 4, 10, 120 and 870 s irradiations. Measurements were made between 10.7 and 12375 s without correction factors for measurements where waiting time was fairly similar to the irradiation time.

3.5 University of Massachusetts Lowell data

A series of experiments were performed under the direction of Schier [34, 35, 36] for thermal fission of ^{235}U and ^{239}Pu, and fast fission of ^{238}U, which notably employed a helium-jet to transport fission fragments from the irradiated sample to counting stations. The flushed fission fragments were embedded into microscopic oil droplets which were carried by a rolling tape which could be varied in speed and distance to detection equipment – allowing measurement at different cooling times. This method resulted in decay heat measurements as short as a few hundred milliseconds. Unfortunately, this method is unable to account for the portion of decay heat attributable to noble gases and a compensation is required in order to reconstruct the total decay heat. For specific fissioning nuclei and cooling times, the decay chains from noble gases can comprise more

than 30% of the decay heat. For comparison with decay heat simulations relevant to most physical systems, the data from UML is highly sensitive to the correction factors generated using CINDER10 with ENDF/B-VI [34, 12].

The thermal experiments used the UML 5.5 MV Van de Graaff accelerator to fire 4.5 MeV protons into a ^{7}Li target which were then thermalised by paraffin. This produced a relatively modest 1E7 neutrons per second incident on the fission target. Fast neutrons were generated using the UML 1MW pool research reactor with a cadmium shield to suppress the thermal fission of residual ^{235}U within the depleted uranium sample.

While the helium-jet method produces unique, and therefore valuable, data in short cooling times, the necessary noble corrections make these data less reliable for cooling periods >10 s, where large discrepancies exist between the UML results and all other experiments.

While the summary report [20] and the set of preliminary reports provide excellent experimental overviews, the PhD theses of the students are the primary sources for all of the data used in this report [34, 35, 36]. As the beta and gamma heat measurements were made with different sets of cooling time, no total decay heat values are provided. In this report no effort has been made to mix or modify the experimental data to generate total heat values.

3.6 Centre d'Etudes Nucléaires de Fontenay-aux-Roses data

Total calorimetric measurements of thermal and fast fission of ^{235}U were made by Lott *et al* [26] for cooling time intervals of 1 minute up to 1 day. The calorimeter sensitivity was 7.6E-4 V/W with a time constant of 115s. The sample was irradiated in a constant power channel of the ZOE pile. Fission rates were measured, relative to a calibration, based on the 1596.2 keV line of ^{140}La assuming a fission product yield of 6.30% for ^{140}Ba. Some efforts were made to quantify the experimental and calculational uncertainties with a proper recognition of the lack of reliable nuclear data considered important in the predictions for cooling time lower than 300s.

3.7 Los Alamos National Laboratory data

Two separate campaigns of irradiations with different measurement techniques were carried out using the Los Alamos Omega West Reactor by Yarnell *et al* [24, 25] and Jurney *et al* [27], which used a 93% enriched fuel. In both, ^{233}U, ^{235}U and ^{239}Pu were irradiated for 2E4s at a flux of approximately 3E13 $\mathrm{n \cdot cm^{-2} s^{-1}}$. The calorimetric measurements were performed using a cryogenic liquid helium boil-off method. This afforded tremendous advantages for short cooling times, bringing the thermal time constant from the 115s of Lott *et al* down to less than 1s. Samples were contained within an aluminum capsule which was loaded into an aluminum dart. The plutonium samples were encased in SS304. The dart was ejected from the reactor at the end of irradiation and would open upon upon striking a target above the calorimeter. The calorimeter was comprised of a 52 kg copper block suspended in a vacuum with a 1.2 L liquid helium bath. The flow of helium vapour was used to measure total decay heat. The average sample characteristics for the set of experiments were 87mg 97.46% ^{233}U, 60mg 93.19% ^{235}U, 66mg

93.59% ^{239}Pu and in all cases some effort was taken to ensure that uncertainty/error due to captures, alternative fissions and gamma losses were accounted for.

Smaller samples of 1.73mg 97.46% ^{233}U, 2.14mg 93.19% ^{235}U and 8.6mg 93.59% ^{239}Pu were irradiated in aluminum disks which were placed inside graphite holders and irradiated for 2E4s. After reactor shutdown, measurements were made using a 6.35cm diameter, 15cm long NaI(Tl) crystal encased in a 25-30cm NaI annulus surrounded by a 7.6cm lead shield.

A separate campaign was performed by Fisher *et al* [33] in 1964 using the Godiva-II device. Samples were irradiated in short bursts, strongly peaked at less than 0.02s, and then transferred by pneumatic tube. Several 0.105 inch disks with 99+% enriched samples of ^{232}Th, ^{233}U, ^{235}U, ^{238}U and ^{239}Pu were then measured using a 4 inch diameter, 4 inch long NaI spectrometer.

3.8 UK Atomic Energy Authority data

The longest cooling times for any experiment in this report are due to fast reactor irradiations performed by Murphy *et al* [32] at the Zebra reactor in Winfrith, UK. To extend the measurements to 2E7s (>200 days), 1E5s irradiations were performed with approximately 1.2E10 $\mathrm{n \cdot cm^{-2} s^{-1}}$ flux. To avoid the large heat contribution from aluminum activation, a aluminised melinex foil on thin perspex ring was used as a fission fragment catcher. After irradiation, samples the catcher foil was recovered and placed against a NE102A plastic scintillator.

Six irradiations each of ^{235}U and ^{239}Pu samples were performed, with the data in this report taken from the 'Irradiation 6' results in both cases. Note that the range of measurements extends from 14.8s to over 45 weeks.

3.9 UK Atomic Weapons Research Establishment data

Irradiations of ^{235}U and ^{239}Pu samples within the HERALD research reactor at AWRE Aldermaston were performed for a range of 10, 10^2, 10^3, 10^4 and 10^5 s by McNair *et al* [30, 31]. Parallel samples were enclosed in either NE 102 or perspex discs, tightly sealed to minimise loss of noble gases. These were calibrated against discs filled with ^{90}Sr and ^{90}Y. Samples were removed to a plastic phosphor scintillation counter for beta heat measurements. Separate calibrations were performed for gamma sensitivity of the detector, disc activity and natural fuel decay. These data are presented as a range of finite irradiation simulations, rather than reconstructed pulse, primarily due to the longer irradiation durations.

3.10 Scottish Research Reactor Centre data

Irradiations of ^{235}U samples were performed by MacMahon *et al* [28] using the UTT-100 reactor at the Scottish Research Reactor Centre in Glasgow. Magnetic fields were employed to separate the beta decay heat from the total signal. Several calibrations were made with ^{32}P (β) and ^{137}Cs (γ) standards, as well as ^{90}Sr + ^{90}Y. The sample foil was placed in an aluminised mylar fission product catcher, which was rotated from

an irradiation station to a NE102A detector. The calibration of the catcher foil was performed by direct measurements of ^{99}Mo and ^{140}Ba activities. As with the AWRE data, these results are presented simply as finite irradiation simulations.

3.11 International fission decay standards data

A separate meta-analysis was performed by Tobias [3, 37] which includes a combination of results from multiple laboratories. This data is not derived from any specific experiment, but statistical treatment of a large sampling of data over different irradiation conditions[7], measurement techniques and cooling times stretching back to the legacy experiments of the 1950s. The UK Atomic Energy Research Establishment Harwell code DEVCOR was used to generate a set of decay heat functions for irradiations ranging from a pulse to 1E5 seconds. **Note that (1)** the report was made in 1989 and does not contain more modern experiments, such as the UM Lowell which better probes times less than 10s and **(2)** the author uses χ^2 analysis to identify experimental "inconsistencies" and subsequently modified uncertainties based on the best fit of all data[8]. A more recent review of the Tobias standard has been performed [38][9] found that inclusion of the Lowell data had a "trivial impact on results from the [gamma] fit". Considering the absence of quality experiments with both irradiations of and measurements at less than 10s (besides the ORNL data), and the discrepancy between the Tobias and Lowell data, this is particularly surprising and suggests errors in the approach taken or in the statistical weighting features of DEVCOR. Given the tremendous uncertainty which was statistically generated by DEVCOR for short cooling times (>50% for ^{239}Pu), re-analysis or a new decay heat standard would be prudent.

Most standards for fission decay heat, such as the ANSI/ANS-5.1 standard, are purposefully conservative meta-analyses of the set of experimental data. While it is common for validation reports to compare against these standards, it is universally understood that they are application specific and not intended to be physically accurate. This report therefore does not compare against meta-analyses other than the Tobias compilation.

4 Simulation of fission decay heat

The fission pulse decay heat is an idealised concept where an instantaneous burst of fissions occur, typically in an individual nuclide. If the beta, gamma and total heat values per fission-second following this infinitesimal irradiation time are $b(t)$, $g(t)$ and $h(t)$, the real irradiation can be approximated by integrating a continuous set of bursts over the irradiation period. Consider the beta heat output $B(t)$ after an irradiation of T_I and waiting period (time between irradiation and start of measurement) of T_W with constant fission rate F. At time $t = 0$ the pulse gives an output of $b(T_I + T_W)Fdt$ toward the measurement at $t = T_W + T_I$ while at the end of irradiation it yields $b(T_W)Fdt$. This is summarised simply as:

$$B(T_I + T_W) = \int_{T_W}^{T_I+T_W} b(t)dt. \tag{2}$$

[7] From pulses to 3E6 second irradiations.
[8] With 21 out of 54 ^{235}U and 9 out of 28 ^{239}Pu experiments receiving modifications.
[9] Those authors were unable to obtain the tabulated data and relied upon plot reading. The report also shows no other analysis besides gamma decay heat in U235.

The ideal experiment employs a neutron pulse irradiation T_I which is much less than the waiting time T_W before measurements:

$$T_W \gg T_I. \tag{3}$$

In these circumstances the heat output is very well approximated by

$$B(T_I + T_W) = T_I b(T_W + T_I/2). \tag{4}$$

In real laboratory conditions the limited flux available for experiments forces longer irradiations in order to accurately measure decay heat. As a result, waiting times will not always be much greater than the irradiation time and corrections are required. Detector limitations generate additional constraints, for example with requisite count rates on spectroscopic measurements. Ideally, the time to make measurements T_M should be much smaller than the waiting time:

$$T_W \gg T_M. \tag{5}$$

As with Equation (3), this is not always possible. To provide a universal 'cooling time' T_C, it is standard practice to define $T_C = T_W + 1/2(T_I + T_M)$ and give all pulse values as functions of this time variable. Whenever these approximations are not valid, a correction must be made to account for the integration of fission events during the irradiation. This is often done by application of a 'correction factor' given by the ratio of calculated values for pulse and longer-irradiation heat outputs. As a specific example, consider the γ energy release from the 10 s fast irradiation of ^{235}U by Akiyama reproduced in Table 3.

Table 3: Akiyama ^{235}U fast fission data for 10 s irradiation

T_W (s)	T_M (s)	T_C (s)	$G(T_I, T_W)$ (MeV/f)	$g(T_C)$ (MeV/f/s)
11	6	19	0.213	3.47E-2
17	8	26	0.208	2.57E-2
25	10	35	0.195	1.94E-2
35	10	45	0.153	1.53E-2
45	10	55	0.126	1.26E-2
55	20	70	0.198	9.86E-3
75	20	90	0.150	7.48E-3

In this case to correct for the duration of the count there is an additional division by T_C. For the 35 second and above measurements there is no correction term while the $T_C = 19$ case includes a correction for the gamma burst function of

$$\eta \equiv \frac{T_I \times g_{calc.}(T_C)}{G_{calc.}(T_I, T_W)} = \frac{0.0347 \times 6}{0.213} = 0.977. \tag{6}$$

This modification reflects the fact that the calculated burst function decreases over the 10 s period around the cooling time of 19 s. Those fissions that occurred earlier in the irradiation period will already have decreased in heat output so that the integrated fissions over that irradiation are slightly less hot than a pulse after 19 s. After one

minute the difference is so negligible that the experiment effectively reproduces a fission pulse.

More generally, an experiment is constrained by maximum achievable fluxes, maximum total heat that a sample can emit, time delays in sample movement systems and a (potentially small) range of count rates that detectors can accurately handle. In order to probe different sections of the fission decay burst function, an experimentalist typically can only adjust the sample irradiation time. Figure 4 shows several total heat curves for irradiations of ^{241}Pu using a 1E14 n/s flux and irradiation times of 0.1, 1, 10, 100 and 1000 seconds. The burst function calculated using a 1E21 flux over 1 ns and the experimental results from Dickens are included for comparison. The non-fission decay heat from ^{241}Pu is included while decay from capture events are excluded.

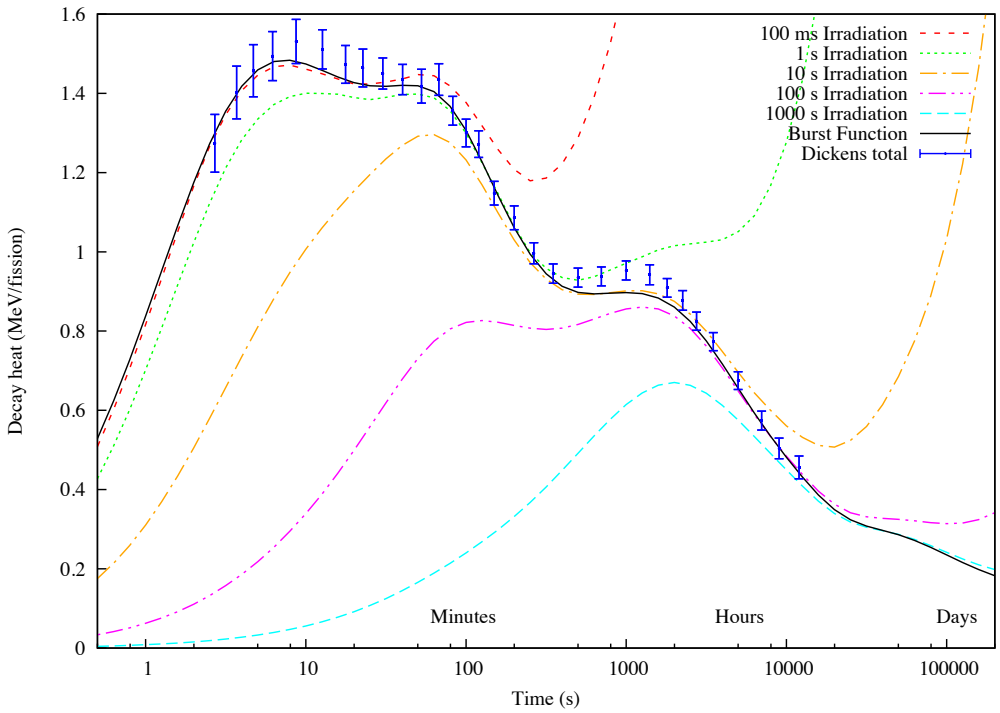

Figure 4: Comparison of ^{241}Pu irradiations against the burst function and Dickens results.

For longer irradiations, the relative contribution from short-lived nuclides becomes less, since some fraction of them have decayed over the irradiation. For example, the 100 s irradiation has a large deviation from the burst function for cooling times less than 100 s and continues to be substantially less than the burst until some 2000 s cooling time. Eventually in all samples the total heat from fission decays will experience non-trivial competition with parent decay and/or capture. In Figure 4, the curve regions with exponential increase above the burst function indicate that the parent decay has become dominant.

4.1 Nuclear data file inputs

Fission yields vary substantially over the set of nuclides of interest for reactor operation, and indeed for incident neutron energy. This results in very different functions of decay heat per fission, which are particularly divergent in the cooling times less than 1000 s (17 min), as shown in Figure 5. Since the products which dominant any given response function are produced in different quantities using the fission yields from different nuclides, the decay heat is intuitively different for each of these cases.

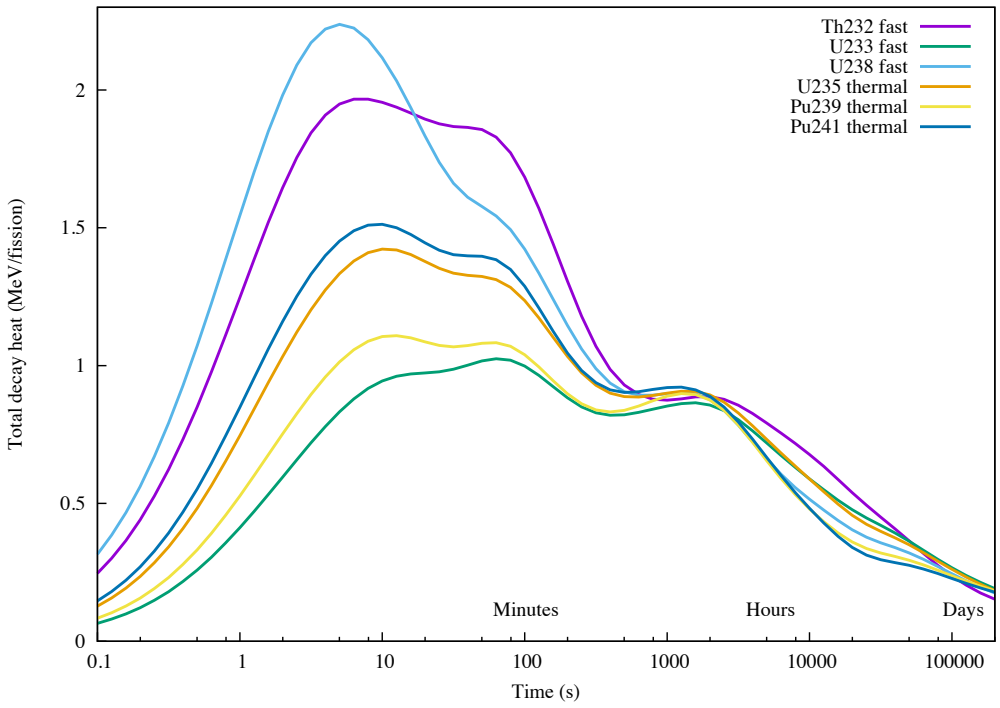

Figure 5: Comparison of total decay heat burst functions for various nuclides of interest for reactor operation. All simulations use GEF-4.2 nFY with ENDF/B-VII.1 decay data.

Another difference in response is due to the variation in fission yield as a function of incident neutron energy. The well-known asymmetry in the mass of daughters of binary fission is not a universal feature of fission. The asymmetric distributions of fission products for well-known fissiles become considerably more broad at higher neutron energy. As a result, the dominant nuclides for some thermal response function, which are the most likely fission products, will have less production in exchange for increased production from the 'shoulders' of the fission yield distribution. The general change in the response function will be a decrease across all time periods, potentially with some new response from a previously minor nuclide. This can be seen in the neutron-energy-dependent decay heat curves from fission pulses calculated with GEF-4.2 fission yields. Two examples are shown in Figures 6 and 7: ^{235}U and ^{239}Pu, respectively.

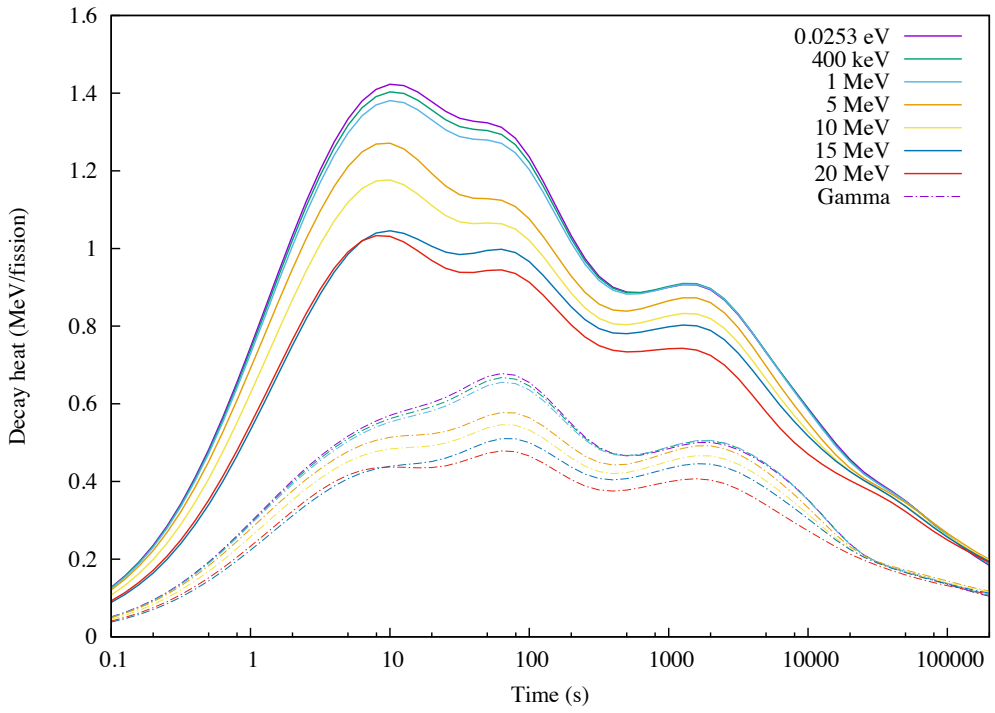

Figure 6: Comparison of total decay heat burst functions of ^{235}U for various neutron energies. All simulations use GEF-4.2 nFY with ENDF/B-VII.1 decay data.

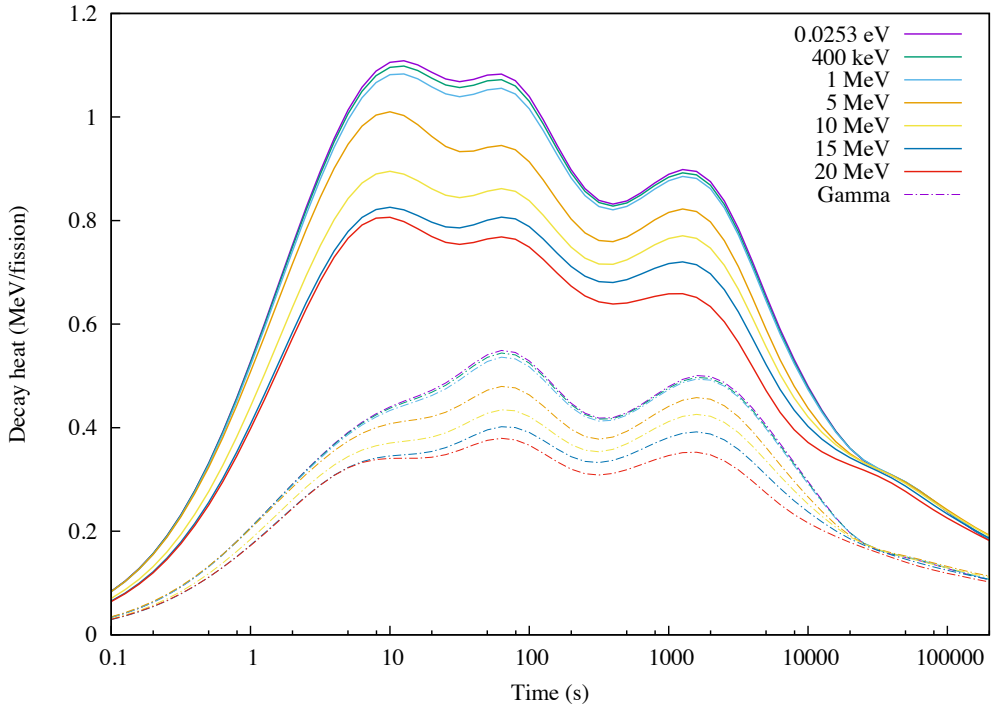

Figure 7: Comparison of total decay heat burst functions of ^{239}Pu for various neutron energies. All simulations use GEF-4.2 nFY with ENDF/B-VII.1 decay data.

The decay heat curves demonstrate a clear trend of decreasing decay heat with increasing

neutron energy, but also advertise an impressive quality of the GEF-4.2 fission yield library: a wealth of data for 49 different energies ranging from thermal, through various fast energies up to 20 MeV. More importantly, the GEF code can be used to generate fission yields for any energy of interest (subject to model applicability). In comparison, the JEFF-3.1.1 fission yield file for ^{239}Pu has only two entries, 0.0253 eV and 400 keV, as seen in Figure 8. While the lack of higher-energy data may not impress some reactor physicists, it should be stressed that standard LWR neutron spectra extend well beyond 10 MeV and for certain regimes 400 keV files will simply not satisfy the simulation requirements.

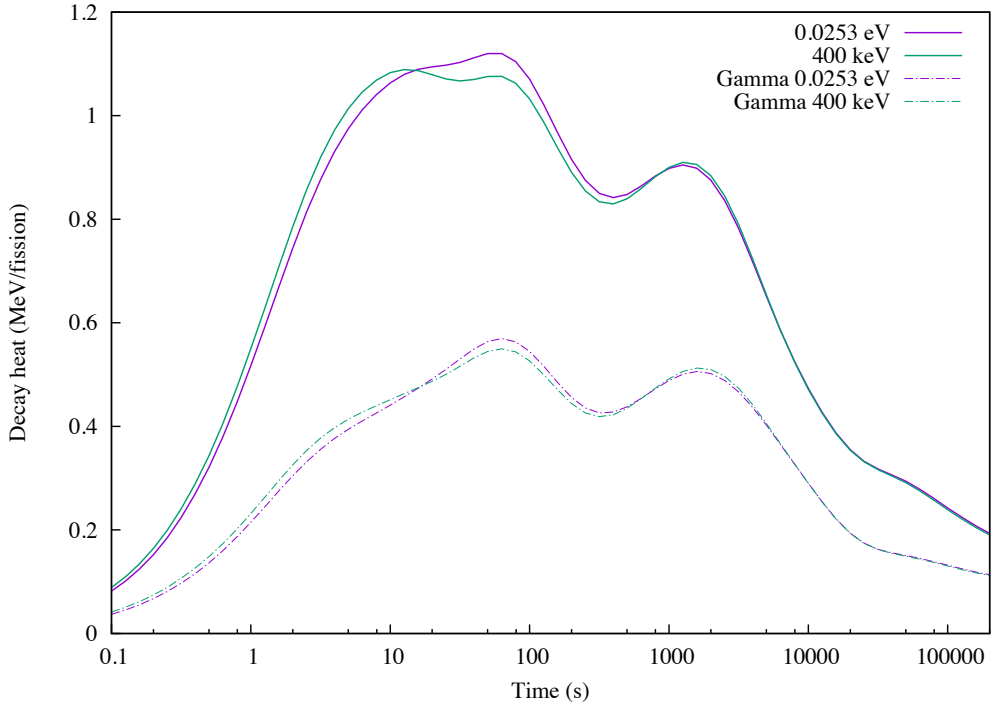

Figure 8: Comparison of total decay heat burst functions of ^{239}Pu for all energies within the JEFF-3.1.1 nFY file.

4.2 FISPACT-II inputs

To faithfully simulate the theoretical fission pulse decay heat a relatively simple input file is required for FISPACT-II, where the majority of the details are merely present to *turn off* features of the code which would result in a more physical simulation. The required inputs to initialise fission calculations are the fission keywords:

```
USEFISSION
FUEL 1
   U235 1.0E+24
FISYIELD  1 U235
FISCHOOSE 1 U235
```

In this case fission simulation has been included with the first line and a specific number of nuclides have been selected with the following two. In order to isolate *only* one nuclide

for fission in a simulation, the FISYIELD and FISCHOOSE keywords can be included to prohibit the fission of any other nuclides in the inventory and pathway calculations, respectively. While one fuel may have been selected initially, other fissile nuclides will be produced through transmutation/decay reactions which should be ignored to isolate only the target fission decay heat. In addition, the decay heat from capture products and the fuel itself (essential for short-lived fissiles, such as Pu238) can be 'turned off' using additional input keywords:

- Removal of capture cross-section using the OVER and ACROSS keywords:

```
OVER U238
  ACROSS U239 0.0
```

- Elimination of parent decay heat using the OVER and ALAM keywords:

```
OVER Pu238
  ALAM 1E30 5
```

In order to verify the accuracy of the simulations, convergence tests of the simulations were run in order to find the strict numerical tolerance settings required. Both absolute and relative tolerances were then tightened by an additional three orders-of-magnitude for all results shown in the report. To prevent decay of short-lived fission products which would affect the earliest cooling times, a 1 μs irradiation of 1E22 n/s was used. In order to isolate the the fission yield file entry for one specific energy, a flux was used which contained only one non-zero entry in the energy group of the desired 0.0253 eV or 400 keV. In all cases, the independent fission yield files were used for pulses and other finite irradiations, although cumulative yields may be read by FISPACT-II using the CUMFYLD keyword.

For inventory calculations, it should be noted that at any given cooling time between 10-5000 s an individual nuclide rarely contributes more than 10% of the total decay heat. Typically, and for the case of U235 in particular, in the first 1000 s the most dominant nuclide comprises 5-7% of the total heat, while each of the top 50 nuclides contribute at least 0.5%. As the sample continues to cool fewer nuclides are present and the heat is concentrated in a smaller set, but generally for times less than 1E6 s a fairly large inventory of 20+ nuclides is required to capture 90% of the total heat. To follow the complete inventory after irradiation, the keywords

```
MIND 1.0
SORTDOMINANT 200 200
```

can be used to retain all nuclides with at least 1 atom, as well as tabulate the top 200 contributors to decay heat. These values may not be necessary for all simulations, and strict tolerance settings must be included to prevent inaccuracies in the modelling of small nuclide concentrations, but in principle all nuclides and decay chains included in the fission yield and decay files can be tracked by FISPACT-II. For the inventory simulations and decay data library comparisons, this is precisely what has been done.

5 Comparison of simulations with experimental data

While the number of fuel isotopes considered is relatively small, irradiation durations and measurement techniques vary over the experimental dataset. This section is organised first by nuclide and all the FISPACT-II simulations for all experiments included in Table 2 are displayed. In each simulation, a variety of nuclear data files have been used to demonstrate the range of values found by varying fission yield and decay data. It is essential to keep in mind that the simulations rely upon data and software working in concert, and that EASY-II is distributed with multiple data libraries precisely so that any user has complete freedom to select whichever they find most suitable. While any fission yield and decay file could be paired, only matching ENDF/B, JENDL and JEFF nFY+decay simulations are shown. A fourth combination using GEF-4.2 nFY with the UKDD-12 library is also included.

Several non-pulse experiments have been carried out with irradiations ranging from a few seconds to several months. While the reconstructed equivalent pulse experimental data is derived from irradiations of up to a few hundred seconds, the non-pulse data explore a variety of fundamentally different decay heat scenarios – for example seconds after a week-long irradiation. While the pulse simulations provide a more robust method of verifying the simulation capabilities of the code and nuclear data system, the non-pulse simulations offer an opportunity to validate the system against application-relevant results important to code users.

All thermal and fast simulations use mono-energetic 0.0253 eV and 400 keV pulses, respectively, to isolate one entry of the nFY files. Partial decay heat curves are depicted using dashed lines whenever they appear alongside the total.

5.1 ^{235}U decay heat

As the primary fuel for nearly every operating nuclear fission plant, ^{235}U has been the subject of the most numerous decay heat experiments which have been used to produce several decay heat standards for reactor operation and many post-irradiation fuel applications. This section includes the Tobias decay heat compilation for comparison with the simulated thermal pulse, as well as the data from Dickens *et al* and Schier *et al*, which show non-negligible differences at several cooling times. Note that the UM Lowell data includes beta and gamma heat measurements made at different cooling times, so that no precise totals can be presented without some mixing/modification of the data, which is not done in this report. This is particularly noticeable at cooling times less than 2.7s, where only the Tobias meta-analysis data, with relatively large uncertainty, are available. This is followed by a simulation comparison with the fast reactor decay heat results from YAYOI reactor due to Akiyama *et al*, which is performed using 400 keV fission yields.

The non-pulse simulations include a comparison with calorimetric measurements made by Baumung *et al* from a 200 second irradiation and Yarnell from a 20000 second irradiation. Both of these are considered independently and are simulated with the same data combinations as with the pulses. These are followed by a series of comparisons against radiation-specific comparisons of experimental datasets including a wide range of irradiation durations.

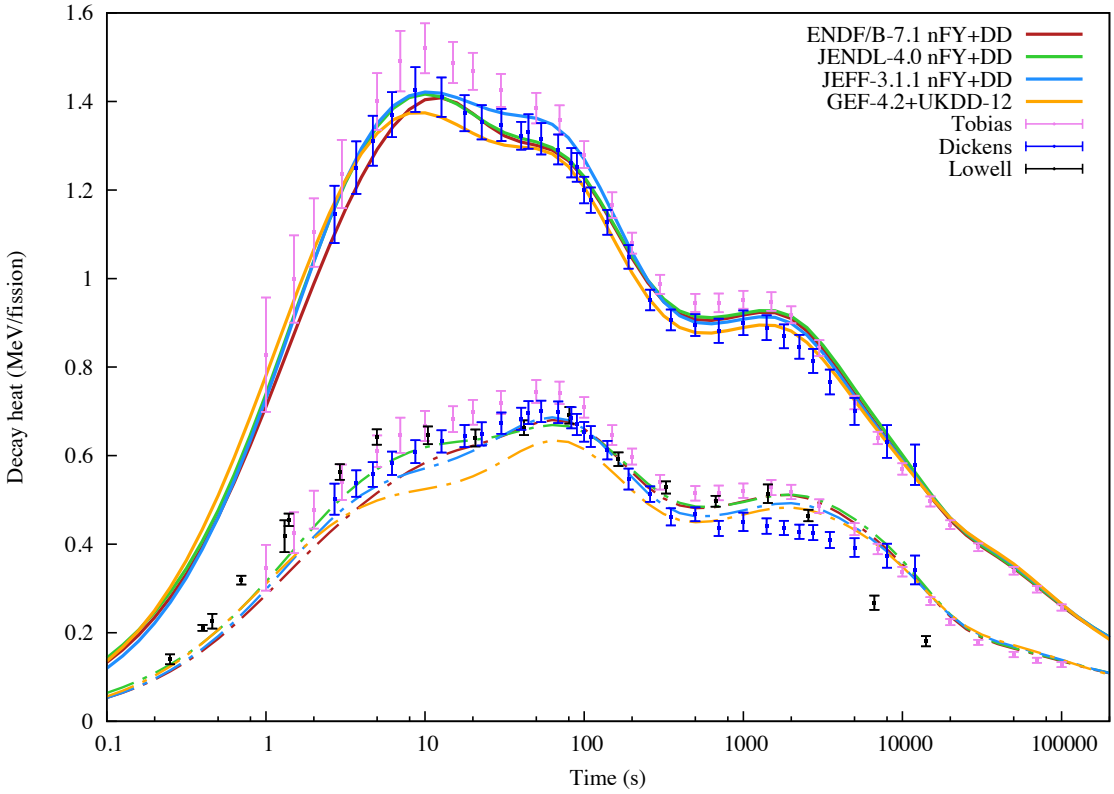

Figure 9: Total (solid) and gamma (dash) decay heat from thermal pulse on ^{235}U.

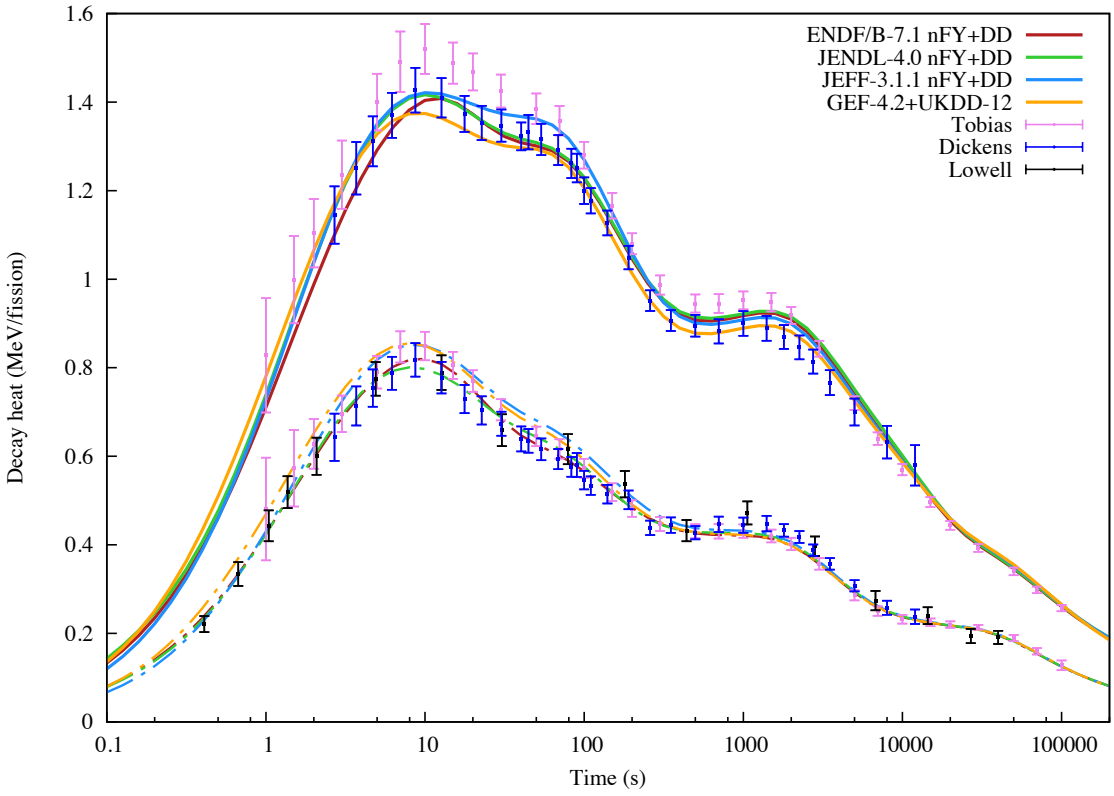

Figure 10: Total (solid) and beta (dash) decay heat from thermal pulse on ^{235}U.

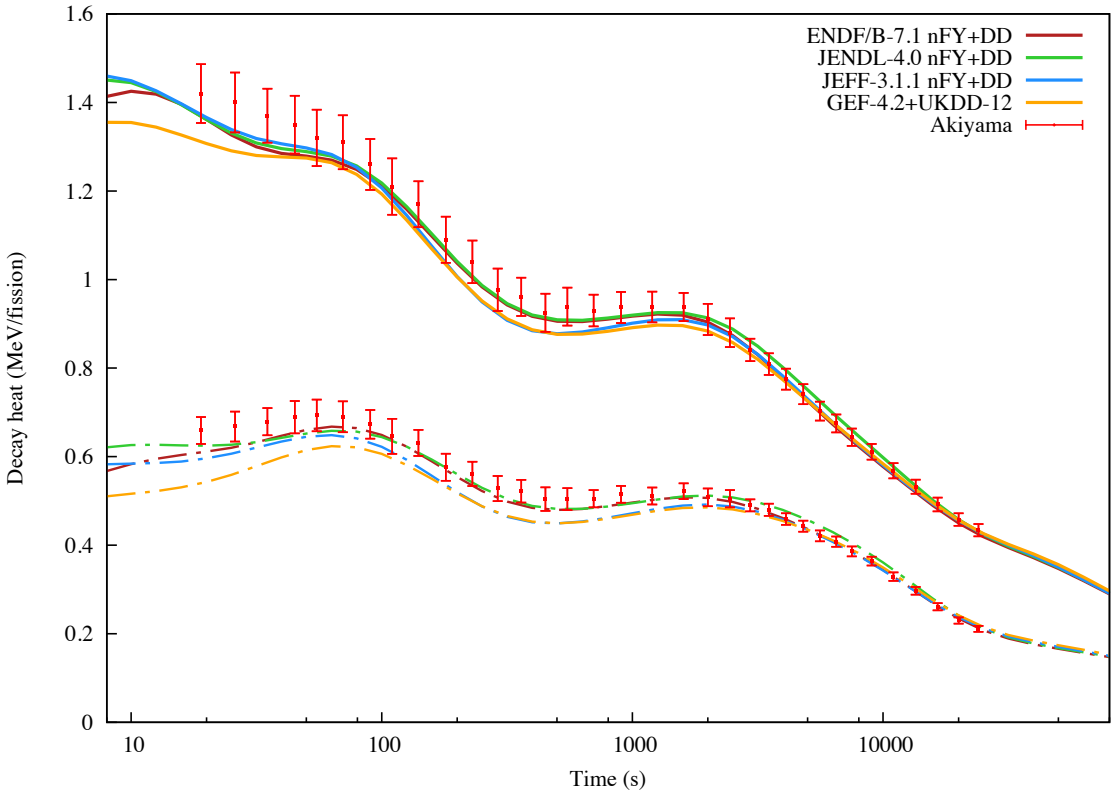

Figure 11: Total (solid) and gamma (dash) decay heat from fast pulse on ^{235}U.

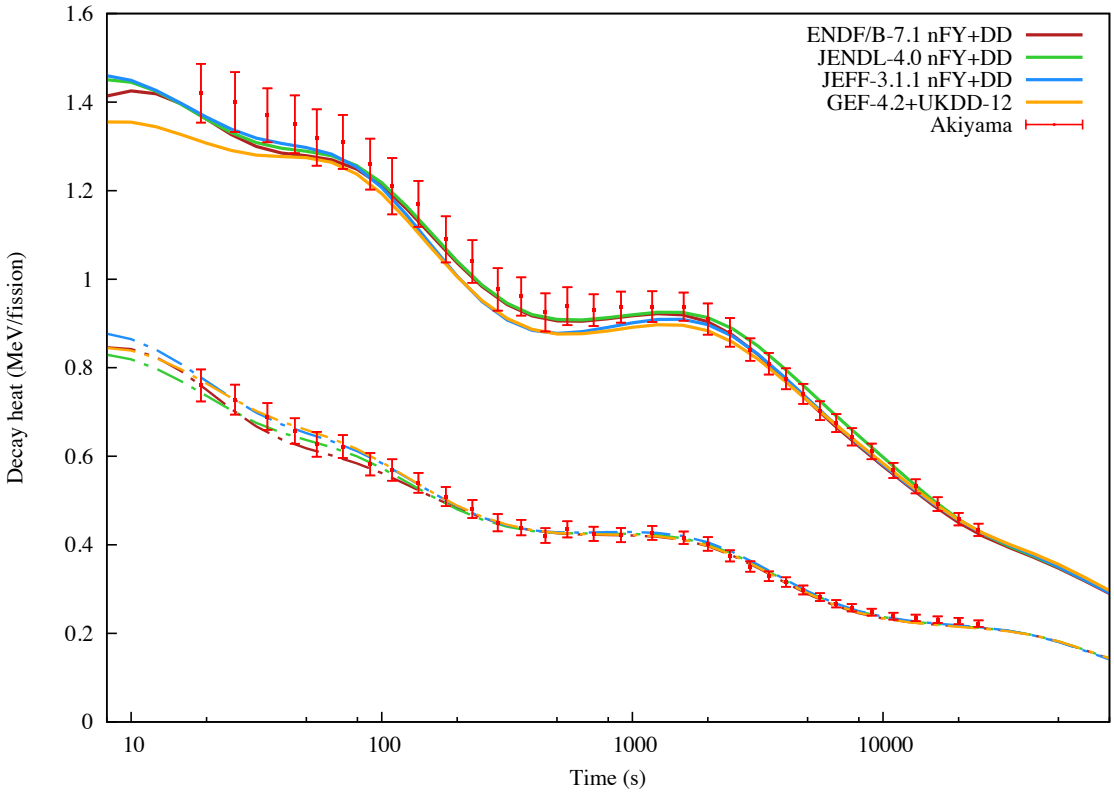

Figure 12: Total (solid) and beta (dash) decay heat from fast pulse on ^{235}U.

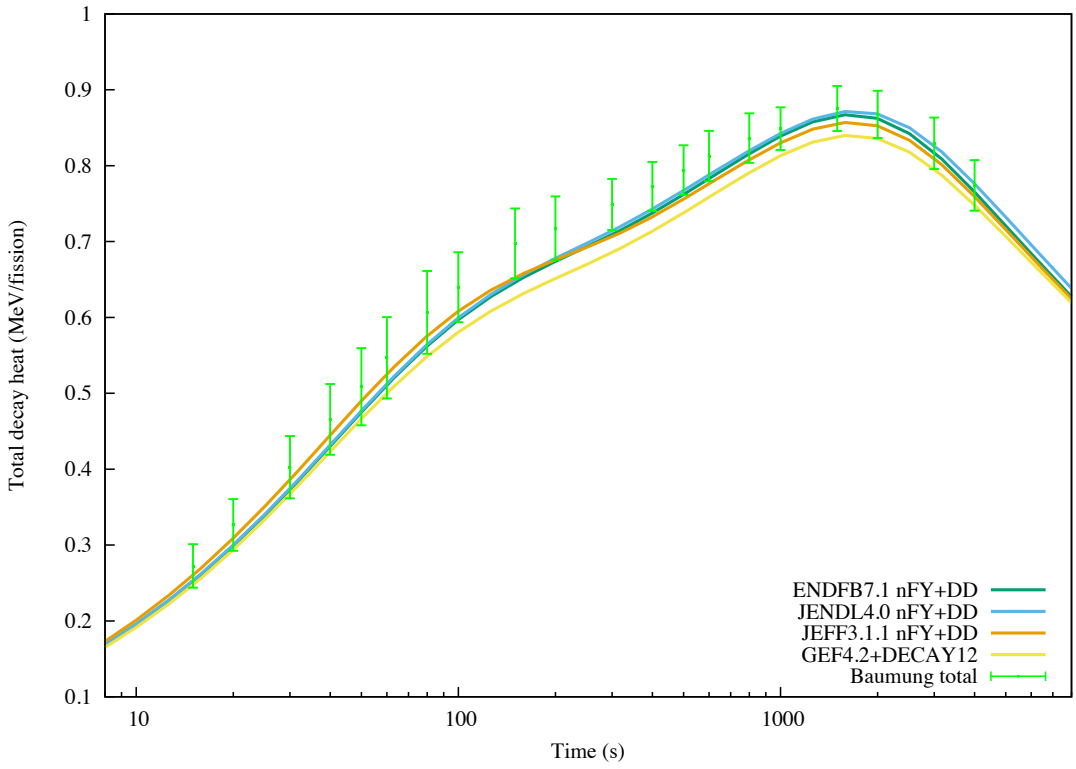

Figure 13: Total decay heat from thermal 200s irradiation of ^{235}U.

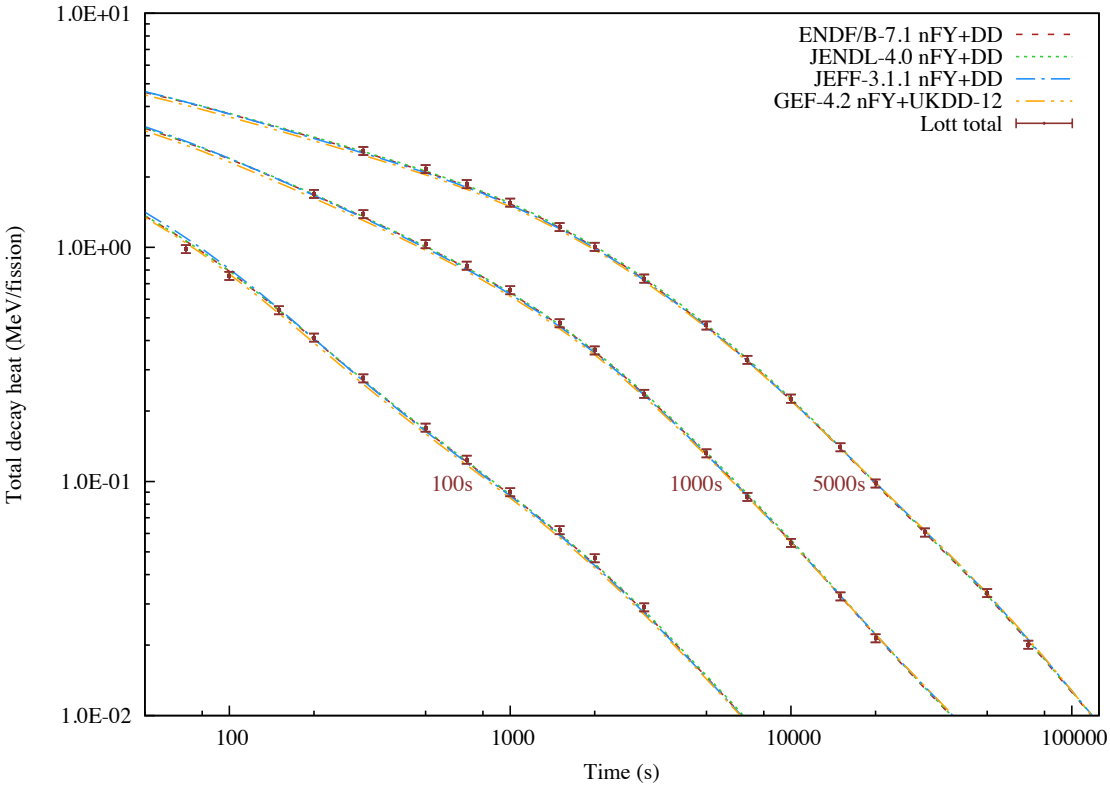

Figure 14: Total decay heat from 100-5000 s irradiations of ^{235}U.

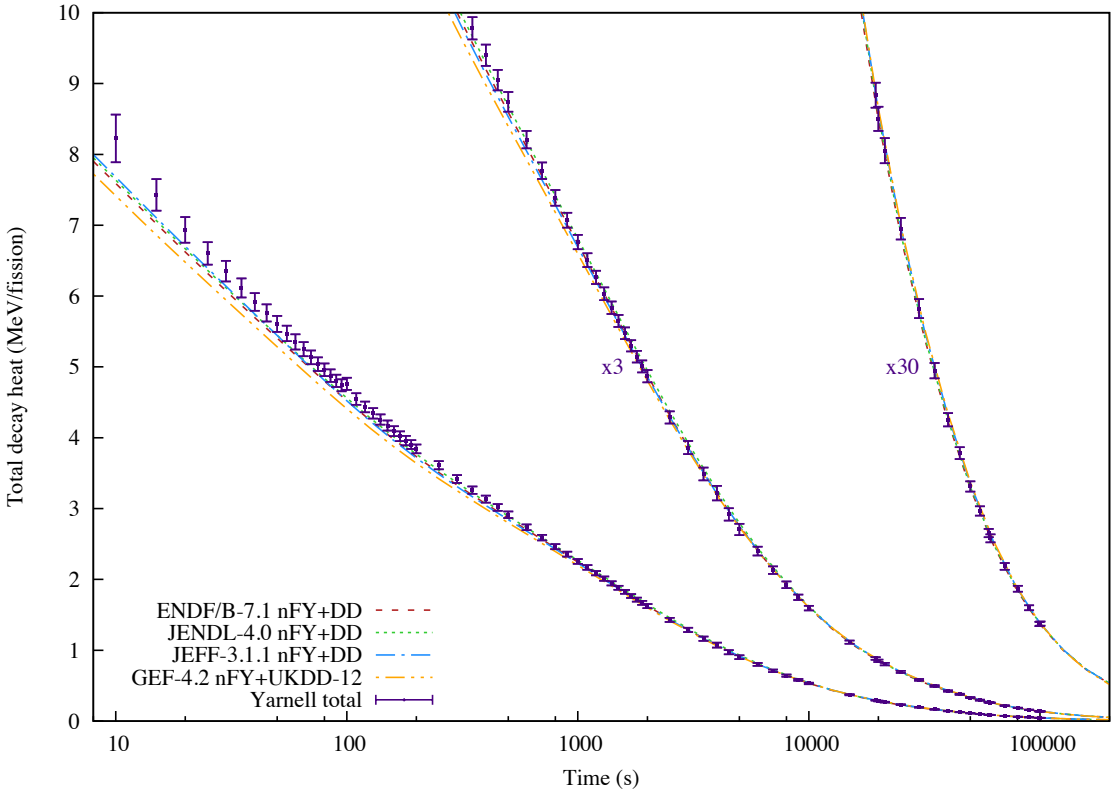

Figure 15: Total decay heat from thermal 2E4s irradiation of ^{235}U.

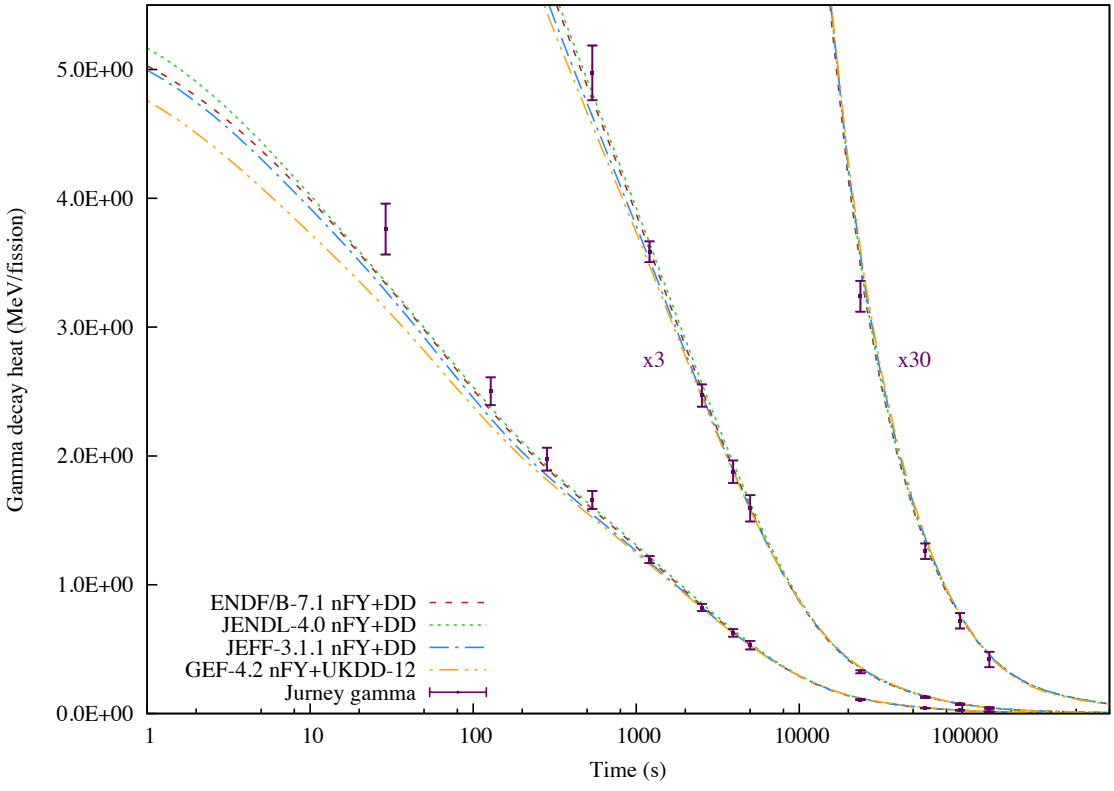

Figure 16: Gamma decay heat from thermal 2E4s irradiation of ^{235}U.

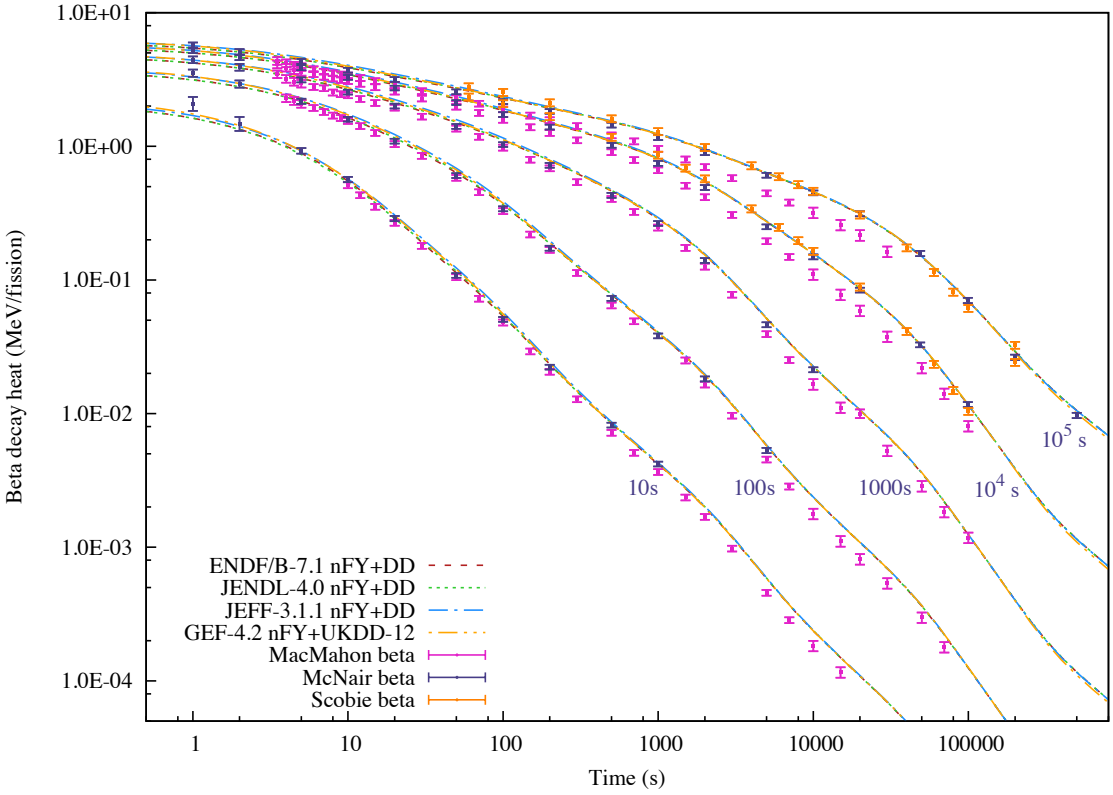

Figure 17: Beta decay heat from 10-100000 s irradiations of ^{235}U.

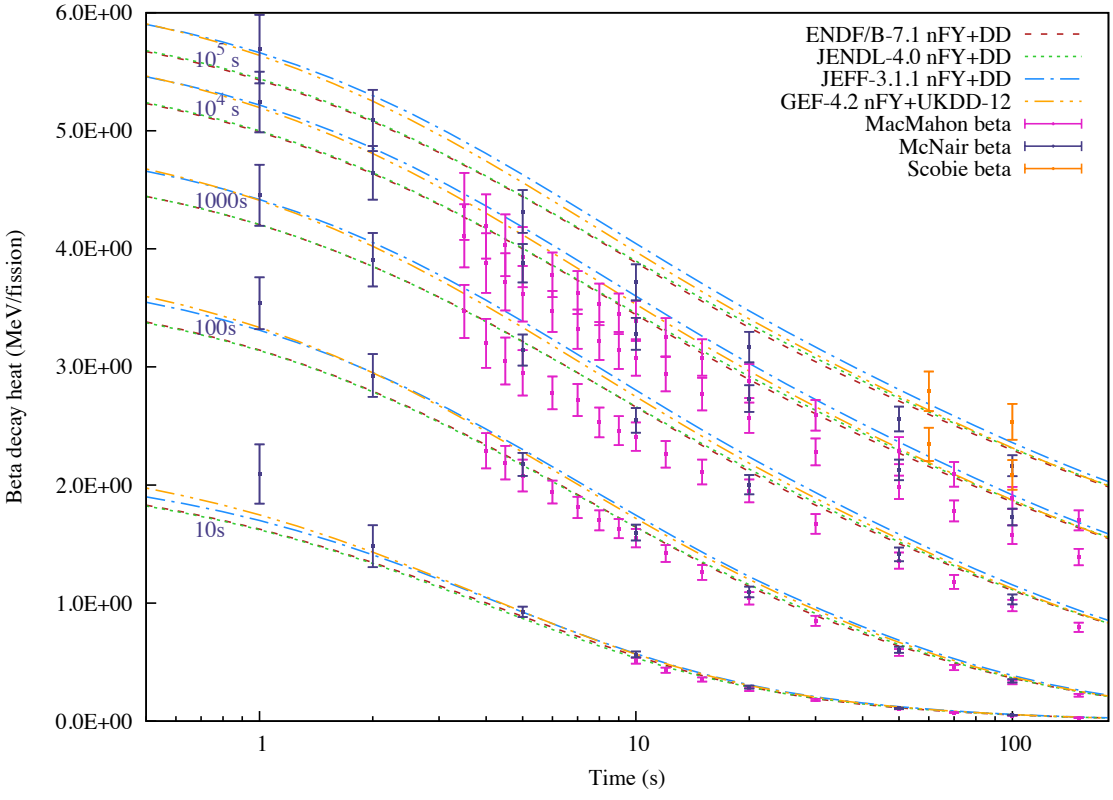

Figure 18: Beta decay heat from 10-100000 s irradiations of ^{235}U for <200 s cooling.

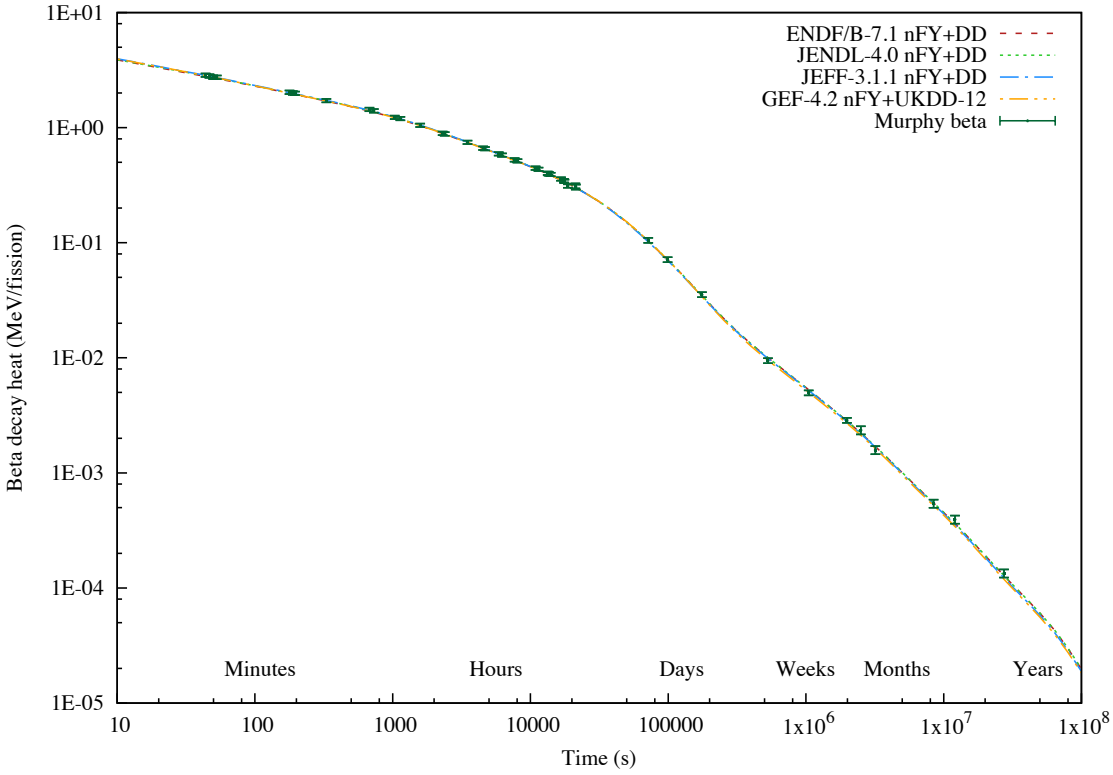

Figure 19: Beta decay heat from 1E5s fast irradiation of ^{235}U.

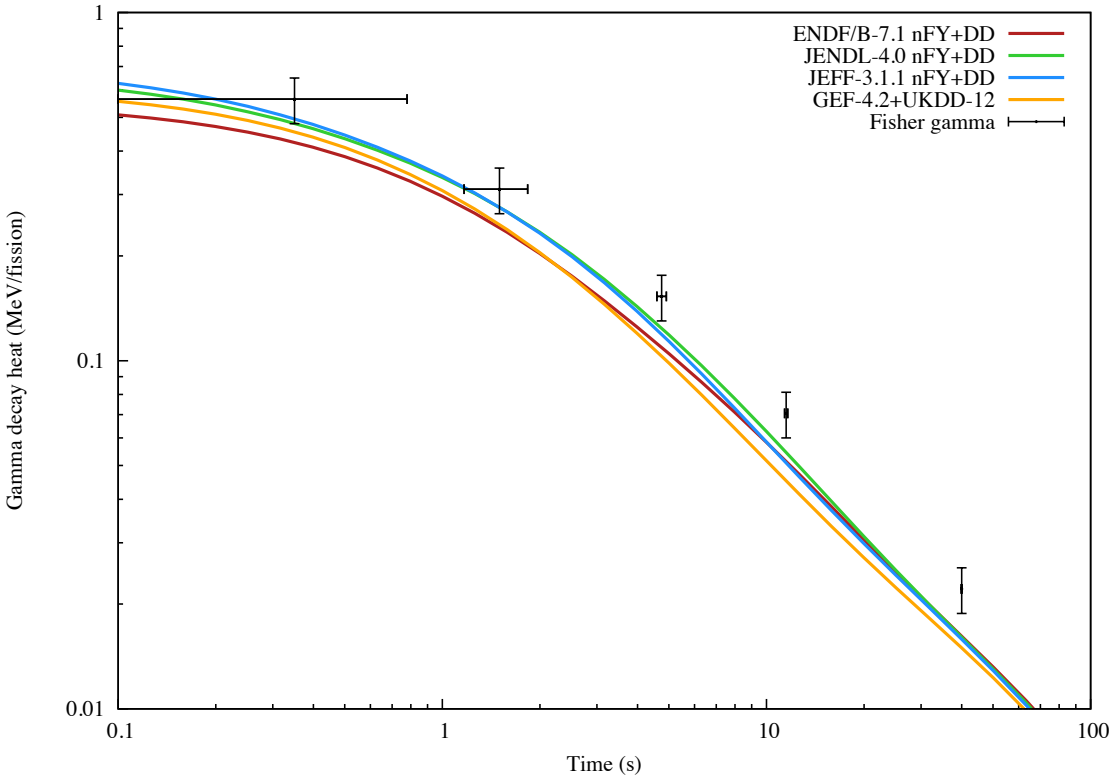

Figure 20: Gamma decay heat from <0.1s irradiations of ^{235}U.

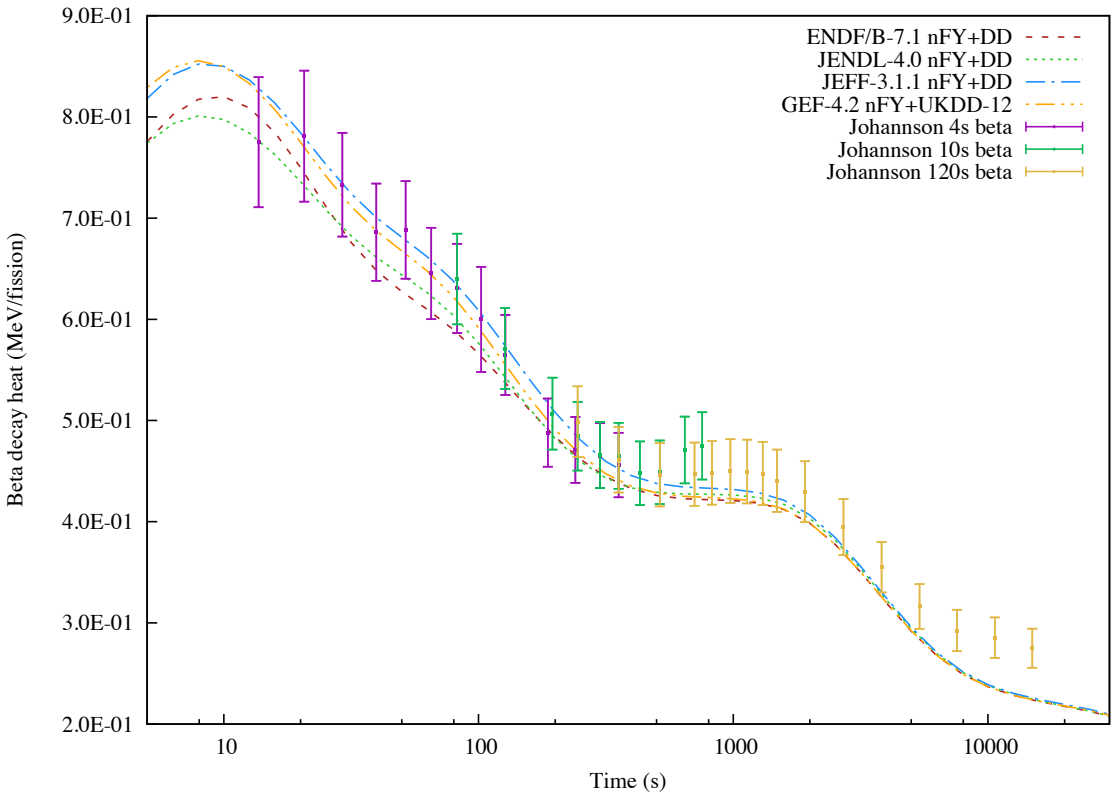

Figure 21: Beta decay heat from 120s irradiation of ^{235}U.

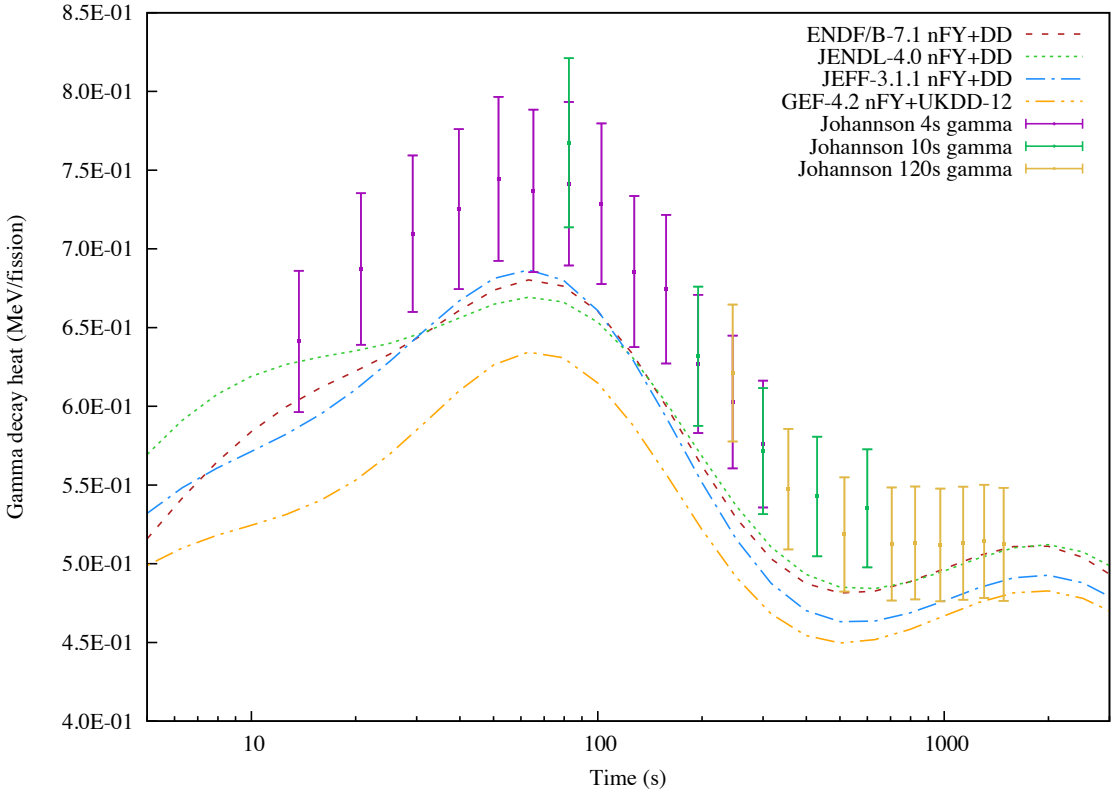

Figure 22: Gamma decay heat from 4-120s irradiations of ^{235}U.

While these simulations demonstrate the ability to calculate complex decay heat responses within the experimental uncertainty for most cases, a few general observations from these comparisons must be clear:

- The most highly regarded experimental data are not in agreement for several cooling times with the most well-known and ubiquitous fissile nuclide
- Consistent discrepancy between gamma heat of experiments and simulation with differing nuclear data for nearly all cooling times
- Total heat simulation and experiment agreement better than spectroscopic heat, suggesting faults with decay data β/γ feeds

The various experiments shown are clearly of different standards and many error estimates should be reconsidered – for example with the beta measurements following longer irradiations. The gamma heat for short cooling times appears to be significantly underpredicted in all relevant experiments, which employ a variety of spectra and experimental techniques.

These substantial differences between simulations with varying nuclear data libraries points toward errors in nuclear data files which can be probed using FISPACT-II. As seen in both the thermal and fast pulse simulations, cooling times between a few seconds and one minute include intriguingly different results including multiple 'cross-overs' between different decay heat functions. This cooling time, as well as that around 1000 seconds, are explored in Section 6.

5.2 ^{239}Pu decay heat

Either as a the constituent of mixed-fissile fuels or as the by-product of ^{238}U capture in standard uranium-fuelled reactors, ^{239}Pu substantially contributes to reactor power and decay heat, making this decay heat standard the second in general importance. This section also includes the Tobias thermal pulse compilation, as well as the Dickens *et al* and Schier *et al* data. Again note that the UM Lowell data includes beta and gamma heat measurements made at different cooling times, so that no precise totals can be presented without some mixing/modification of the data, which is not done in this report. This is particularly noticeable at cooling times less than 2.7s, where only the Tobias meta-analysis data, with tremendous uncertainty, are available. Fast fission decay heat from the YAYOI reactor (Akiyama) is also included for a separate pulse comparison.

The non-pulse results of 20000s irradiation calorimetric measurements by Yarnell *et al* are then compared against all four nuclear data simulations, followed by several spectroscopic heat measurements collected by measurement technique, which are compared with results from Dicken *et al*, McNair & Keith, Jurney *et al* and Murphy *et al*.

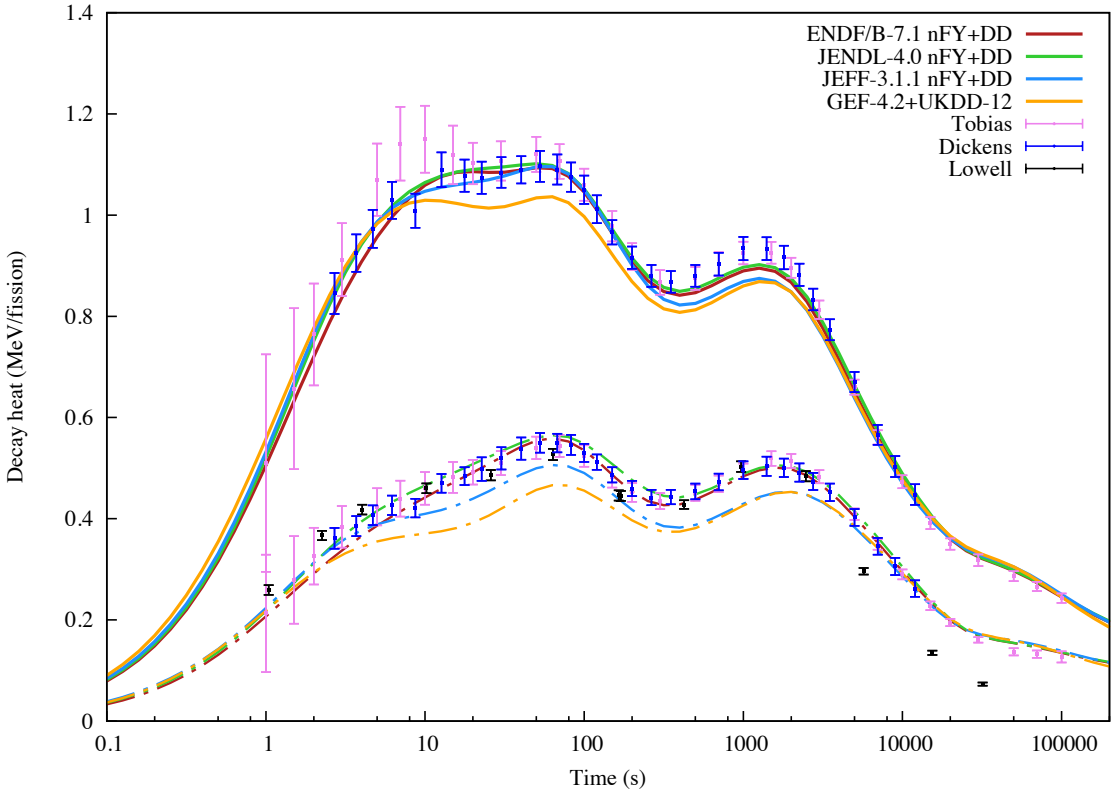

Figure 23: Total (solid) and gamma (dash) decay heat from thermal pulse on ^{239}Pu.

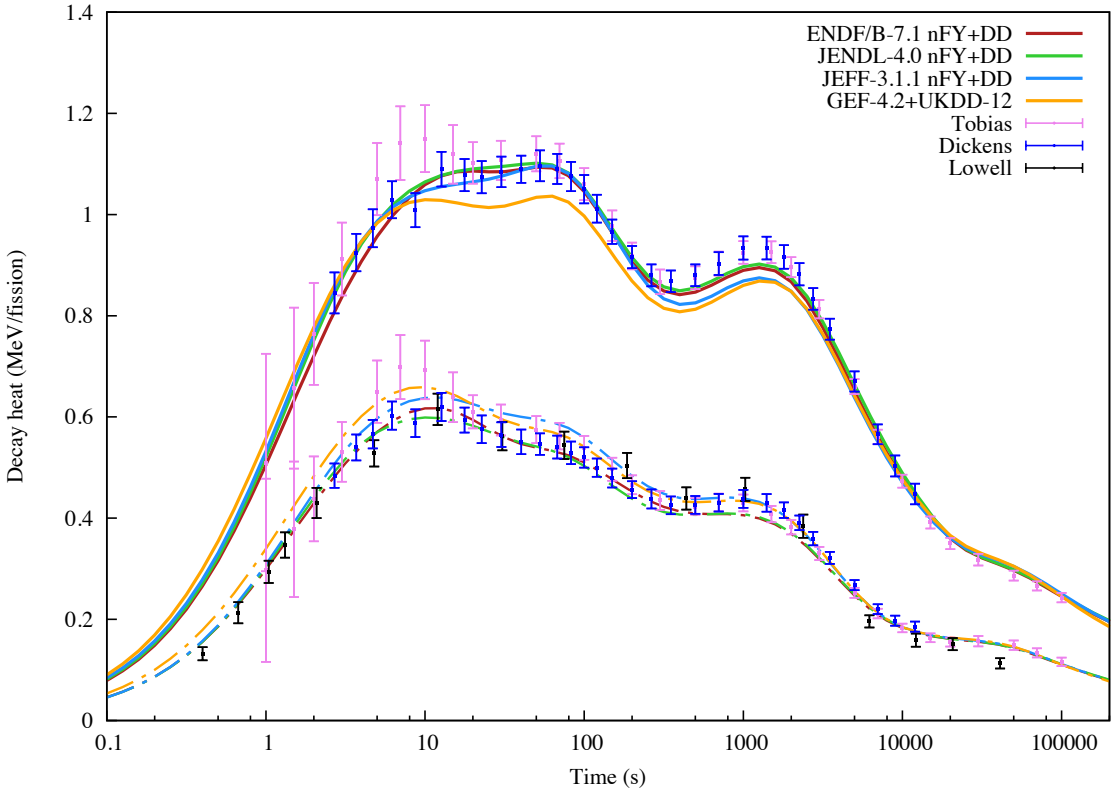

Figure 24: Total (solid) and beta (dash) decay heat from thermal pulse on ^{239}Pu.

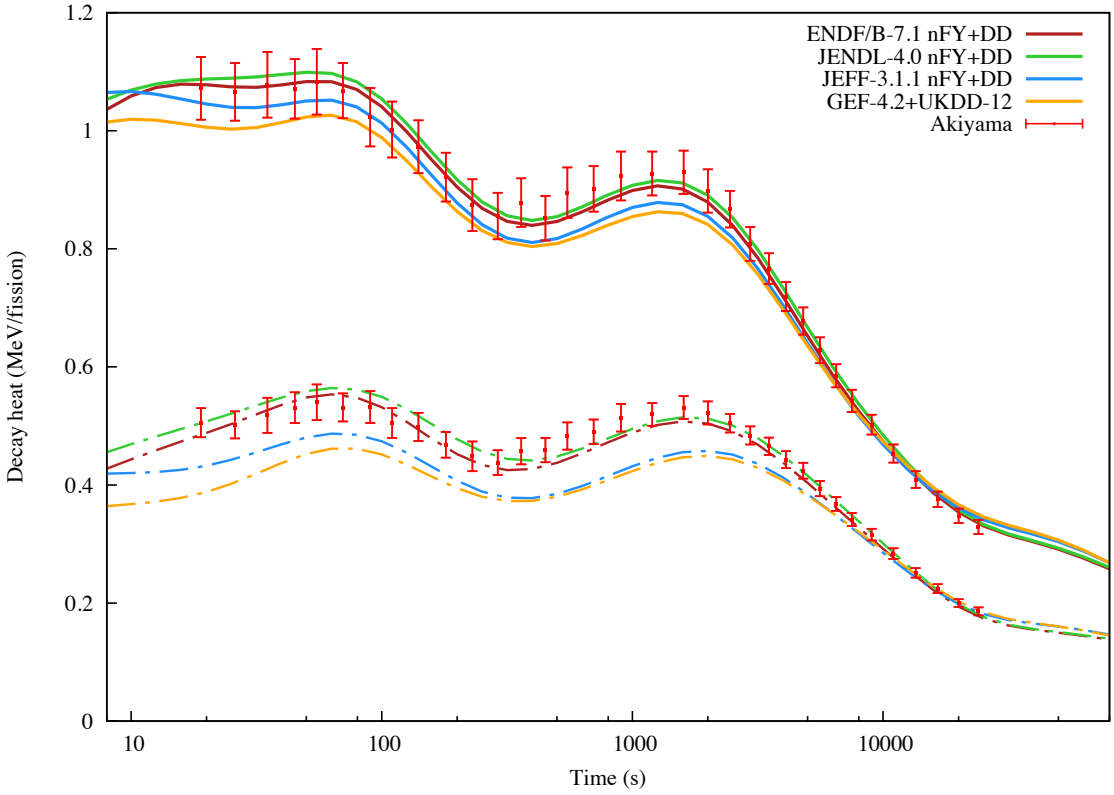

Figure 25: Total (solid) and gamma (dash) decay heat from fast pulse on ^{239}Pu.

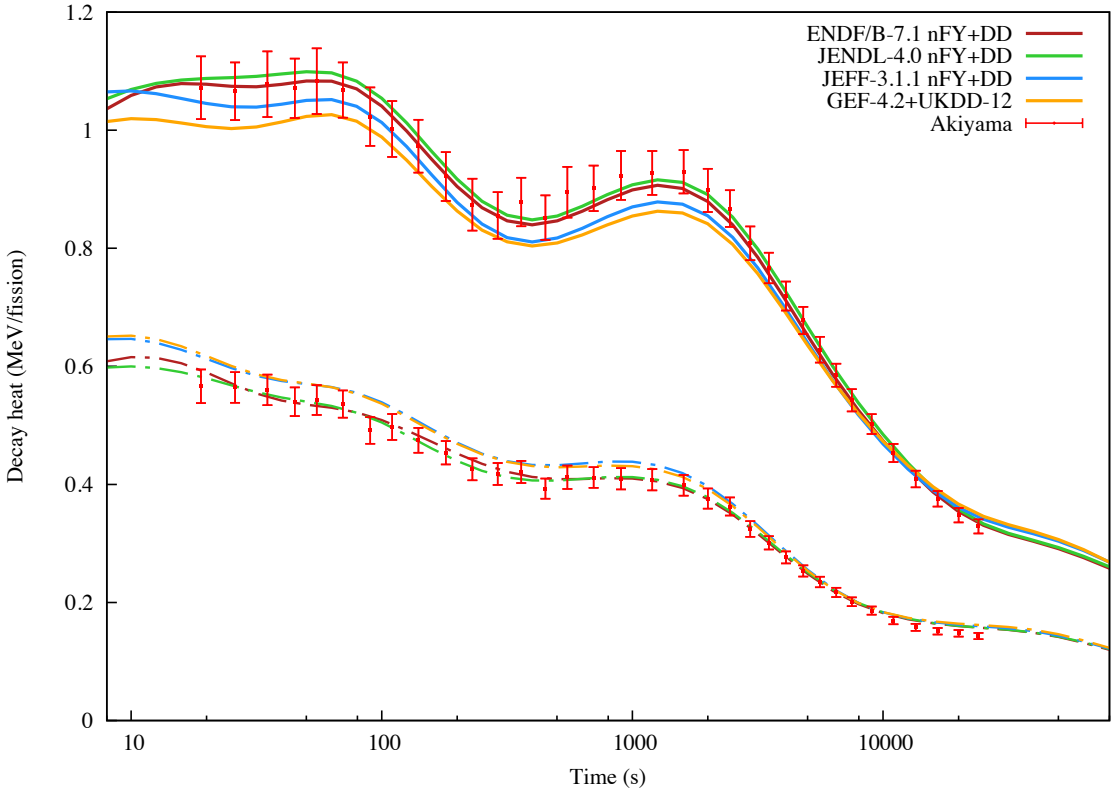

Figure 26: Total (solid) and beta (dash) decay heat from fast pulse on ^{239}Pu.

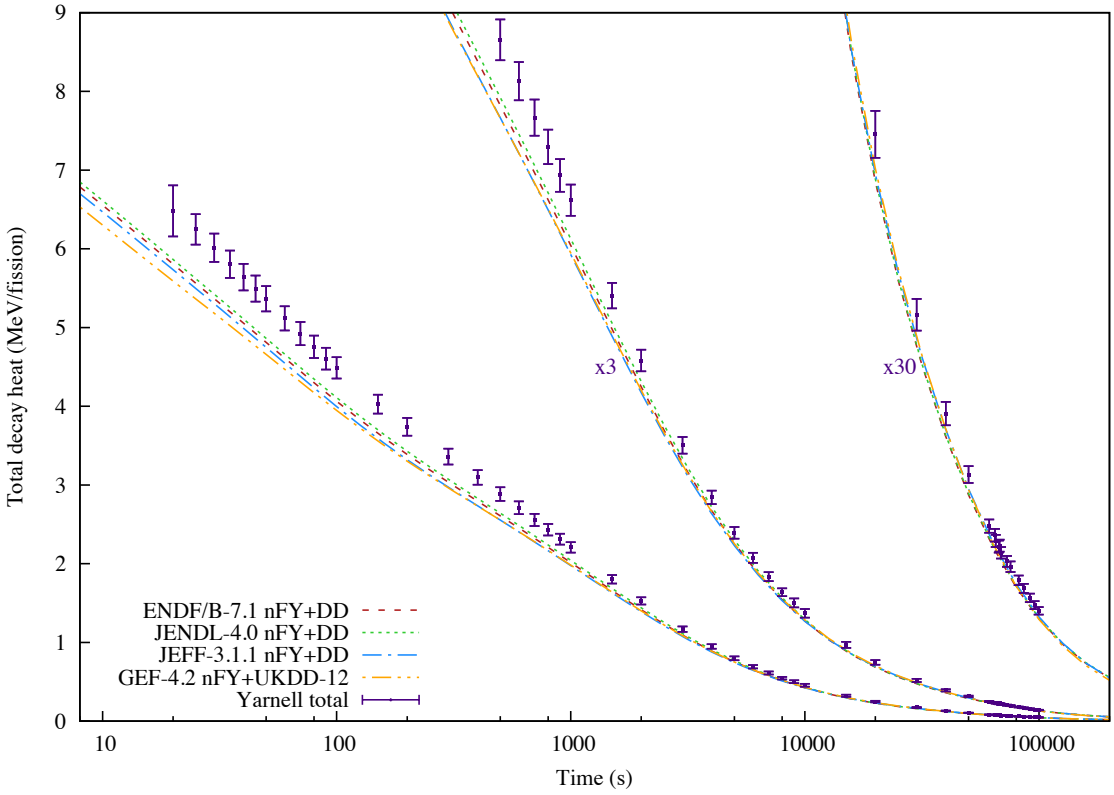

Figure 27: Total decay heat from thermal 2E4s irradiation of ^{239}Pu.

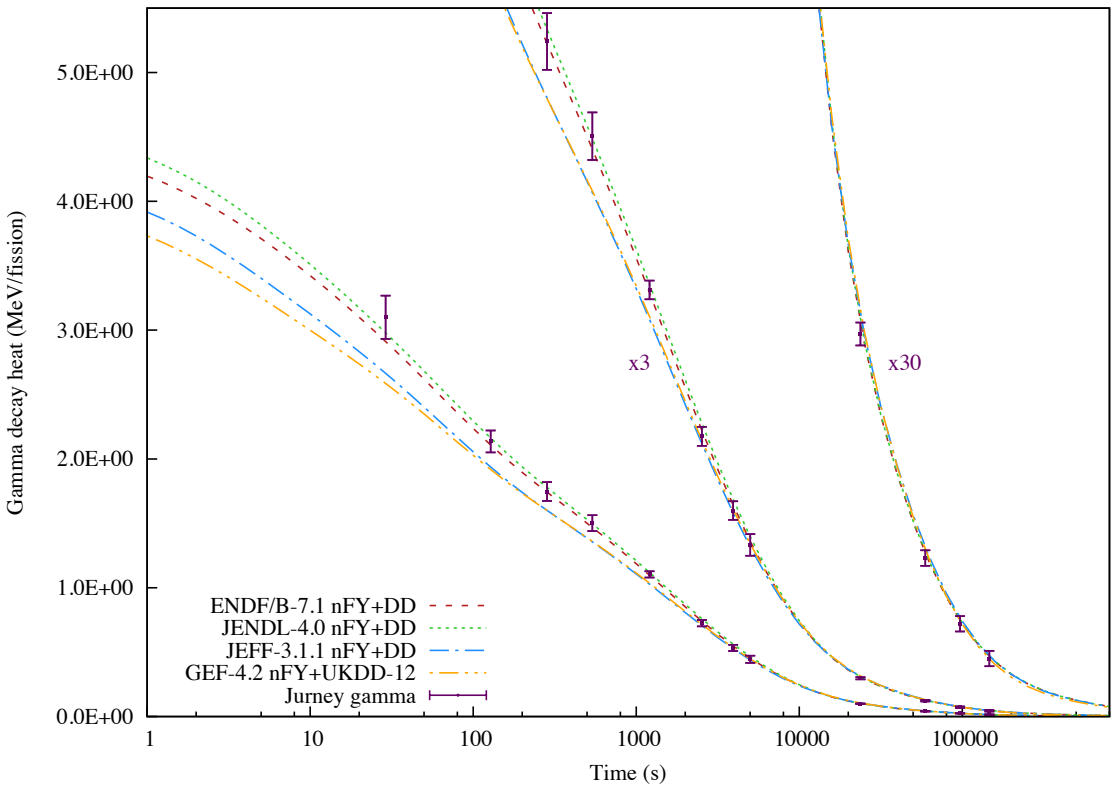

Figure 28: Gamma decay heat from thermal 2E4s irradiation of ^{239}Pu.

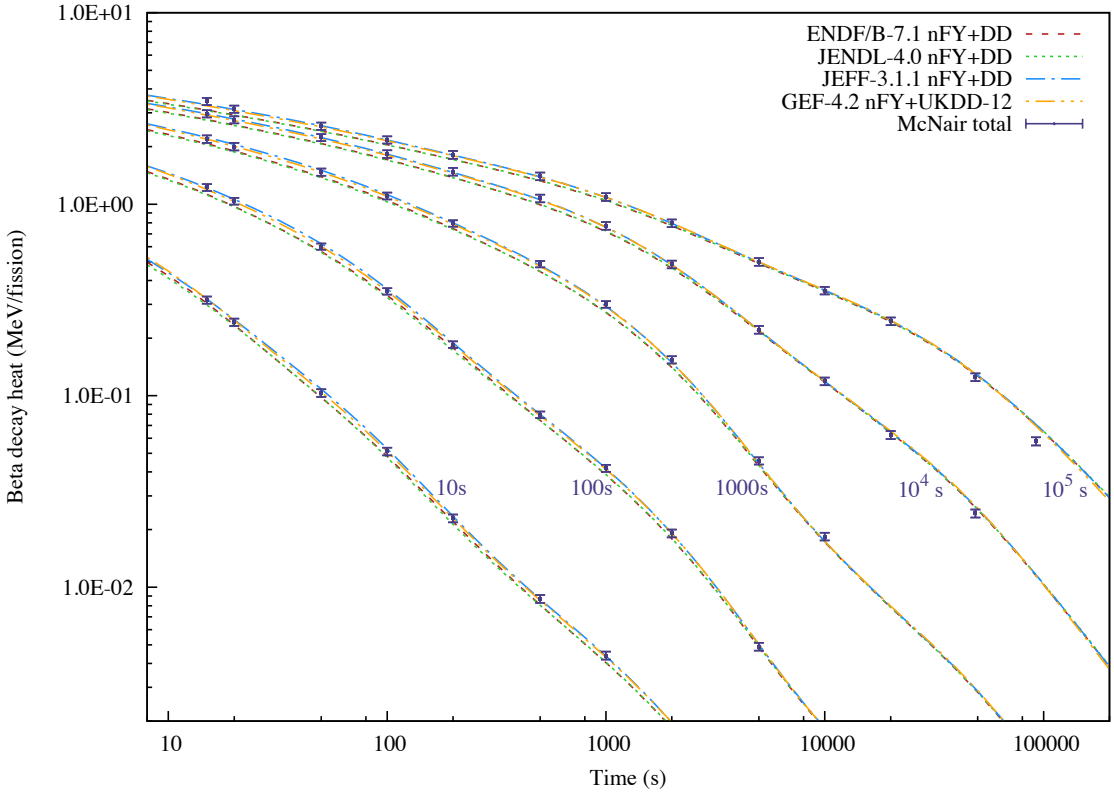

Figure 29: Beta decay heat from 10-100000 s thermal irradiation of ^{239}Pu.

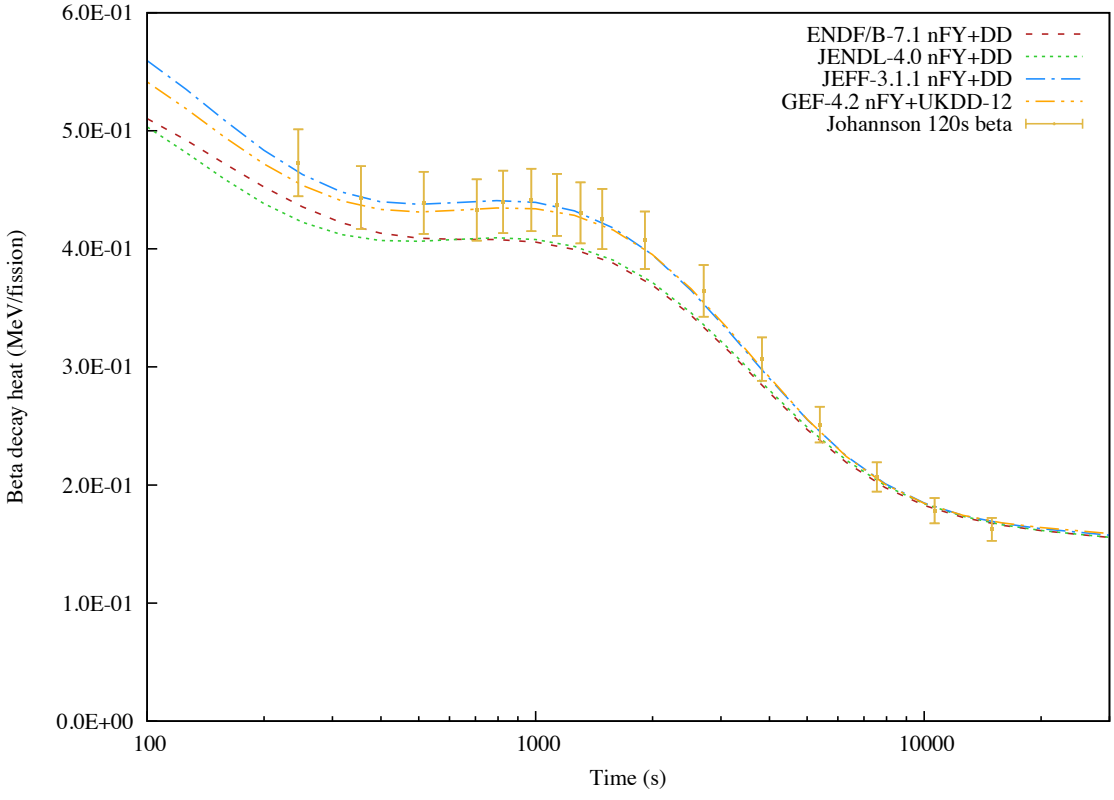

Figure 30: Beta decay heat from 4-120s irradiations of ^{239}Pu.

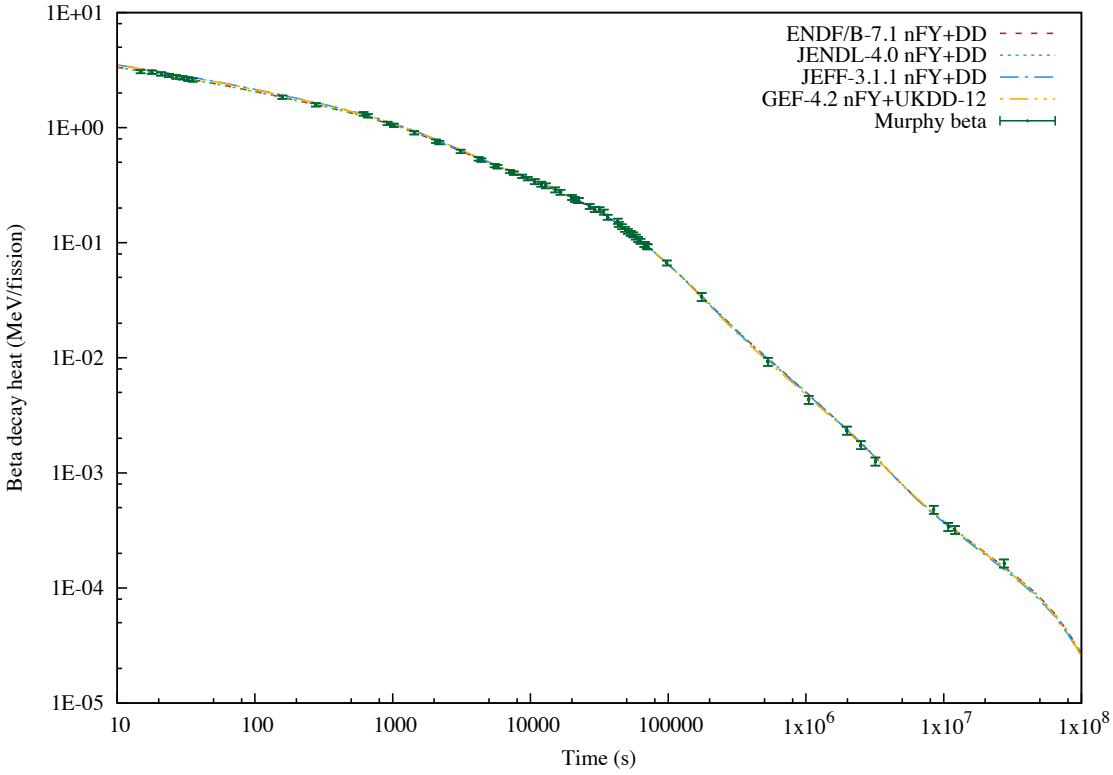

Figure 31: Beta decay heat from 1E5s fast irradiation of ^{239}Pu.

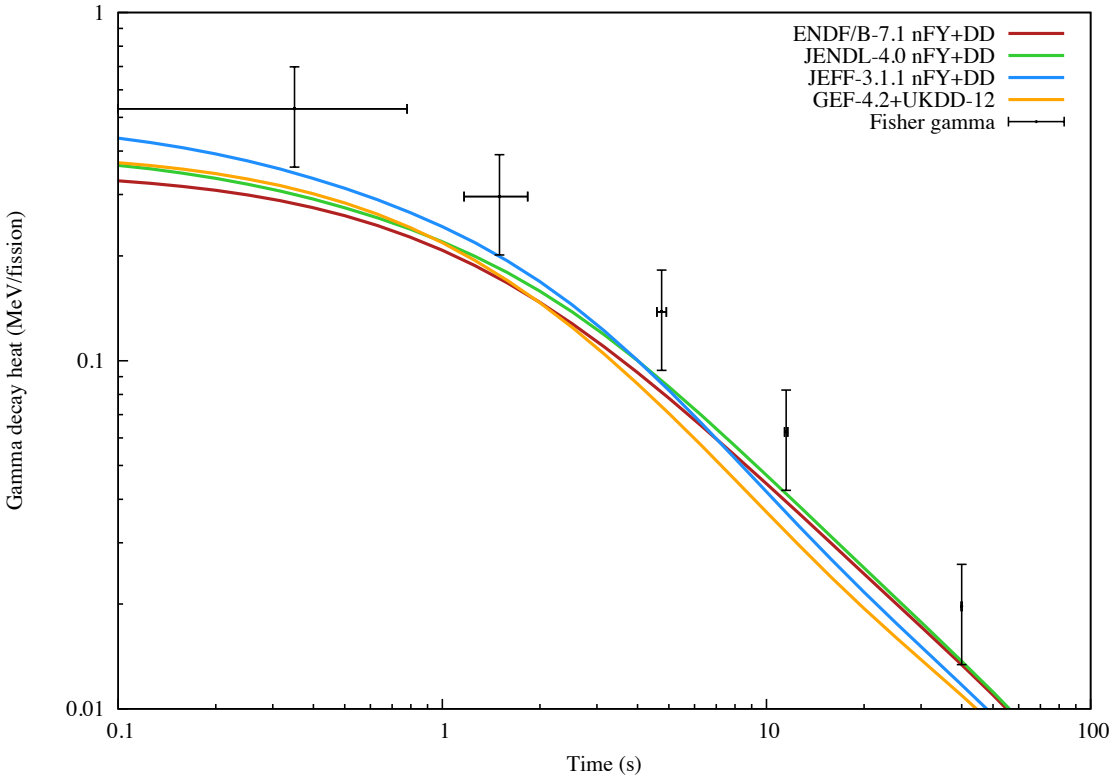

Figure 32: Gamma decay heat from <0.1s irradiations of ^{239}Pu.

As with the U235 simulations, the result of the Pandemonium effect is a general over-prediction of beta heat with under-prediction of gamma heat. The under-prediction for total heat from simulations using GEF-4.2 nFY with UKDD-12 for cooling times between 10-100 s are particularly significant, although general disagreement between experimental data for early cooling times prevents more detailed comparison. Note that the uncertainty from the Tobias meta-analysis reaches values above 50% for the shortest cooling times due to the very few, and relatively poor measurements that were available (UM Lowell data was not available). The Dickens results were in fact the only measurements made with cooling times and irradiations less than 10 s. Any other contribution to the analysis for these cooling times are extrapolations of much longer irradiations and/or heat measurements from cooling times after 10 s.

The fast fission decay heat shows a rather clear separation between simulations made using ENDFB-7.1/JENDL-4.0 and those with JEFF-3.1.1/GEF-4.2/UKDD-12. The gamma heat, in particular, remains 10% lower for a large range of cooling times between 10-1000 s.

5.3 ^{232}Th decay heat

While the uranium/plutonium fuel cycle has remained the worldwide focus for fission power generation, increased interest in a thorium cycle employing fertile ^{232}Th and the capture-product ^{233}U has led to a variety of studies, including the IAEA report on Th/U fuel decay data requirements [39]. The experimental results for this report come from the YAYOI fast reactor and Godiva-II gamma heat measurements made by Akiyama *et al* and Fisher & Engle. Combined with the ^{233}U measurements in the next section, these give some general guidance for decay heat simulation, but the comparisons between simulations using different libraries and information from decay heat simulation of other nuclides provide complementary data.

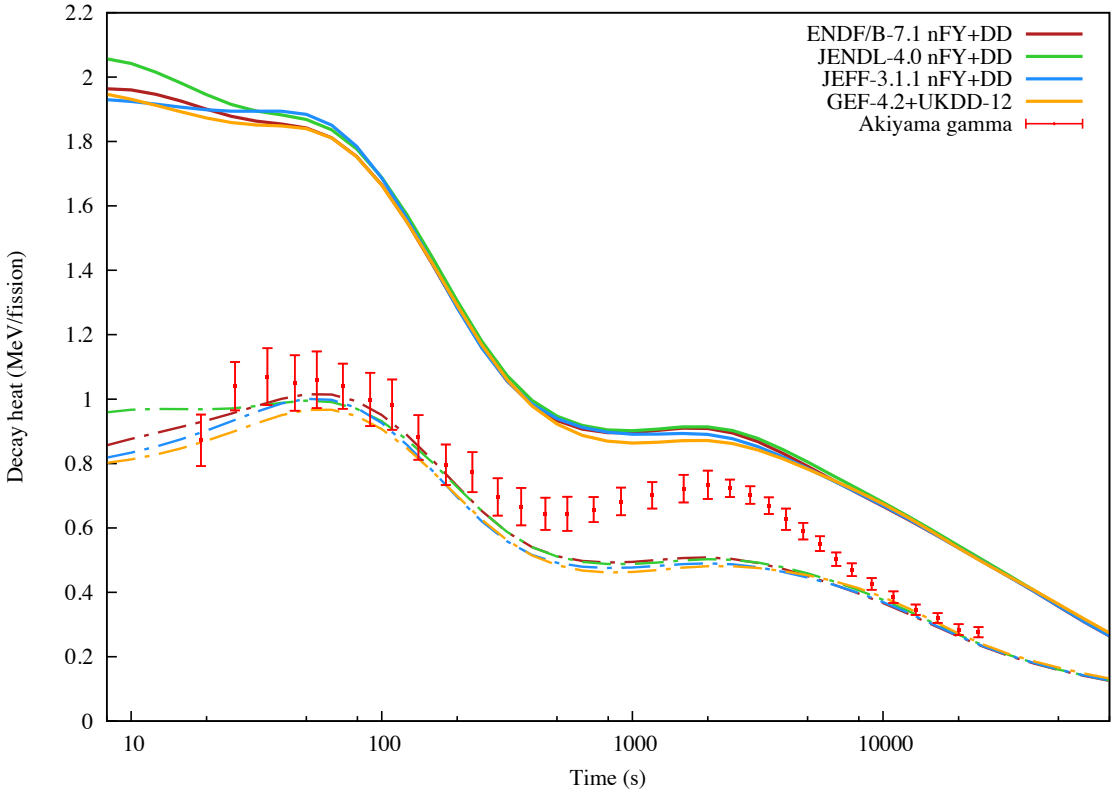

Figure 33: Total (solid) and gamma (dash) decay heat from fast pulse on ^{232}Th.

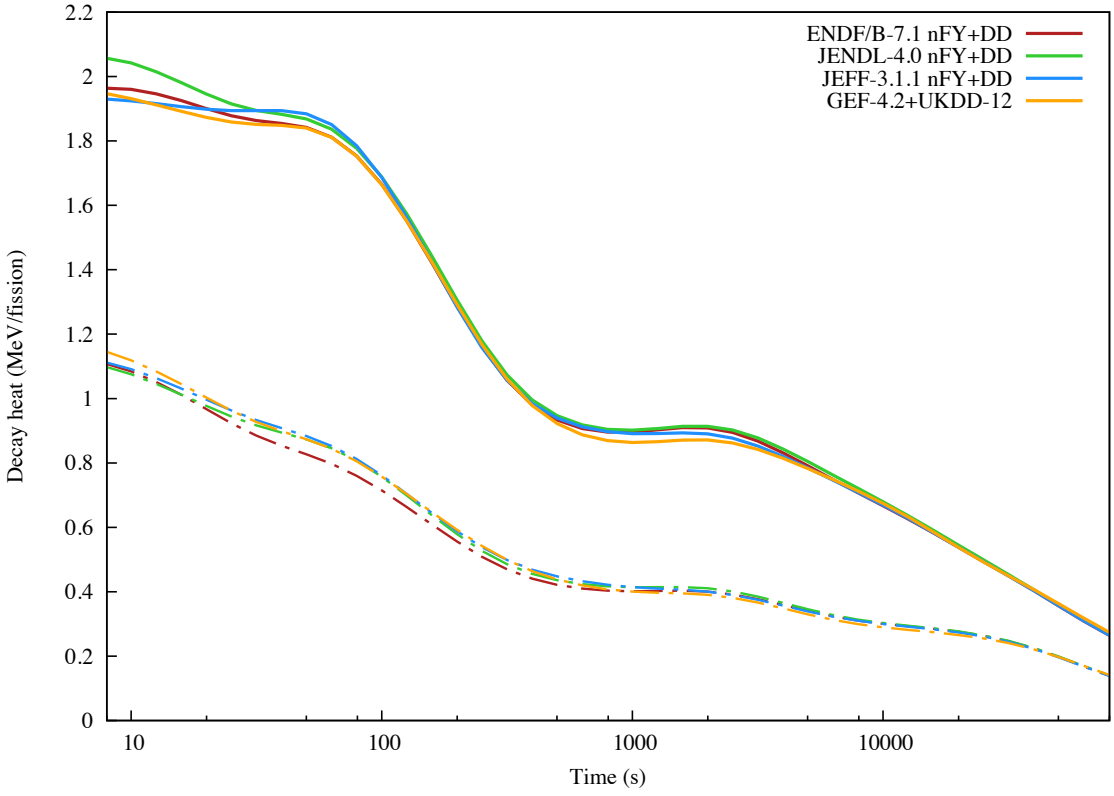

Figure 34: Total (solid) and beta (dash) decay heat from fast pulse on ^{232}Th.

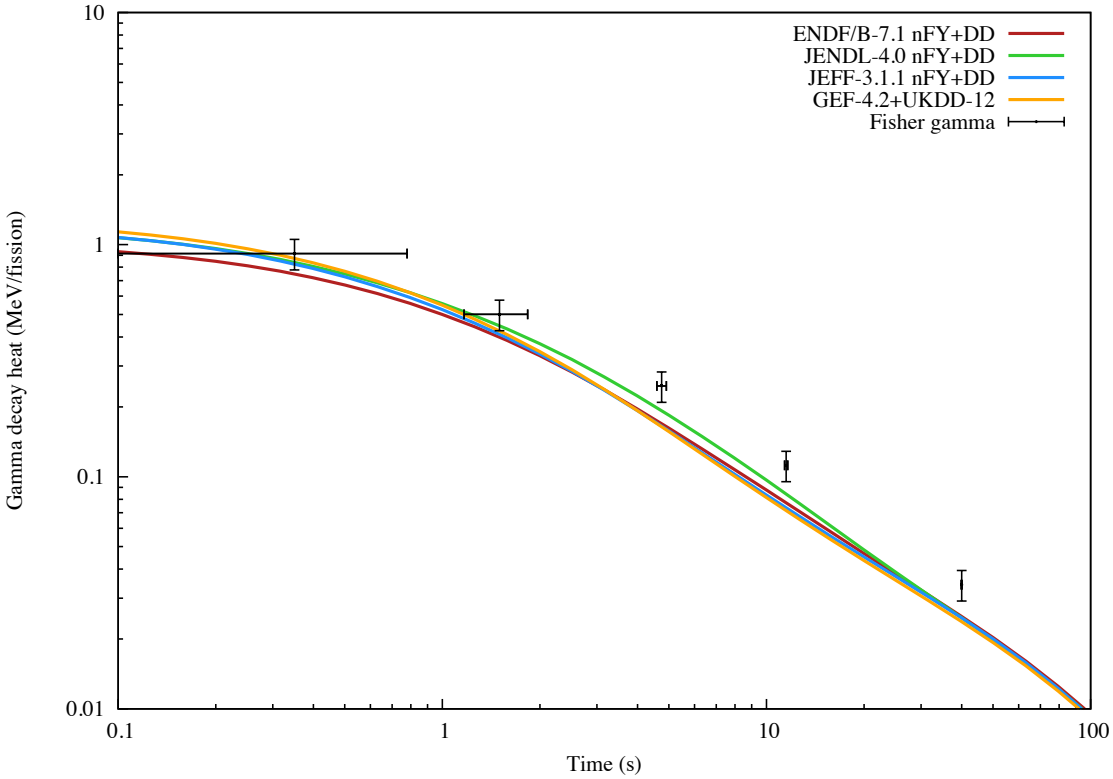

Figure 35: Gamma decay heat from <0.1s irradiations of ^{232}Th.

All simulations show remarkable agreement between 20-50000 s, although the time between 200-8000 s appears quite different from the experimental data. This is precisely the decay period of the capture product, ^{233}Th, with a half-life of 1310 s. The precise calibration for the capture decay requires knowledge of the capture rate for this experiment and, although apparent corrections for this phenomenon are shown graphically within the published literature, no tabular data or detailed methodology for the capture/fission ratio could be found for this report.

The LANL data probes a different time-scale which, as with these measurements for all other nuclides considered, suggests an under-prediction in gamma heat for cooling times less than 100s.

5.4 ^{233}U decay heat

As the main fissile isotope for the thorium fuel cycle, the accurate simulation of ^{233}U fission decay heat would be of considerable importance for the deployment of reactors using this fuel source. ^{233}U is commonly produced through neutron capture of ^{232}Th, followed by two beta decays, and can be bred in a variety of proposed reactor designs which employ thermal and fast neutron spectra. A relatively small number of fission decay heat experiments were found for this report, including those of the YAYOI fast reactor and thermal neutron irradiation at the LANL Omega West Reactor. While a series of experiments were carried out at YAYOI to reconstruct the fission burst function, longer irradiations of 2E4s were carried out in total calorimetric and γ-heat measurements at LANL. Gamma heat measurements from Godiva-II are also presented.

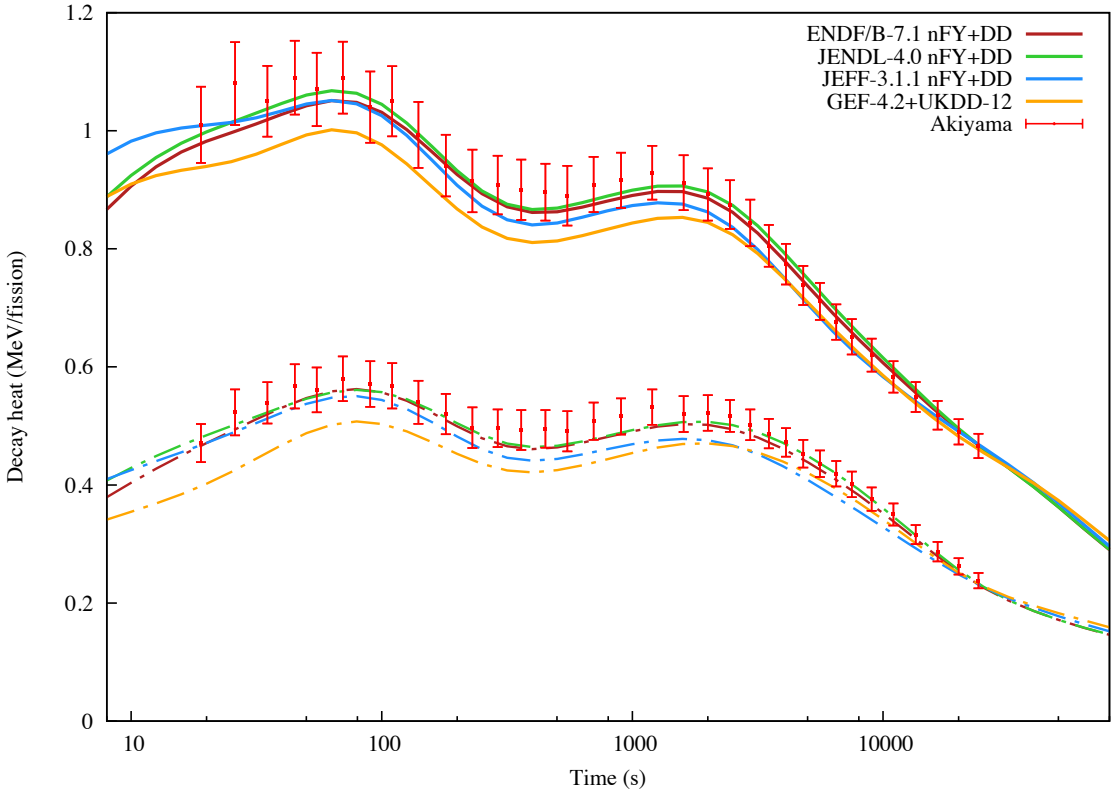

Figure 36: Total (solid) and gamma (dash) decay heat from fast pulse on ^{233}U.

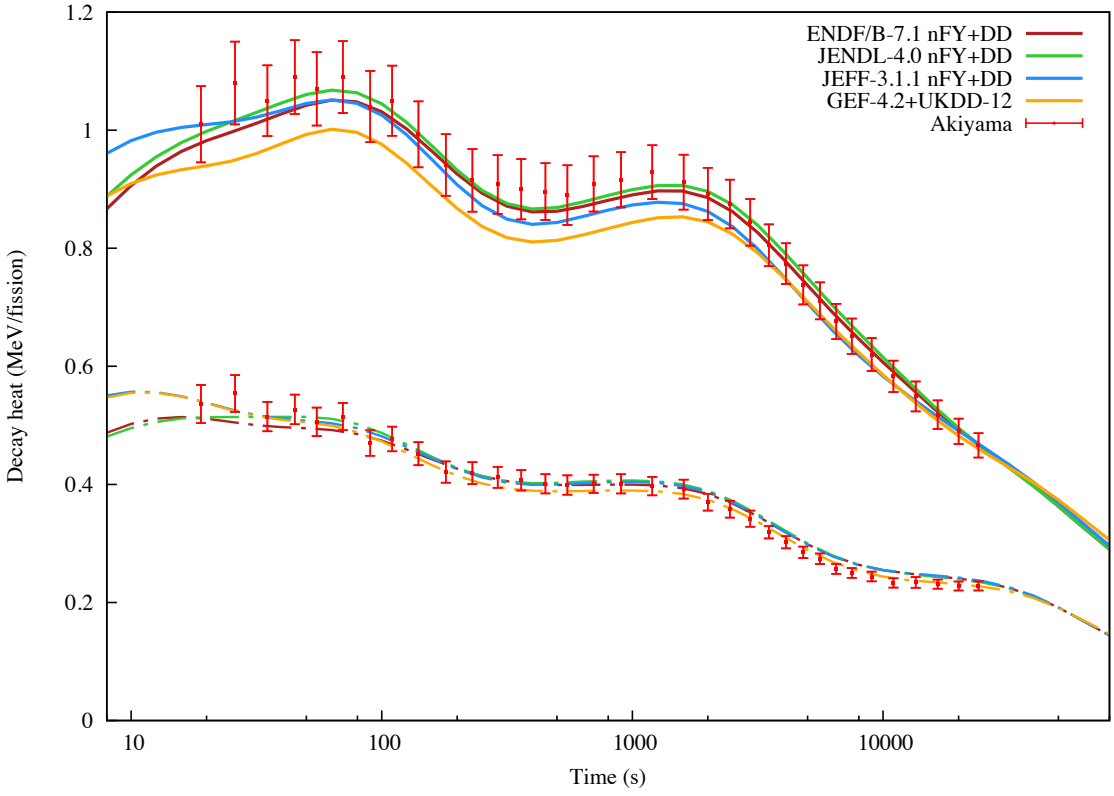

Figure 37: Total (solid) and beta (dash) decay heat from fast pulse on ^{233}U.

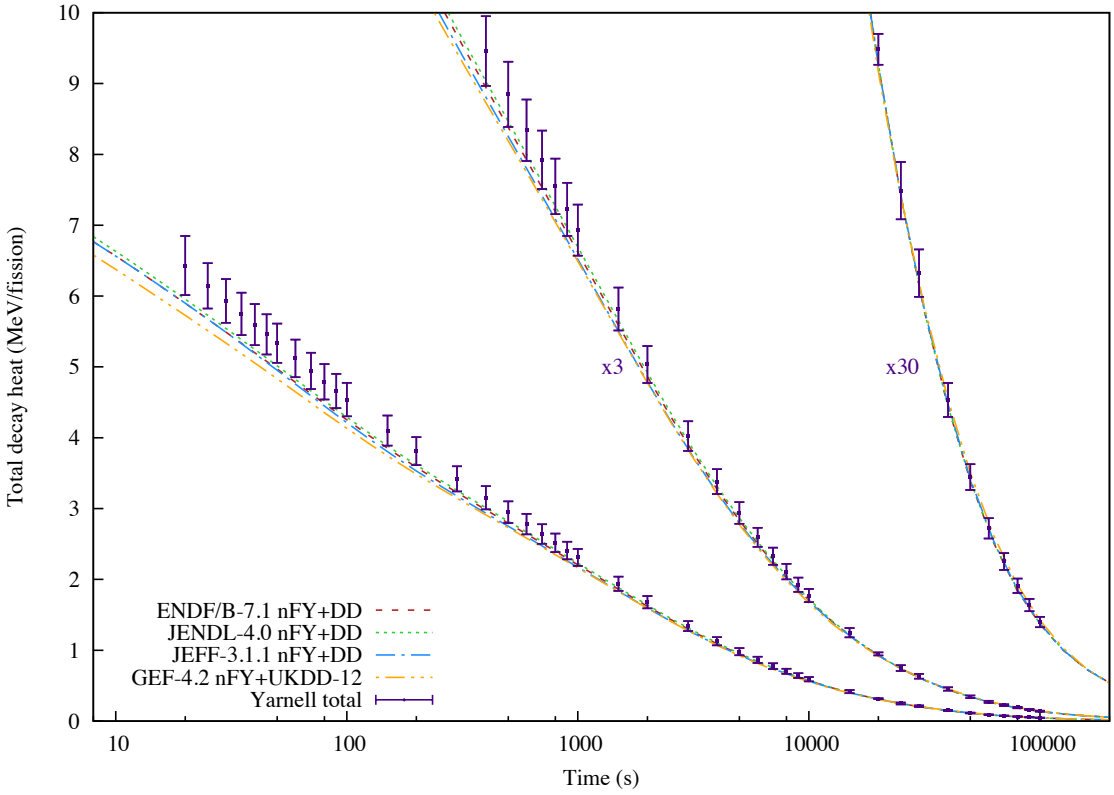

Figure 38: Total decay heat from thermal 2E4s irradiation of ^{233}U.

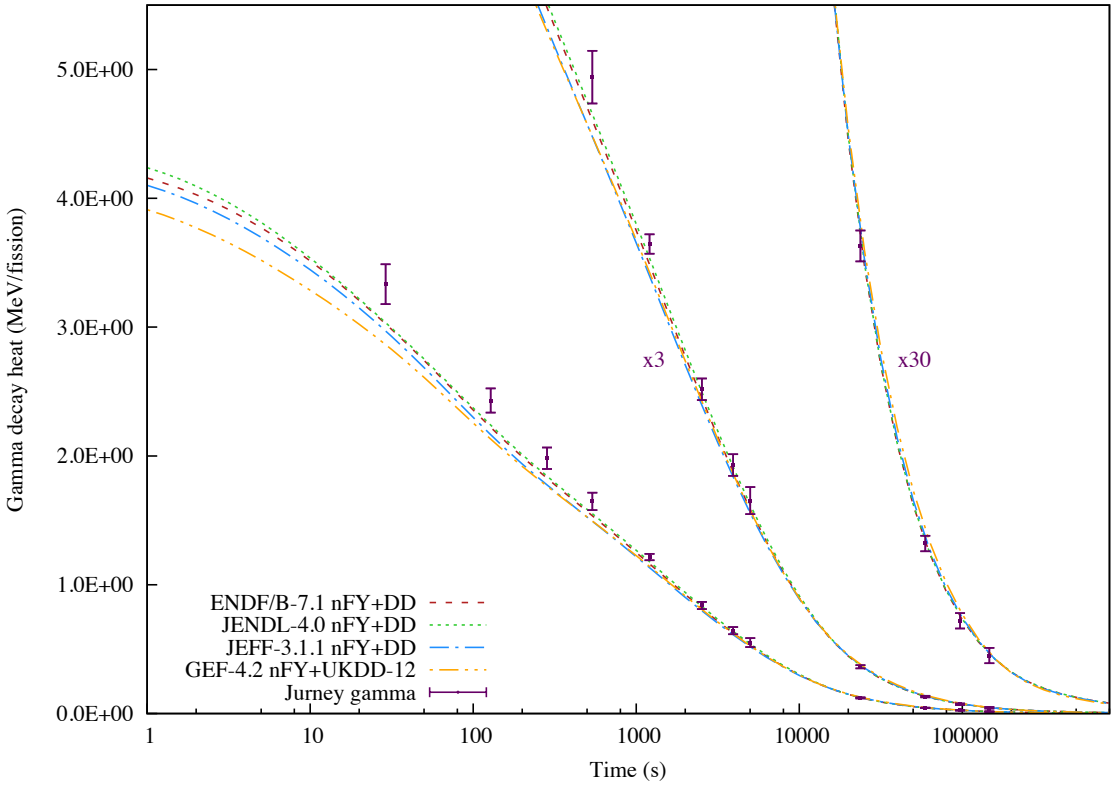

Figure 39: Gamma decay heat from thermal 2E4s irradiation of ^{233}U.

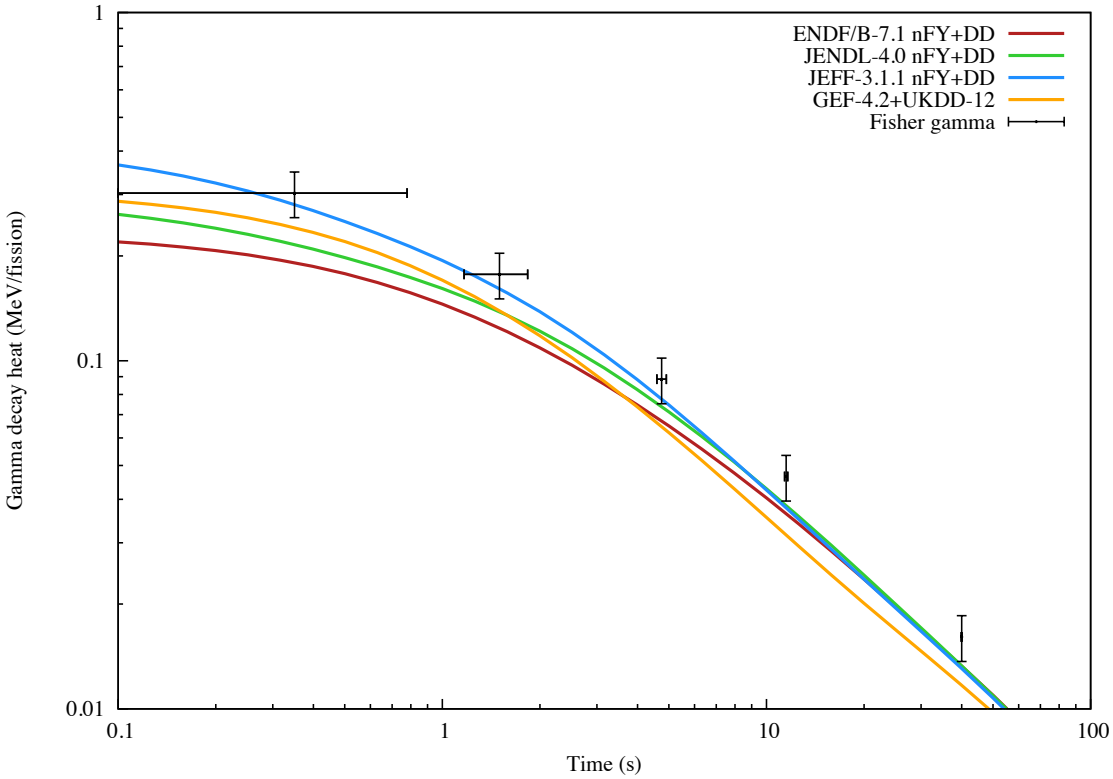

Figure 40: Gamma decay heat from <0.1s irradiations of ^{233}U.

While there is reasonably good C/C agreement between simulations with all major libraries and the total heat from the YAYOI experiments, the LANL calorimetic measurements suggest an under-prediction which approaches 10% in cooling times less than 1000 s – outside the quoted experimental uncertainty. The gamma heat is generally under-estimated by the simulations for cooling times less than a few thousand seconds, with all LANL data suggesting a slightly more pronounced difference.

The beta heat measurements are in relatively good agreement and the overall data generally suggests that some gamma heat is not being accounted for within the nuclear data – either through some effect such as Pandemonium or some more subtle error.

5.5 ^{238}U decay heat

Besides its role in breeding plutonium ^{238}U will fission, particularly with higher-energy neutrons where the $\sigma_{fission}/\sigma_{capture}$ ratio rises above 1. The data from the YAYOI and UM Lowell fast reactors has been reconstructed for fission pulses and are presented together. Note that the Lowell data probes much lower cooling times, while for longer time-scales some systematic errors were never fully corrected. LANL data from the Godiva-II device are also presented.

The UM Lowell data includes beta and gamma heat measurements made at different cooling times, so no precise totals can be presented without some mixing/modification of the data, which is not done in this report. This is particularly noticeable at cooling times less than 20s, where no experimental total decay heat values are available.

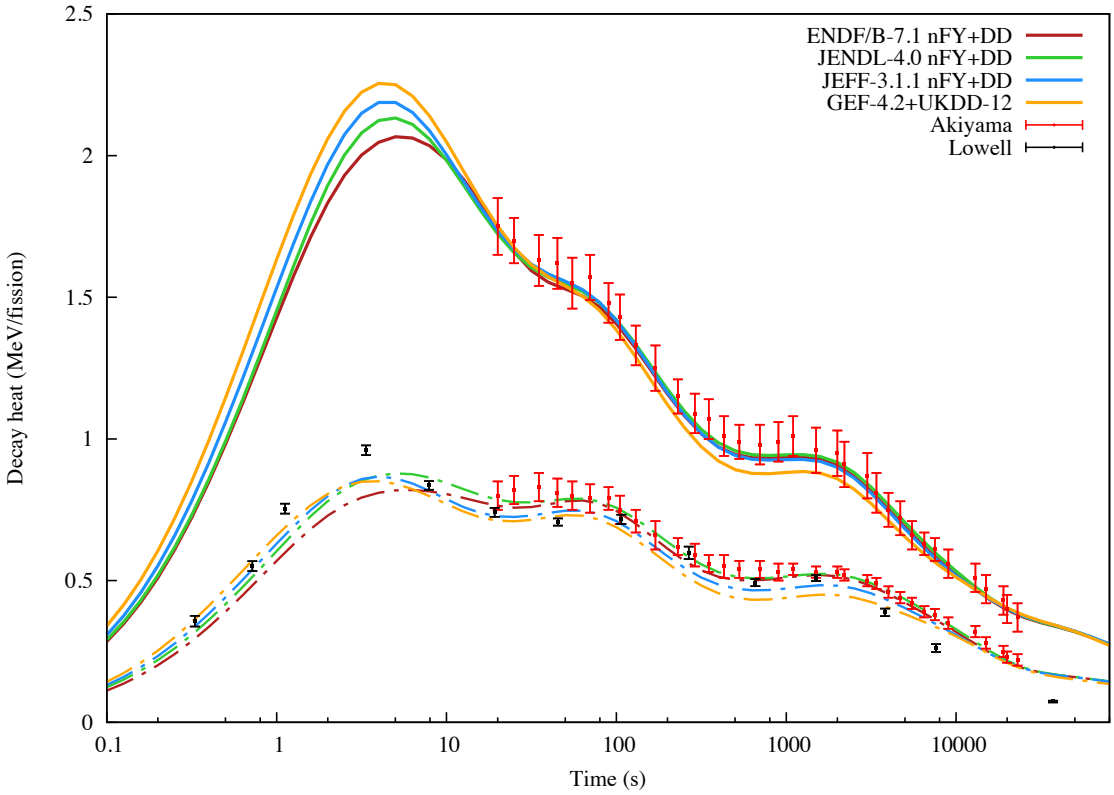

Figure 41: Total (solid) and gamma (dash) decay heat from fast pulse on ^{238}U.

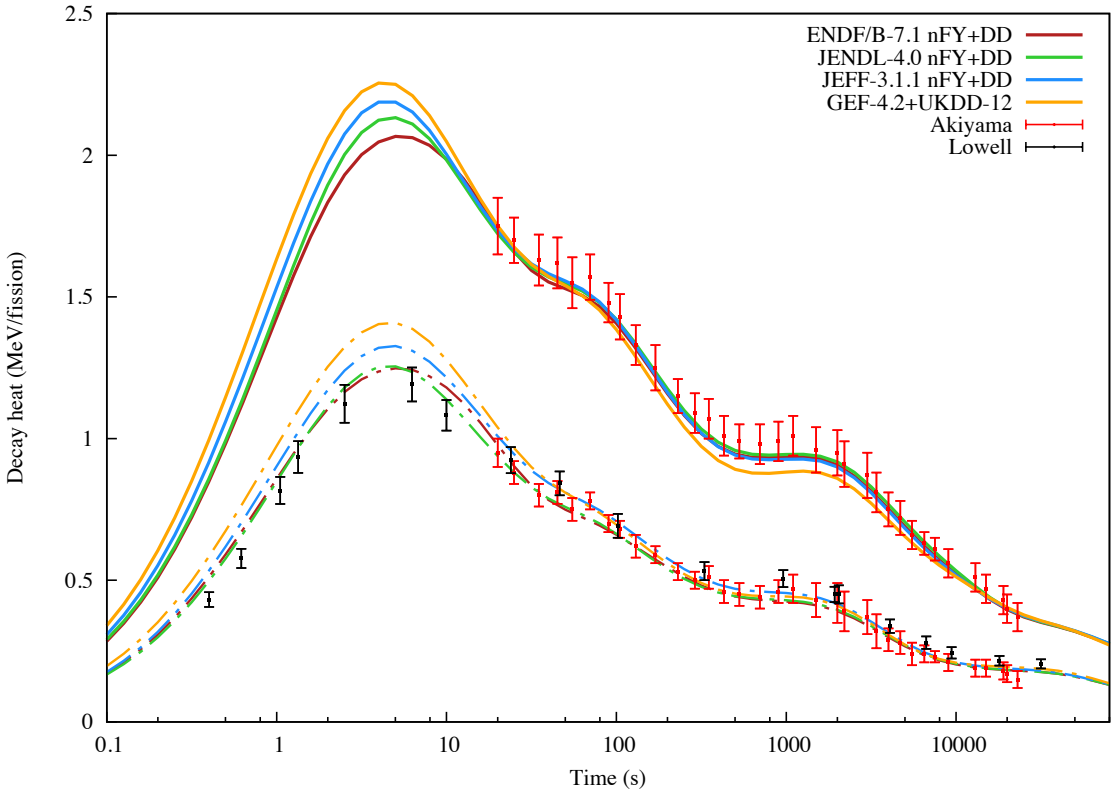

Figure 42: Total (solid) and beta (dash) decay heat from fast pulse on ^{238}U.

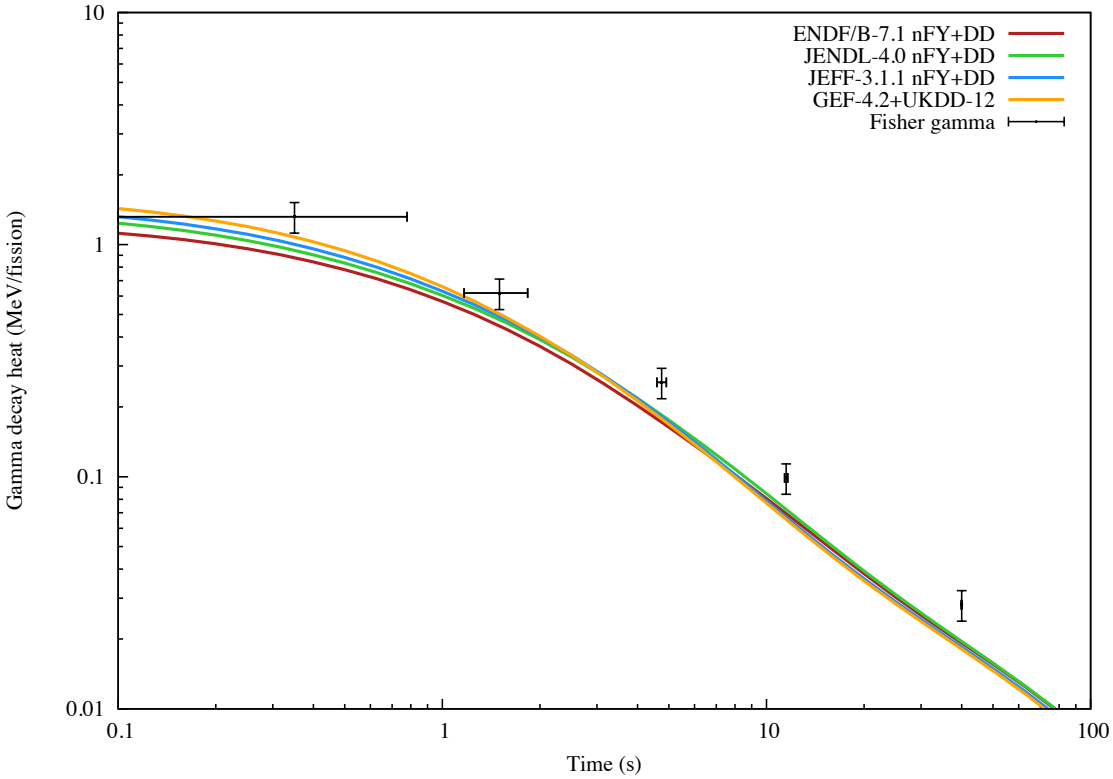

Figure 43: Gamma decay heat from <0.1s irradiations of ^{238}U.

Although the data is rather sparse in comparison with major fuel isotopes, this nuclide provides one of the most clear examples of Pandemonium in cooling times less than 100s. As with all of the other Godiva-II measurements, gamma heat around a few seconds appears to be substantially under-predicted, while the 1s and 4s Lowell measurements strengthen this concern and suggest the existence of Pandemonium nuclides not corrected in any major decay library. This cooling time is explored in Section 6.

5.6 ^{237}Np decay heat

This fissile nuclide is commonly produced in fission reactors through successive capture reactions from ^{235}U or through (n,2n) reactions on either ^{238}U or ^{238}Pu, followed by β decay or EC, respectively. It is also produced through α decay of ^{241}Am with a half-life of 433 years, making it a concern for reactor waste. This report only considers the data reported by Ohkawachi *et al* using the YAYOI reactor.

Gamma heat measurements were published which suffered from additional heat contribution from the capture product ^{238}Np. An effort to correct for this contribution was made using the 500s irradiation data, although the resulting data shows unphysical spread indicating substantial uncertainty. In general, the conversion from the finite irradiation to burst irradiation involved correction factors greater than 2 at certain cooling times – suggesting very large experimental and correction uncertainties. Total and beta heat calculations are also shown to give the reader the whole picture of the decay heat simulation. No uncertainty or error estimates were available and only the nominal data are presented.

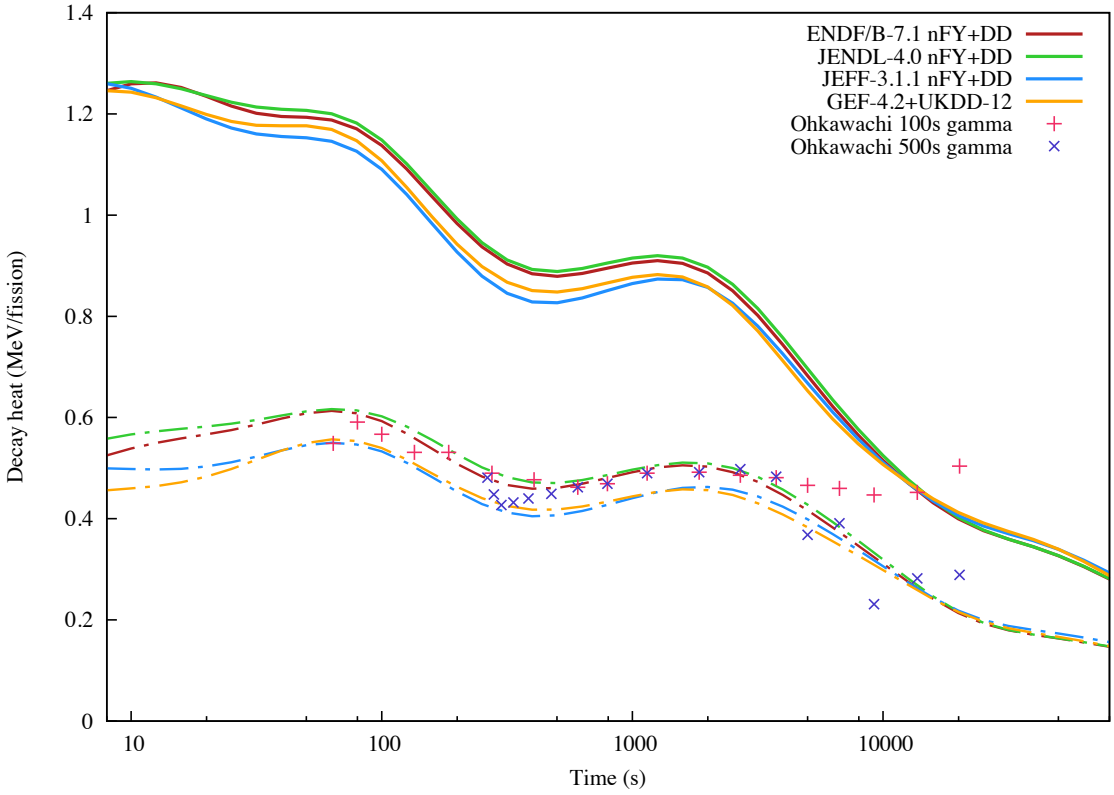

Figure 44: Total (solid) and gamma (dash) decay heat from fast pulse on ^{237}Np.

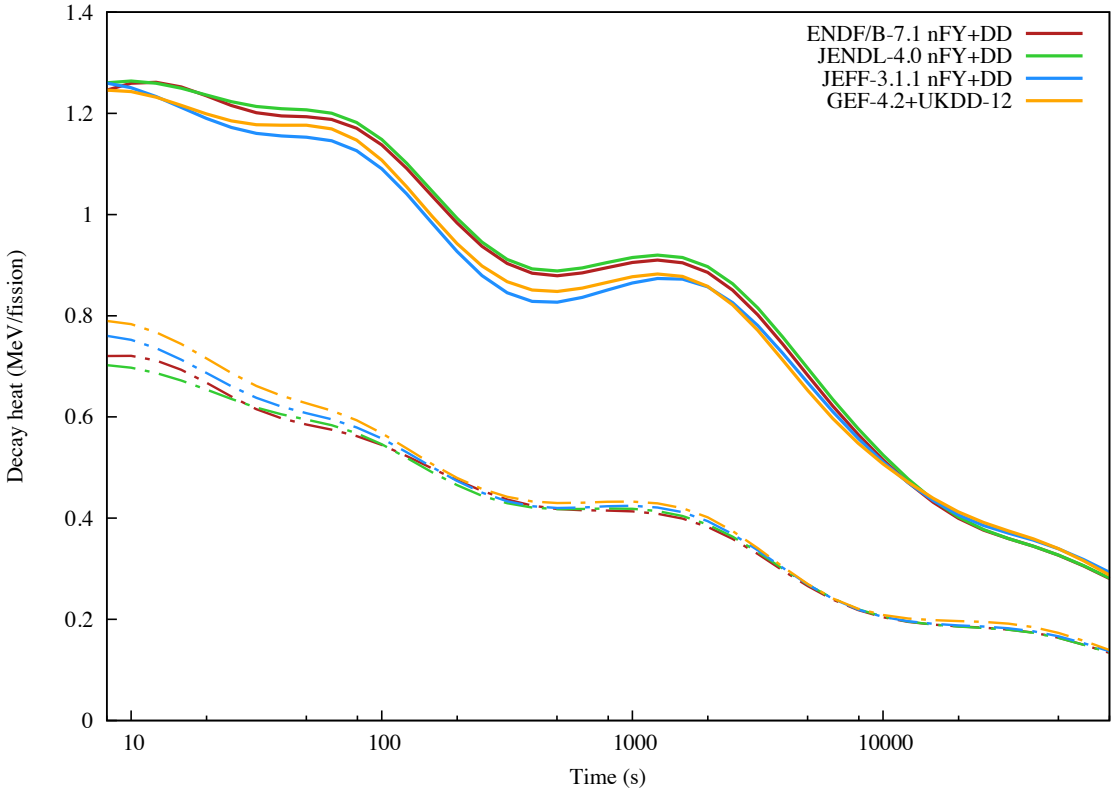

Figure 45: Total (solid) and beta (dash) decay heat from fast pulse on ^{237}Np.

5.7 ^{241}Pu decay heat

Much more fissile than the intermediary ^{240}Pu, ^{241}Pu is produced in increasing quantities with higher burn-up. Either in MOX fuel or as an additional, minor component in standard uranium fuels, ^{241}Pu decay heat is sufficiently important to warrant an experimental campaign at ORNL. A full set of gamma and beta heat measurements were made for cooling times between 2 and 14000s. With a shortest irradiation period of 1s, the $<$ 10s cooling time is not exceptionally well probed, but the general agreement between the major libraries and the experiment, for total heat, is quite good. TAGS corrections in ENDF/B-VII.1 and JENDL-4.0 have resulted in excellent agreement for gamma heat, while beta heat measurements lie between the simulations using generally corrected and un-corrected decay data – particularly in cooling times between 20-200s, where some under-prediction may exist in the simulation.

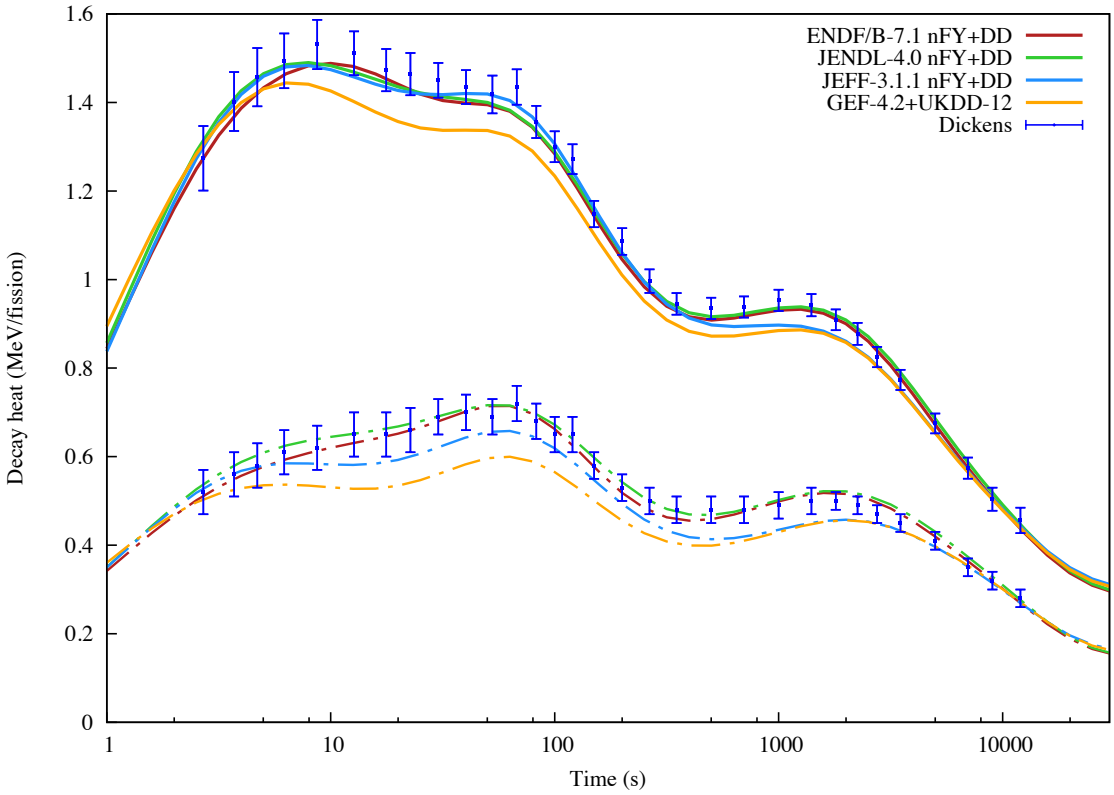

Figure 46: Total (solid) and gamma (dash) decay heat from thermal pulse on ^{241}Pu.

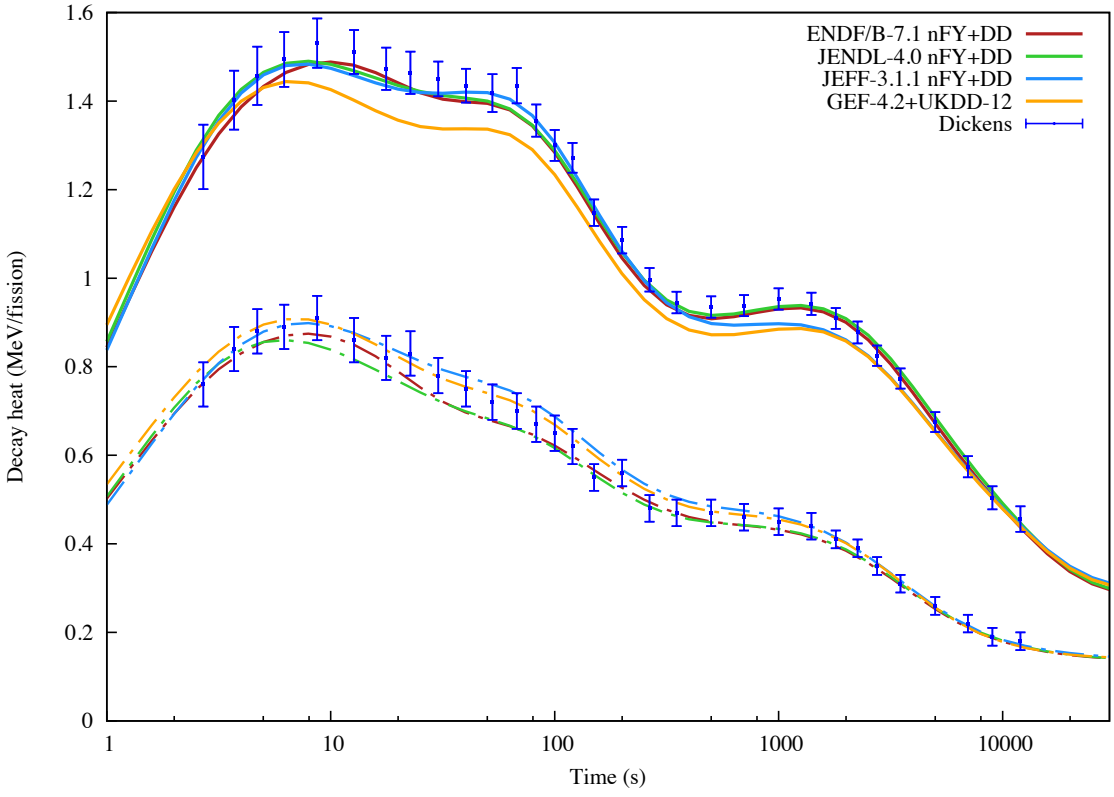

Figure 47: Total (solid) and beta (dash) decay heat from thermal pulse on ^{241}Pu.

6 Nuclear data comparisons

As has been demonstrated in the previous sections, the use of different nuclear data libraries can have a profound effect on the simulation of decay heat for all fissile nuclides – including the main constituents of LWR fuel. To better understand the root cause of these differences, FISPACT-II can be employed by swapping individual decay or fission files and comparing heat and inventories at a selection of cooling times. By doing this, the effects of library differences can be easily discovered and nuclides which both contribute non-negligibly to decay heat and have discrepant yields or decays can be identified. While the comparisons can be easily performed for any nuclide, spectrum, irradiation, cooling time or library permutation, we show only those from 1E16 neutron pulses of either 0.025 eV or 400 keV neutrons over 1 μs, striking 1E24 atoms of an individual nuclide. The daughter nuclide heat outputs are shown for specified cooling times following the pulse and is in units of kW. In all cases, the same fission cross-section and thus fission rates are simulated, while either decay or nFY data are varied.

In all simulations, the top 200 dominant nuclides are recorded for gamma, beta and total heat, while only the top 50 are shown – ensuring that any discrepancy where a heat contribution *does not* appear in one simulation truly indicates at least an order-of-magnitude difference[10].

For the nuclides which suffer from the Pandemonium effect, the beta heat is over-expressed due to mis-allocation of the heat due to high-energy gammas. This is not the only error possible with decay data files – misreading of data from ENSDF, dubious splitting of totals and simple typographical mistakes could also be at fault – but it is the most prevalent problem. To find the root cause, the decay data files must be interrogated by hand (ultimately by decay data evaluators). For select nuclides this is done for the examples that follow. Fission yield files are more subtle in their evaluation and there are no systematic inaccuracies (such as Pandemonium) that the authors of this report are aware of. The minor actinides which demonstrated considerable variation are probed in the following sections for the consideration of future evaluations.

One data library must be selected to calculate ratios of simulated decay heat from individual nuclides and, for several reasons ENDF/B-VII.1 was chosen for this purpose. This was primarily due to the complete absence of gamma heat contributions from other libraries for several nuclides which contribute more than 0.5% of the gamma heat at one of the four cooling times: 10s, 100s, 1000s or 10000s. In these cases no evaluation has been performed for some nuclides and direct processing of ENSDF has resulted in $EEM = 0$ decay files.

6.1 Comments on ^{235}U 0.0253 eV pulse decay heat

As the main fissile nuclide for nearly every fission reactor, it was surprising to find disagreement between decay heat simulations, both when broken down into γ/β contributions and in total. As shown in Figures 9 and 10, the various heat values in cooling times between approximately 10-100s, as well as 1000-5000s, show substantial simulation differences, as well as disagreement between the experimental data. In Figures 48 and 49, the top 50 dominant gamma heat nuclides are shown with the values from simulation

[10]This prevents nuclides from hiding 'beneath the flotation line', *ie* just beneath the dominant list.

using different decay libraries. These are accompanied by Tables 4 and 5 which give all numbers shown in those figures.

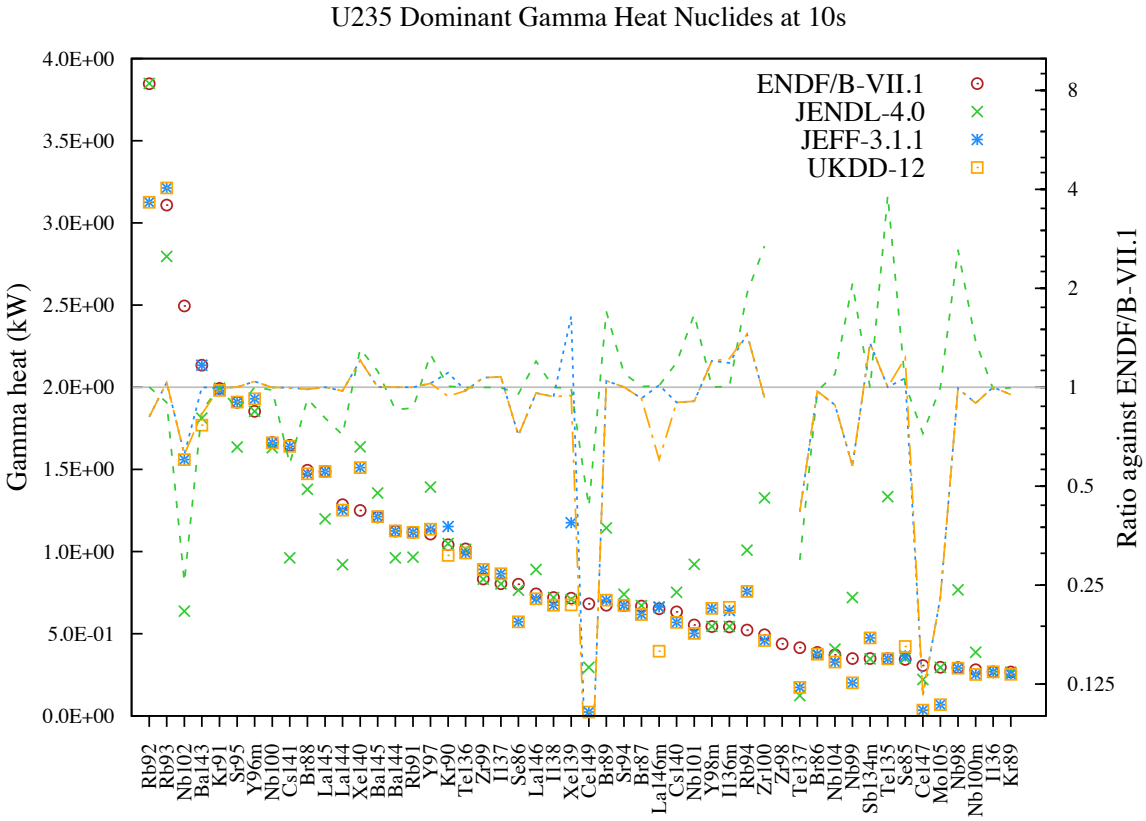

Figure 48: Gamma decay data comparison for U235 fission pulse after 10s cooling.

Table 4: Gamma decay heat (in kW) decay data comparison for U235 fission pulse after 10s cooling.

Nuclide	% Heat	ENDF/B-7.1	JENDL-4.0	JEFF-3.1.1	UKDD-12
Rb92	7.0	3.85E+00	3.85E+00	3.13E+00	3.13E+00
Rb93	5.7	3.11E+00	2.80E+00	3.21E+00	3.21E+00
Nb102	4.5	2.50E+00	6.37E-01	1.56E+00	1.56E+00
Ba143	3.9	2.13E+00	1.81E+00	2.13E+00	1.77E+00
Kr91	3.6	1.99E+00	2.00E+00	1.98E+00	1.98E+00
Sr95	3.5	1.91E+00	1.64E+00	1.91E+00	1.91E+00
Y96m	3.4	1.85E+00	1.85E+00	1.93E+00	1.93E+00
Nb100	3.0	1.66E+00	1.63E+00	1.66E+00	1.66E+00
Cs141	3.0	1.65E+00	9.62E-01	1.64E+00	1.64E+00
Br88	2.7	1.50E+00	1.38E+00	1.47E+00	1.47E+00
La145	2.7	1.49E+00	1.20E+00	1.49E+00	1.49E+00
La144	2.3	1.28E+00	9.20E-01	1.25E+00	1.25E+00
Xe140	2.3	1.25E+00	1.64E+00	1.51E+00	1.51E+00
Ba145	2.2	1.21E+00	1.36E+00	1.21E+00	1.21E+00
Ba144	2.0	1.12E+00	9.61E-01	1.13E+00	1.13E+00
Rb91	2.0	1.12E+00	9.66E-01	1.12E+00	1.12E+00
Y97	2.0	1.11E+00	1.39E+00	1.14E+00	1.14E+00

Nuclide	% Heat	ENDF/B-7.1	JENDL-4.0	JEFF-3.1.1	UKDD-12
Kr90	1.9	1.04E+00	1.05E+00	1.15E+00	9.77E-01
Te136	1.8	1.02E+00	1.01E+00	9.92E-01	9.92E-01
Zr99	1.5	8.33E-01	8.32E-01	8.91E-01	8.91E-01
I137	1.5	8.05E-01	8.03E-01	8.65E-01	8.65E-01
Se86	1.5	8.01E-01	7.64E-01	5.72E-01	5.72E-01
La146	1.4	7.42E-01	8.91E-01	7.13E-01	7.13E-01
I138	1.3	7.20E-01	7.20E-01	6.74E-01	6.74E-01
Xe139	1.3	7.16E-01	7.09E-01	1.18E+00	6.76E-01
Ce149	1.2	6.82E-01	2.95E-01	2.39E-02	2.39E-02
Br89	1.2	6.73E-01	1.14E+00	7.04E-01	7.04E-01
Sr94	1.2	6.71E-01	7.40E-01	6.72E-01	6.72E-01
Br87	1.2	6.68E-01	6.71E-01	6.17E-01	6.17E-01
La146m	1.2	6.52E-01	6.59E-01	6.62E-01	3.93E-01
Cs140	1.2	6.33E-01	7.53E-01	5.69E-01	5.69E-01
Nb101	1.0	5.54E-01	9.23E-01	5.02E-01	5.02E-01
Y98m	1.0	5.44E-01	5.44E-01	6.54E-01	6.54E-01
I136m	1.0	5.41E-01	5.44E-01	6.42E-01	6.61E-01
Rb94	0.9	5.22E-01	1.01E+00	7.57E-01	7.57E-01
Zr100	0.9	4.94E-01	1.33E+00	4.59E-01	4.59E-01
Zr98	0.8	4.38E-01	—	—	—
Te137	0.8	4.15E-01	1.24E-01	1.74E-01	1.74E-01
Br86	0.7	3.86E-01	3.76E-01	3.75E-01	3.75E-01
Nb104	0.7	3.71E-01	4.07E-01	3.28E-01	3.28E-01
Nb99	0.6	3.49E-01	7.21E-01	2.01E-01	2.01E-01
Sb134m	0.6	3.49E-01	3.47E-01	4.75E-01	4.75E-01
Te135	0.6	3.47E-01	1.33E+00	3.48E-01	3.48E-01
Se85	0.6	3.43E-01	3.51E-01	3.66E-01	4.23E-01
Ce147	0.6	3.06E-01	2.21E-01	3.53E-02	3.53E-02
Mo105	0.5	2.95E-01	2.94E-01	6.77E-02	6.77E-02
Nb98	0.5	2.93E-01	7.67E-01	2.91E-01	2.91E-01
Nb100m	0.5	2.81E-01	3.87E-01	2.52E-01	2.52E-01
I136	0.5	2.68E-01	2.65E-01	2.68E-01	2.68E-01
Kr89	0.5	2.67E-01	2.66E-01	2.53E-01	2.53E-01

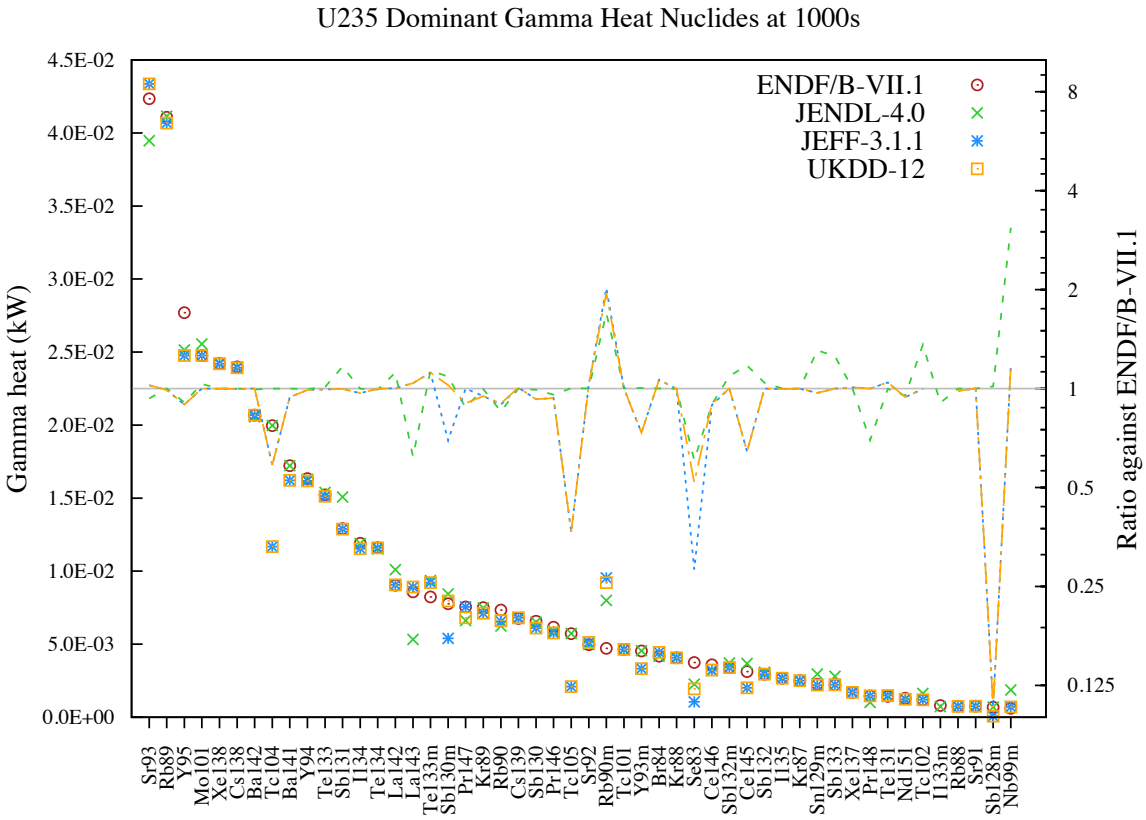

Figure 49: Gamma decay data comparison for U235 fission pulse after 1000s cooling.

Table 5: Gamma decay heat (in kW) decay data comparison for U235 fission pulse after 1000s cooling.

Nuclide	% Heat	ENDF/B-7.1	JENDL-4.0	JEFF-3.1.1	UKDD-12
Sr93	9.2	4.23E-02	3.95E-02	4.34E-02	4.34E-02
Rb89	8.9	4.11E-02	4.11E-02	4.07E-02	4.07E-02
Y95	6.0	2.77E-02	2.51E-02	2.48E-02	2.48E-02
Mo101	5.4	2.48E-02	2.56E-02	2.48E-02	2.48E-02
Xe138	5.2	2.42E-02	2.42E-02	2.42E-02	2.42E-02
Cs138	5.2	2.40E-02	2.40E-02	2.39E-02	2.39E-02
Ba142	4.5	2.07E-02	2.06E-02	2.07E-02	2.07E-02
Tc104	4.3	2.00E-02	2.00E-02	1.17E-02	1.17E-02
Ba141	3.7	1.72E-02	1.72E-02	1.62E-02	1.62E-02
Y94	3.5	1.63E-02	1.63E-02	1.62E-02	1.62E-02
Te133	3.3	1.52E-02	1.54E-02	1.51E-02	1.51E-02
Sb131	2.8	1.29E-02	1.51E-02	1.29E-02	1.29E-02
I134	2.6	1.19E-02	1.19E-02	1.15E-02	1.15E-02
Te134	2.5	1.16E-02	1.15E-02	1.16E-02	1.16E-02
La142	2.0	9.04E-03	1.01E-02	9.06E-03	9.06E-03
La143	1.9	8.59E-03	5.33E-03	8.92E-03	8.92E-03
Te133m	1.8	8.24E-03	9.36E-03	9.21E-03	9.21E-03
Sb130m	1.7	7.77E-03	8.44E-03	5.40E-03	7.96E-03
Pr147	1.6	7.56E-03	6.62E-03	7.56E-03	6.81E-03
Kr89	1.6	7.51E-03	7.48E-03	7.13E-03	7.13E-03

Nuclide	% Heat	ENDF/B-7.1	JENDL-4.0	JEFF-3.1.1	UKDD-12
Rb90	1.6	7.34E-03	6.25E-03	6.56E-03	6.62E-03
Cs139	1.5	6.76E-03	6.76E-03	6.81E-03	6.81E-03
Sb130	1.4	6.57E-03	6.51E-03	6.10E-03	6.10E-03
Pr146	1.3	6.16E-03	5.90E-03	5.77E-03	5.77E-03
Tc105	1.2	5.72E-03	5.73E-03	2.09E-03	2.09E-03
Sr92	1.1	4.97E-03	4.98E-03	5.13E-03	5.13E-03
Rb90m	1.0	4.72E-03	8.00E-03	9.54E-03	9.22E-03
Tc101	1.0	4.64E-03	4.65E-03	4.64E-03	4.64E-03
Y93m	1.0	4.53E-03	4.55E-03	3.33E-03	3.33E-03
Br84	0.9	4.17E-03	4.18E-03	4.44E-03	4.44E-03
Kr88	0.9	4.07E-03	4.06E-03	4.06E-03	4.06E-03
Se83	0.8	3.74E-03	2.26E-03	1.05E-03	1.94E-03
Ce146	0.8	3.59E-03	3.21E-03	3.20E-03	3.23E-03
Sb132m	0.7	3.40E-03	3.71E-03	3.40E-03	3.40E-03
Ce145	0.7	3.13E-03	3.68E-03	2.01E-03	2.01E-03
Sb132	0.6	2.95E-03	3.07E-03	2.95E-03	2.95E-03
I135	0.6	2.67E-03	2.68E-03	2.67E-03	2.67E-03
Kr87	0.5	2.51E-03	2.51E-03	2.50E-03	2.50E-03
Sn129m	0.5	2.27E-03	2.96E-03	2.20E-03	2.20E-03
Sb133	0.5	2.23E-03	2.80E-03	2.23E-03	2.23E-03
Xe137	0.4	1.69E-03	1.69E-03	1.70E-03	1.70E-03
Pr148	0.3	1.45E-03	1.01E-03	1.46E-03	1.46E-03
Te131	0.3	1.42E-03	1.42E-03	1.48E-03	1.49E-03
Nd151	0.3	1.31E-03	1.24E-03	1.23E-03	1.23E-03
Tc102	0.3	1.20E-03	1.63E-03	1.20E-03	1.20E-03
I133m	0.2	8.01E-04	—	—	—
Rb88	0.2	7.54E-04	7.54E-04	7.42E-04	7.42E-04
Sr91	0.2	7.54E-04	7.54E-04	7.54E-04	7.54E-04
Sb128m	0.1	6.86E-04	6.96E-04	7.36E-05	7.36E-05
Nb99m	0.1	6.05E-04	1.87E-03	7.08E-04	7.08E-04

The most substantial deviations for total gamma heat arise from the dominant nuclides, but with less than 10% attributable to any one nuclide, the differences in each are relatively important and the variation over the set which contribute more than 0.5% is tremendous. Several of the major TAGS corrections can be identified in these tables, although many which appear here are not on any IAEA list for past or future measurements.

The lack of gamma heat from Zr98 in any library except ENDF/B-VII.1 and I133m gamma heat missing from both JEFF-3.1.1 and UKDD-12 are worth specific consideration. It is necessary to read the decay files to verify why $EEM = 0$ for all those cases which returned zero gamma heat in a FISPACT-II simulation[11]. For these nuclides, the decay file states quite clearly how it has been assembled. The JENDL-4.0 decay file for Zr98 reads:

```
JENDL FP Decay Data File 2011                                0 0  0    0
```

[11]Not only is $EEM = 0$, but often there is no spectral information for the beta decay, as well.

```
 40-Zr- 98 JAEA NDC   EVAL-JAN11 J. KATAKURA                        4049 1451    5
                      DIST-JUL12                          20120123   4049 1451    6
----JENDL/FPD-2011    MATERIAL 4049                                  4049 1451    7
-----DECAY DATA                                                      4049 1451    8
------ENDF-6 FORMAT                                                 4049 1451    9
  98ZR B- DECAY  (30.7 S 4)       ENSDF DATE 201011                  4049 1451   10
      DISCRETE DATA ARE FROM ENSDF                                   4049 1451   11
  REFERENCES                                                         4049 1451   12
    QB: G.AUDI, W.MENG, D.LUNNEY, B.PFEIFFER                         4049 1451   13
           - ATOMIC MASS EVALUATION 2009 (2009)                      4049 1451   14
    COMPILATION: J.KATAKURA - JAEA-DATA/CODE 2011-025 (2012)         4049 1451   15
```

while the JEFF-3.1.1 is an exact duplicate outside `MF=1`. In comparison, the ENDF/B-VII.1 file comments explain what evaluation has taken place:

```
 $Rev:: 584      $  $Date:: 2011-12-19#$                             1 0  0    0
 40-Zr- 98  BNL        EVAL-AUG11 Conv. from CGM                   1049 1451    5
 /ENSDF/                                           20111222        1049 1451    6
----ENDF/B-VII.1      Material 1049                                 1049 1451    7
-----RADIOACTIVE DECAY DATA                                         1049 1451    8
------ENDF-6 FORMAT                                                1049 1451    9
********************** Begin Description ********************** 1049 1451   10
**         ENDF/B-VII.1 RADIOACTIVE DECAY DATA FILE            ** 1049 1451   11
************************ Energy  Balance ************************ 1049 1451   12
Mean Gamma Energy:     4.486E2 keV                                  1049 1451   13
Mean Beta Energy:      7.007E2 keV                                  1049 1451   14
Mean Neutron Energy:   0.000E0 keV                                  1049 1451   15
Mean Neutrino Energy:  1.101E3 keV                                  1049 1451   16
Sum:                   2.250E3 keV                                  1049 1451   17
Efective Q-value       2.238E3 keV                                  1049 1451   18
Source of Data:                                                     1049 1451   19
Parent Excitation Energy: 0.000E0 keV                               1049 1451   20
%Pn=0.00E0 from Kawano & Moller Calculations                        1049 1451   21
T1/2=30.7 S from ENSDF                                              1049 1451   22
Spin and Parity from ENSDF                                          1049 1451   23
Masses from the 2011 update of the Atomic Mass Evaluation by        1049 1451   24
Audi et al.                                                         1049 1451   25
Beta Strength Functions: P. Moller (LANL)                           1049 1451   26
Statistical Model Calculations:                                     1049 1451   27
S. Holloway, T. Kawano, H. Little(LANL)                             1049 1451   28
Translated into ENDF format by:                                     1049 1451   29
T. Johnson, E. McCutchan & A.A. Sonzogni (BNL)                      1049 1451   30
************************ End Description ************************ 1049 1451   31
```

It is not generally true that all ENDF/B-VII.1 decay files have detailed evaluations while other libraries are mere reflections of ENSDF with AME, but there are ubiquitous discrepancies between the libraries which strongly support ENDF/B-VII.1 decay data and are the reason for its use as the standard in this report.

The total heat comparisons in Figures 50 and 51 show less variation, although still a great number of nuclides which contribute more than 0.5% of the total heat differ by more than 20%. That the net total over all nuclides agrees between libraries should raise concerns. Some differences are due to allocation of heat to isomers, but the majority are not.

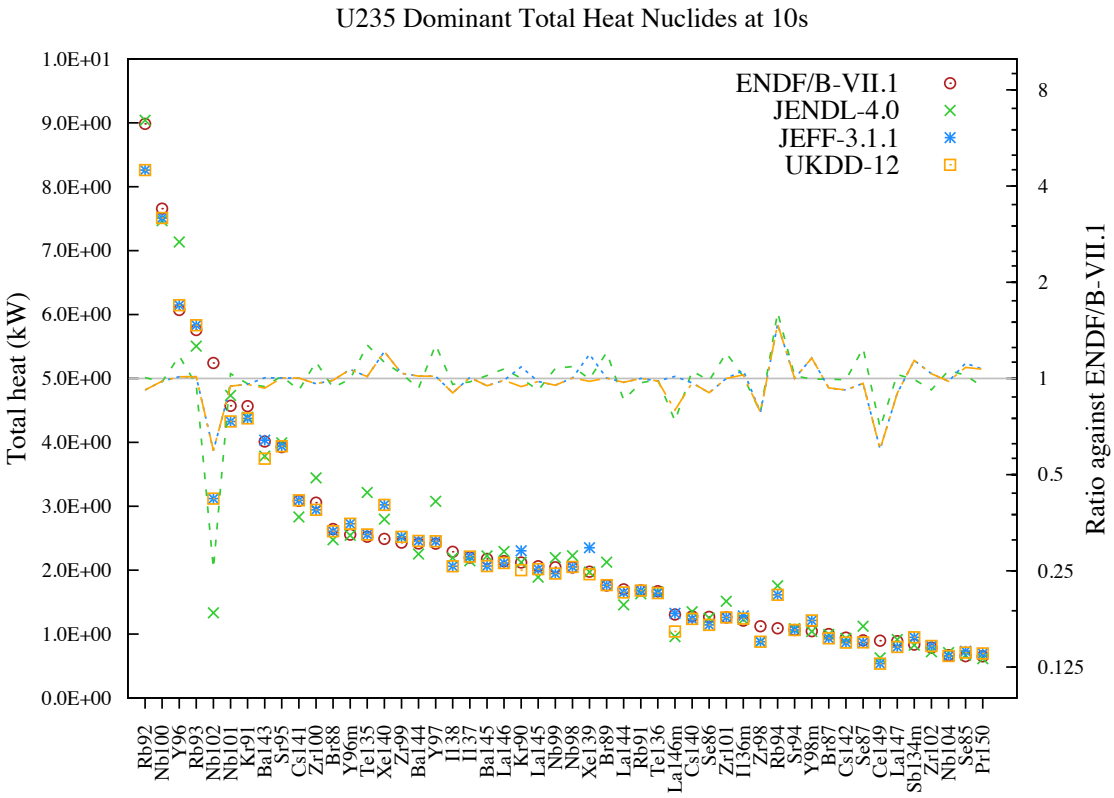

Figure 50: Decay data comparison for U235 fission pulse after 10s cooling.

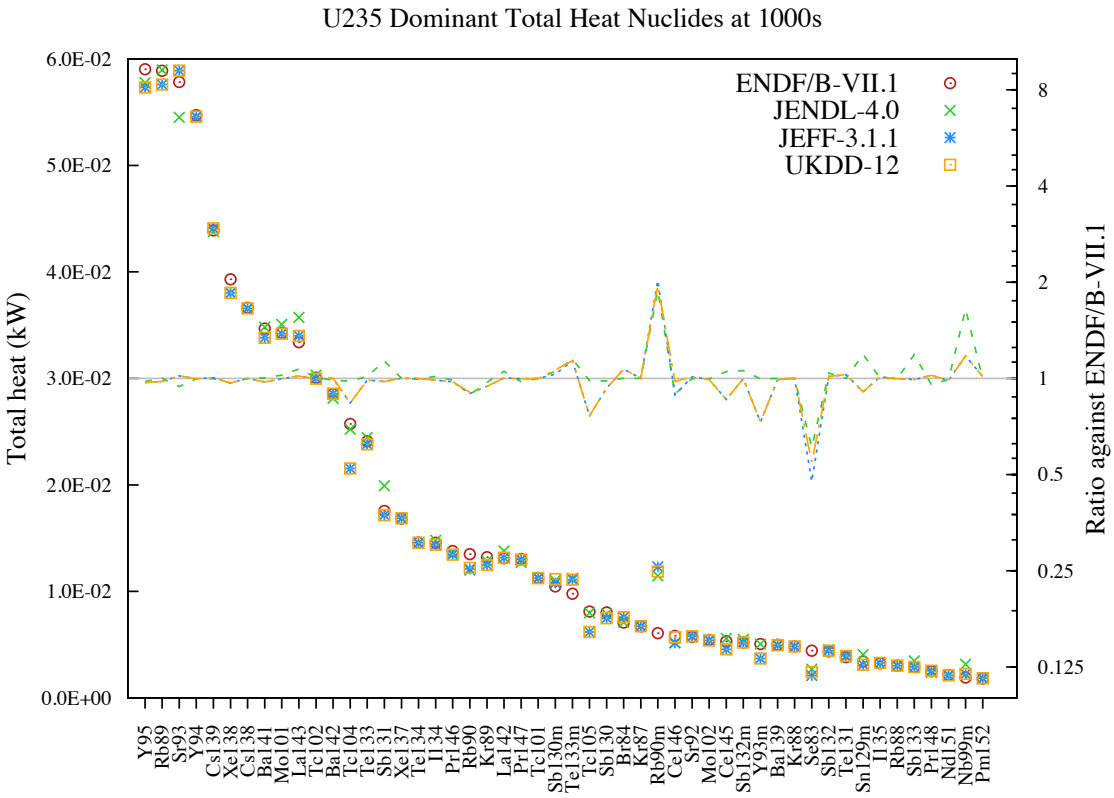

Figure 51: Decay data comparison for U235 fission pulse after 1000s cooling.

6.2 Comments on ^{239}Pu 0.0253 eV pulse decay heat

Each fissile generally has a different fission yield distribution for the smaller of the binary products, so that for any given cooling time the inventory and decay heat will vary between fission nuclide. To avoid overloading the reader with surfeit data, only the 100s gamma decay inventory is shown, in Figure 52. As with the ^{235}U case above, the gamma contributions are scattered. New Pandemonium nuclides appear with large differences, such as the technetium and molybdenum isotopes (which incidentally have considerable EEM variation amongst the decay libraries due to incomplete adoption of TAGS data). Additionally, an evaluation for ^{110m}Rh has been performed for ENDF/B-VII.1 which draws away the contribution from the ground state which appears in JEFF-3.1.1 and UKDD-12.

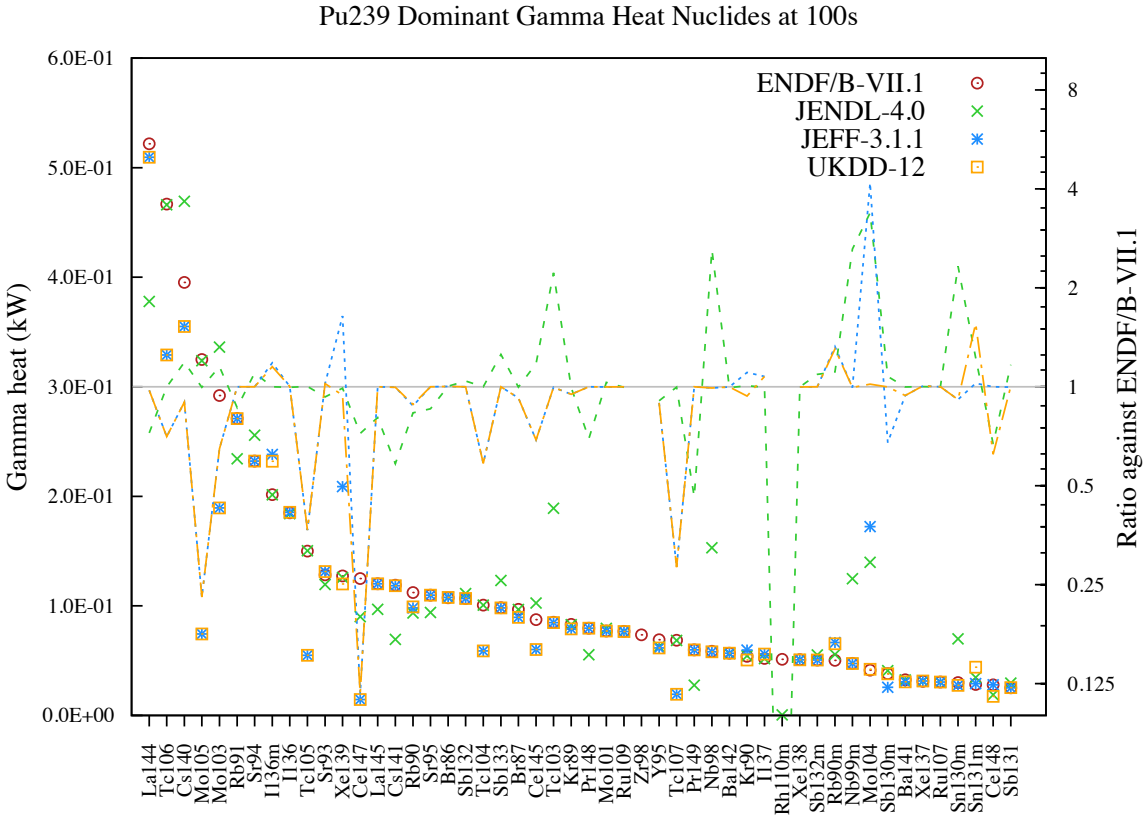

Figure 52: Decay data comparison for Pu239 fission pulse after 100s cooling.

6.3 Comments on ^{233}U 400 keV pulse decay heat

As with the plutonium example, for ^{233}U only one sample plot is provided at a period of interest – 10s post irradiation gamma heat from a fast pulse. Most of the sample 10s culprits appear again with ^{233}U and the ratios between libraries should be nearly identical to those found for other fissiles.

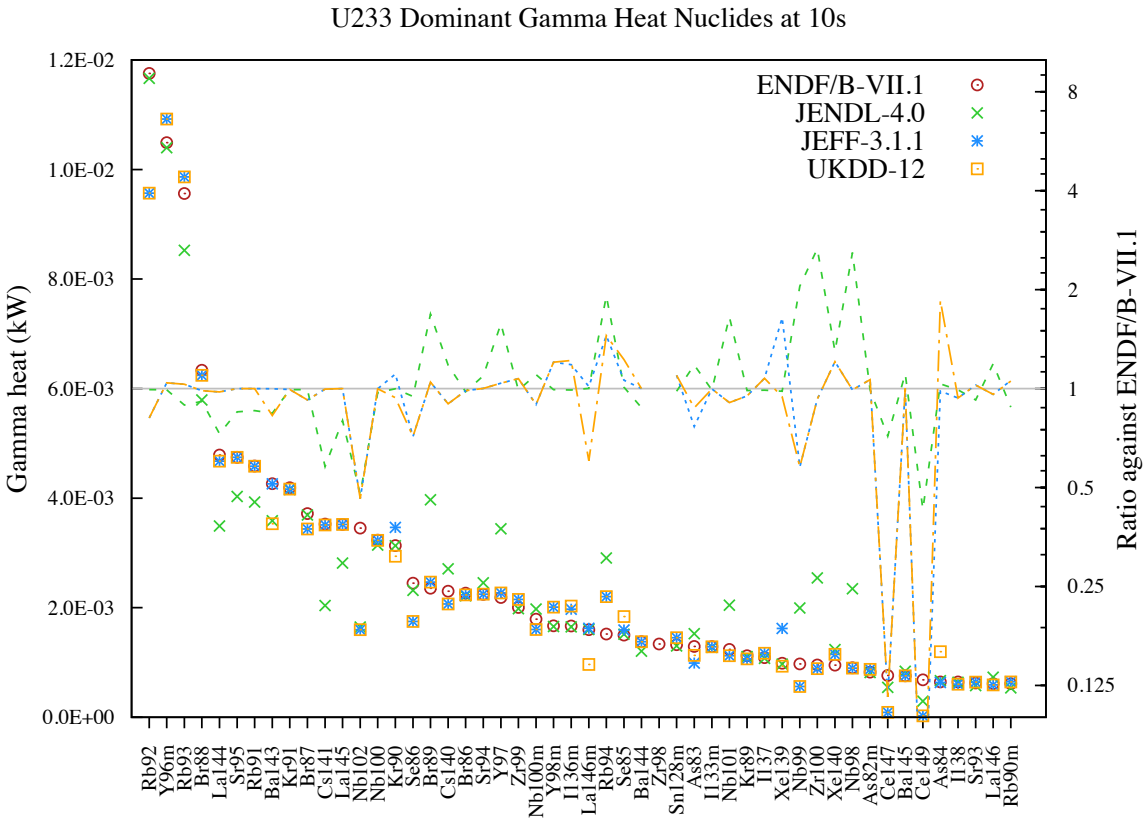

Figure 53: Decay data comparison for U233 fission pulse after 10s cooling.

Figure 54 reflects variation of the fission yield rather than the decay data. The same nuclides appear, although in somewhat different ordering due to the use of the JEFF-3.1.1 simulation as the reference nFY. The decay data used throughout is ENDF/B-VII.1. **Note also** that the color scheme has changed and UKDD-12 has been replaced by GEF-4.2. All of these variations are due to the fission yield files and are not a direct consequence of the Pandemonium errors. While many isomers show the greatest differences, the majority of the 50 most dominant gamma heat contributors (and of course the totals, since this is not a decay feeding problem) have more than 20% difference between the major fission yield libraries. Considering that ^{233}U is the major fuel in the thorium fuel cycle, additional effort in measurement and/or data evaluation should be a high priority.

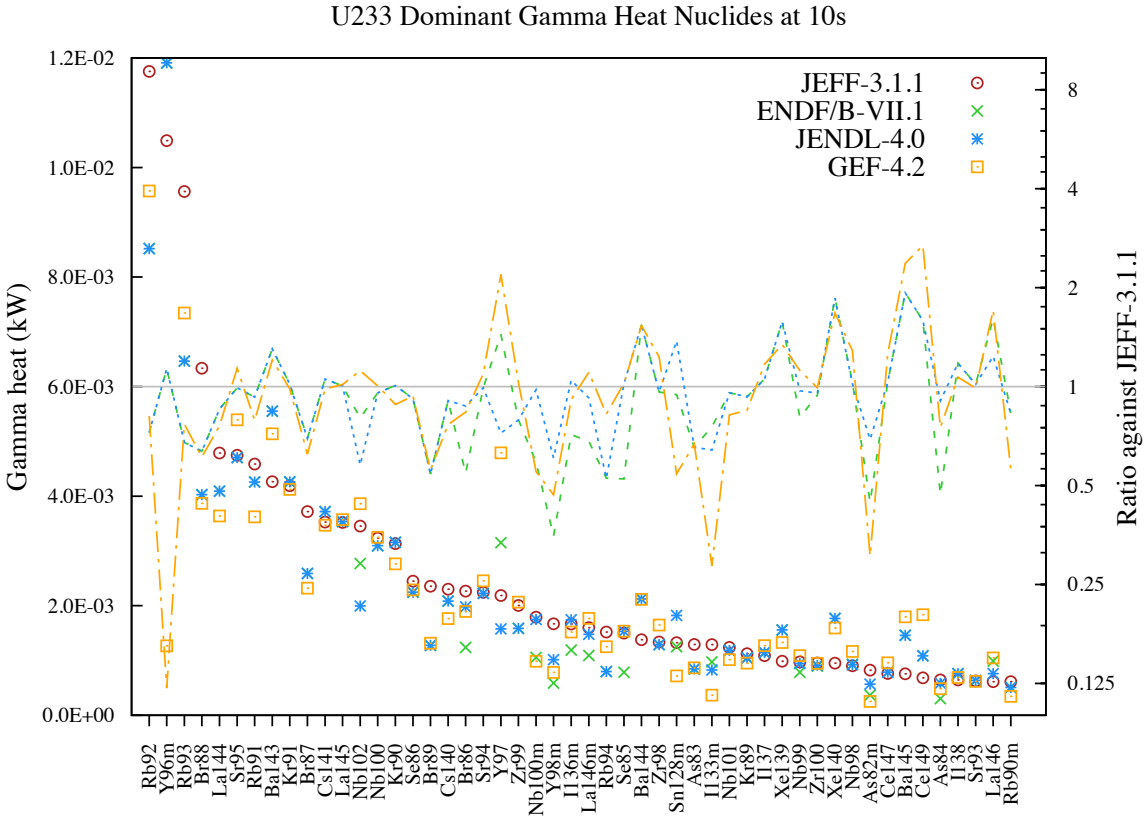

Figure 54: Fission yield comparison for U233 fission pulse after 10s cooling.

These comparisons, both with decay and fission yield data, can be performed for all fissile nuclides with any irradiation pattern and any cooling times. While the well-known fuels generally have good agreement for total heat over the fission products, those which are not ^{235}U or ^{239}Pu are quite different, as shown for ^{233}U above. Many other minor actinides undergo fission in a conventional reactor and can play a substantial role with partially-burned fuel or in reactors designed to burn these nuclides. The library variation for each of these minor actinides is generally greater than those shown above, as can be seen in the supplements to this report.

7 Discussion

What began as a verification and validation exercise for the FISPACT-II code quickly became a study into the discrepancies caused by rotating nuclear data libraries. While the Pandemonium problem was well known and more than 100 nuclides have been the subject of improved measurements, it is clear that varying evaluation quality and progress in TAGS data adoption has resulted in decay libraries with non-trivial differences.

By digging just a bit further in one of the following directions, relatively tremendous discrepancies can be found:

- More cooling times (particularly less than 100s)

- Nuclides underneath the top 70% of the total
- Incident-neutron energies other than 0.0253 eV or 400 keV
- Any fissiles other than ^{235}U or ^{239}Pu

The validation of the decay heat predictions has been demonstrated at least at the level set by other inventory codes, but the verification of the methods is best shown by the ability to rigorously interrogate the decay and fission yield files, find errors and feed back the results for data improvement. The supplements to this report [40, 41] probe all of the major fissiles and minor actinides with the same approach as in Section 6.

The detailed results exemplified in this report raise the problem posed when an engineered solution is preferred to the physical one in order to satisfy a single application. The total decay heat simulation from fission event was never badly predicted, due to the compensation between the beta and gamma components. However, the detailed spatial heat distributions is much more affected by the lack of robustness in the two components: the gamma radiation generally travels further than the beta.

It is worth noticing that the problems arising from the misallocation of the the β/γ decay feeds do not only influence the quality of decay heat simulations but also any responses derived from the decay schemes, such as shutdown gamma dose rates – a particularly important case for D-T fusion reactors. In that case the consequences are far more unfavorable due to the fact that the missing high-energy lines are likely to be the most predominant contributor to the dose.

The results in this report and its counterpart covering the decay from fusion event [42] can be used to develop simulation guidance and uncertainty quantification and propagation in decay heat and inventory predictions for all applications with inventory code FISPACT-II and its attached libraries.

References

[1] K.-H. Schmidt, B. Jurado, and C. Amouroux. General view on nuclear fission. pages 1–208, 2014.

[2] K.-H. Schmidt. GEFY: GEF-based fission-fragment Yield library in ENDF format, 2015. www.khs-erzhausen.de/GEFY.html.

[3] A. Tobias. Decay heat. Technical report, Central Electricity Generating Board, Berkeley Nuclear Laboratories, Berkeley, Gloucestershire GL13 9PB, England, 1979.

[4] I. Gauld. Validation of ORIGEN-S Decay Heat Predications for LOCA Analysis. In *PHYSOR-2006, ANS Topical Meeting on Reactor Physics*. Canadian Nuclear Society, Vancouver, BC, Canada, September 2006.

[5] I. Gauld, G. Illas, B. D. Murphy, and C. F. Weber. Validation of SCALE 5 Decay Heat Predictions for LWR Spent Nuclear Fuel. Technical Report NUREG/CR-6972, USNRC, 2010.

[6] J. Hardy, L. Carraz, B. Jonson, and P. Hansen. The essential decay of pandemonium: A demonstration of errors in complex beta-decay schemes . *Physics Letters B*, 71(2):307 – 310, 1977. ISSN 0370-2693. doi:http://dx.doi.org/10.1016/0370-2693(77)90223-4.

[7] R. C. Greenwood, R. G. Helmer, and M. H. Putnam. Measurement of beta-decay intensity distributions of several fission-product isotopes using a total absorption gamma-ray spectrometer. *Nuclear Instruments and Methods in Physics Research A*, 390:95–154, 1997.

[8] T. Yoshida. International Evaluation Co-operation Volume 25: Assessment of Fission Product Decay Data for Decay Heat Calculations. Technical Report NEA No. 6284, OECD NEA, 2007.

[9] J.-Ch. Sublet, et al. EASY-II: a system for modelling of n, d, p, γ and α activation and transmutation processes. *Joint International Conference on Supercomputing in Nuclear Applications and Monte Carlo*, October 2013.

[10] J.-Ch. Sublet, J. W. Eastwood, and J. G. Morgan. The FISPACT-II User Manual. Technical Report CCFE-R(11) 11 Issue 6, CCFE, 2014. http://www.ccfe.ac.uk/EASY.aspx.

[11] A. Koning, et al. The JEFF-3.1 Nuclear Data Library. Technical Report NEA No. 6190, OECD NEA, 2006.

[12] M. Chadwick, et al. ENDF/B-VII.1 Nuclear Data for Science and Technology: Cross Sections, Covariances, Fission Product Yields and Decay Data . *Nuclear Data Sheets*, 112(12):2887 – 2996, 2011. ISSN 0090-3752. doi:http://dx.doi.org/10.1016/j.nds.2011.11.002. Special Issue on ENDF/B-VII.1 Library.

[13] K. Shibata, et al. JENDL-4.0: A New Library for Nuclear Science and Engineering. *Journal of Nuclear Science and Technology*, 48(1):1–30, 2011. doi:10.1080/18811248.2011.9711675.

[14] R. A. Forrest. The European Activation File: EAF-2007 decay data library. Technical Report UKAEA FUS 537, EURATOM/CCFE, 2007.

[15] J. K. Dickens, et al. Fission Product Energy Release for Times Following Thermal-Neutron Fission of U235 Between 2 and 14000 Seconds. Technical Report ORNL/NUREG-14, Oak Ridge National Laboratory, 1979.

[16] J. K. Dickens. Current status of decay heat measurements, evaluations and needs. Technical Report ORNL/TM-10094, Oak Ridge National Laboratory, 1986.

[17] M. Akiyama, et al. Measurement of gamma-ray decay heat of fission products for fast neutron fissions of 235U, 239Pu and 233U. 24(9):709–722, 1982.

[18] M. Akiyama, et al. Measurements of beta-ray decay heat of fission products for fast neutron fissions of 235U, 239Pu and 233U. 24(10):803–816, 1982.

[19] P. Johansson. Integral Determination of the Beta and Gamma Heat in Thermal Neutron Induced Fission of 235U and 239Pu, and of the Gamma Heat in Fast Fission of 238U. In *Proceedings of the Specialists Meeting on Data for Decay Heat Predictions*, NEA-CRP-L–302, pages 211–223. Studsvik, Sweden, September 1987.

[20] W. A. Schier and G. P. Couchell. Beta and gamma Decay Heat Measurements Between 0.1 s - 50,000 s for Neutron Fission of 235U, 238U, and 239Pu: Final Report. Technical Report DOE/ER/40723-4, University of Massachusetts Lowell, 1997.

[21] M. Akiyama. *Doctoral dissertation to the University of Tokyo*. Ph.D. thesis, University of Tokyo, 1983. UTNL-R 0151 [in Japanese].

[22] Y. Ohkawachi and A. Shono. Decay Heat Measurement of Actinides at YAYOI. *Nuclear Science and Technology*, pages 493–496, August 2002.

[23] K. Baumung. Messung der Nachzerfallsleistung von ^{235}U im Zeitbereich von 15 s bis 4000 s. Technical Report KfK 3262, Kernforschungszentrum Karlsruhe, December 1981.

[24] J. L. Yarnell and P. J. Bendt. Decay heat from products of 235U thermal fission by fast response boil-off calorimetry. Technical Report LA-NUREG-6713, Los Alamos National Laboratory, 1977.

[25] J. L. Yarnell and P. J. Bendt. Calorimetric fission products decay heat measurements of 239Pu, 233U and 235U. Technical Report LA-7452-MS, NUREG-/CR-0349, Los Alamos National Laboratory, 1978.

[26] M. Lott, G. Lhiaubet, and F. Defreche. Puissance Résiduelle Totale Émise par les Produits de Fission Thermique de 235U. *Journal of Nuclear Energy*, 27:597–605, 1973.

[27] E. Jurney, P. Bendt, and T. England. Fission Product Gamma Spectra. Technical Report LA-7620-MS, Los Alamos National Laboratory, 1979.

[28] T. D. MacMahon, R. Wellum, and H. W. Wilson. Energy Released by Beta Radiation Following Fission. Part I - 235U Data. 24:493–501, 1970.

[29] J. Scobie, R. D. Scott, and H. W. Wilson. Beta Energy Release Following the Thermal Neutron Induced Fission of 233U and 235U. *Journal of Nuclear Energy*, 25:1–10, 1971.

[30] A. McNair, F. Bannister, R. Keith, and H. W. Wilson. A Measurement of the Energy Released as Kinetic Energy of Beta-Particles Emitted in the Radioactive Decay of the Fission Products of 235U. *Journal of Nuclear Energy*, 23:73–86, 1969.

[31] A. McNair and R. Keith. A Measurement of the Beta Decay Energy from the Fission Products of 239Pu. *Journal of Nuclear Energy*, 23:697–703, 1969.

[32] M. Murphy, W. Taylor, D. Sweet, and M. March. Experiments to determine the rate of beta energy release following fission of pu239 and u235 in a fast reactor. Technical Report AEEW-R 1212, UK Atomic Energy Authority, 1979.

[33] P. Fisher and B. Engle. Delayed Gammas from Fast-Neutron Fission of Th232, U233, U235, and Pu239. *Physical Review B*, I(1959), 1964.

[34] S. Li. *Beta Decay Heat Following 235U, 238U and 239Pu Neutron Fission.* Ph.D. thesis, University of Massachusetts Lowell, Department of Physics, April 1997.

[35] H. V. Nguyen. *Gamma-ray Spectra and Decay Heat Following 235U Thermal Neutron Fission.* Ph.D. thesis, University of Massachusetts Lowell, Department of Physics, April 1997.

[36] E. H. Seabury. *Gamma-ray Decay Heat Measurements Following 238U(n,f) and 239Pu(n,f).* Ph.D. thesis, University of Massachusetts Lowell, Department of Physics, January 1997.

[37] A. Tobias. Derivation of decay heat benchmarks for U235 and Pu239 by a least squares fit to measured data. Technical report, Central Electricity Generating Board, 1989.

[38] C. J. Dean, T. D. Newton, and G. Hosking. Review of the Tobias Decay Heat Standard. Technical Report SA/NST/18923/W003 Issue 1, Serco Assurance, February 2007.

[39] M. Gupta, M. Kellett, A. Nichols, and O. Bersillon. Decay Heat Calculations: Assessment of Fission Product Decay Data Requirements for Th/U Fuel. Technical Report INDC(NDS)-0577, IAEA, 2010.

[40] M. Fleming and J.-Ch. Sublet. Decay data comparisons for decay heat and inventory simulations of fission events. Technical Report CCFE-R(15)28/S1, CCFE, June 2015. http://www.ccfe.ac.uk/EASY.aspx.

[41] M. Fleming and J.-Ch. Sublet. Fission yield comparisons for decay heat and inventory simulations of fission events. Technical Report CCFE-R(15)28/S2, CCFE, June 2015. http://www.ccfe.ac.uk/EASY.aspx.

[42] J.-Ch. Sublet and M. Gilbert. Decay heat validation, FISPACT-II & TENDL-2014, JEFF-3.2, ENDF/B-VII.1 and JENDL-4.0 nuclear data libraries. Technical Report CCFE-R(15)25, CCFE, 2015. http://www.ccfe.ac.uk/EASY.aspx.